

FACIES AND BED TYPE ANALYSIS OF A THIN-BED
DOMINATED TURBIDITE SUCCESSION IN THE MIOCENE
TEMBURONG FORMATION, KAMPUNG BEBULOH,
LABUAN, MALAYSIA

FARAH SYAFIRA BINTI BURHANUDDIN

DEPARTMENT OF GEOLOGY
FACULTY OF SCIENCE
UNIVERSITI MALAYA
KUALA LUMPUR

2023

**FACIES AND BED TYPE ANALYSIS OF A THIN-
BED DOMINATED TURBIDITE SUCCESSION IN
THE MIOCENE TEMBURONG FORMATION,
KAMPUNG BEBULOH, LABUAN, MALAYSIA**

FARAH SYAFIRA BINTI BURHANUDDIN

**THESIS SUBMITTED IN FULFILMENT OF THE
REQUIREMENTS FOR THE DEGREE
OF MASTER OF SCIENCE**

**DEPARTMENT OF GEOLOGY
FACULTY OF SCIENCE
UNIVERSITI MALAYA
KUALA LUMPUR**

2023

UNIVERSITY OF MALAYA
ORIGINAL LITERACY WORK DECLARATION

Name of Candidate: **FARAH SYAFIRA**

Matric No.: **17044102/3**

Name of Degree: **MASTER OF SCIENCE**

Title of Thesis ("this Work"):

**FACIES AND BED TYPE ANALYSIS OF A THIN-BED
DOMINATED TURBIDITE SUCCESSION IN THE MIOCENE TEMBURONG
FORMATION, KAMPUNG BEBULOH, LABUAN, MALAYSIA**

Field of Study:

SEDIMENTOLOGY

I do solemnly and sincerely declare that:

- (1) I am the sole author/writer of this Work;
- (2) This Work is original;
- (3) Any use of any work in which copyright exists was done by way of fair dealing and for permitted purposes and any excerpt or extract from, or reference to or reproduction of any copyright work has been disclosed expressly and sufficiently and the title of the Work and its authorship have been acknowledged in this Work;
- (4) I do not have any actual knowledge nor do I ought reasonably to know that the making of this work constitutes an infringement of any copyright work;
- (5) I hereby assign all and every rights in the copyright to this Work to the University of Malaya ("UM"), who henceforth shall be owner of the copyright in this Work and that any reproduction or use in any form or by any means whatsoever is prohibited without the written consent of UM having been first had and obtained;
- (6) I am fully aware that if in the course of making this Work I have infringed any copyright whether intentionally or otherwise, I may be subjected to legal action or any other action as may be determined by UM.

Candidate's Signature

Date:

Subscribed and solemnly declared before,

Witness's Signature

Date:

Name:

Designation:

FACIES AND BED TYPE ANALYSIS OF A THIN-BED DOMINATED TURBIDITE SUCCESSIONS IN THE MIOCENE TEMBURONG FORMATION, KAMPUNG BEBULOH, LABUAN, MALAYSIA

ABSTRACT

Thin-bedded turbidites are important hydrocarbon-bearing reservoirs in many mature fields throughout the world. The type of turbidite depositional setting strongly influences reservoir vertical and horizontal continuity. However, differentiation between lobe and levee associated thin-bedded turbidites is still challenging because of the generally similar facies characteristics. This study aims to solve this problem by conducting a detailed bed-scale facies and bed-type analysis on the Early Miocene Temburong Formation exposed at Kampung Bebuloh, Labuan, Malaysia, which may uncover features that can help in differentiating both depositional types. Six bed types are recognised in the Temburong Formation, which are interpreted as low density turbidites (BT1 – 4), hybrid event beds (BT 5), sustained turbidites (BT6) and possible densite muds (some BT3). Detailed facies and ichnology analysis reveal features which are consistent with a lobe fringe deposit rather than levee-associated environment interpretation, including tabular bed geometries, presence of hybrid event beds, and the absence of thick-bedded channel-fill sandstones. Five bed type associations are identified and interpreted as representing sub-environments within an overall lobe depositional setting. A diverse trace fossil assemblage, comprising the *Nereites* ichnofacies is consistent with a deep marine environment. Further identification of the *Paleodictyon* and *Nereites* sub-ichnofacies indicates a distal turbidite system setting, most likely lobe fringe. Based on the thick accumulation of FA2 and FA3 and no distinct observable vertical trend, the Early Miocene Temburong Formation in Labuan is interpreted as turbidites deposited at the fringes of lobe complexes rather than a single lobe fringe. Earlier works into the Temburong Formation in SW Labuan propose a middle slope to proximal basin floor

setting where the thin-bedded intervals were interpreted as potentially representing either levee deposits or the fringes of confined lobe deposits. Conversely, the Temburong Formation at Kampung Bebuloh exhibits characteristics of an unconfined lobe setting, suggesting an evolutionary change in depositional conditions over time.

Keyword: thin-bedded turbidite, lobe fringe, bed type analysis, facies analysis, hybrid event beds, Temburong Formation

Universiti Malaya

ANALISIS FASIES DAN ‘BED TYPE’ BAGI TURBIDIT YANG DI DOMINASI OLEH LAPISAN NIPIS DALAM MIOSEN FORMASI TEMBURUNG DI KAMPUNG BEBULOH, LABUAN, MALAYSIA

ABSTRAK

Lapisan nipis endapan turbidit merupakan takungan minyak yang penting di kebanyakan lapangan matang di serata dunia. Jenis persekitaran pemendapan turbidit memainkan peranan yang penting dalam kesinambungan takungan, dari segi menegak dan juga mendatar. Walau bagaimanapun, pembezaan antara endapan lob dan levi yang berkaitan dengan turbidit lapisan nipis masih mencabar kerana ciri-ciri fasies yang agak serupa. Kajian ini bertujuan untuk menyelesaikan masalah ini dengan melakukan analisis terperinci untuk fasies dan “bed type” di Formasi Temburong yang terdedah di Kampung Bebuloh, Labuan, yang mungkin mendedahkan ciri yang boleh membantu dalam membezakan kedua-dua jenis pemendapan. Enam jenis “bed type” dikenalpasti di Formasi Temburong, yang ditafsirkan sebagai turbidit bertumpatan rendah (BT 1 – 4), lapisan hibrid (BT5), turbidit mampan (BT6), dan kemungkinan lumpur yg tumpat (sebahagian BT3). Analisis fasies dan fosil surih yang terperinci mendedahkan ciri-ciri yang konsisten dengan deposit pinggir lobus dan bukannya tafsiran persekitaran yang berkaitan dengan tambak, berdasarkan ciri-ciri geometri, kehadiran katil acara hibrid dan ketiadaan batu pasir yang menunjukkan ciri-ciri sungai. Lima “bed type association” (BTA) dikenal pasti dan ditafsirkan sebagai mewakili sub-persekitaran dalam tetapan pemendapan lobus keseluruhan. Himpunan fosil surih yang pelbagai, yang terdiri daripada ichnofacies *Nereites* adalah konsisten dengan persekitaran marin yang dalam. Pengenalpastian lanjut sub-ichnofacies *Paleodictyon* dan *Nereites* menunjukkan tetapan sistem turbidit distal, kemungkinan besar pinggir lobus. Berdasarkan pengumpulan tebal FA2 dan FA3 dan tiada kecenderungan aliran menegak yang ketara, Formasi Temburong Miosen Awal di Labuan ditafsirkan sebagai turbidit yang dimendapkan di pinggir

kompleks lobus dan bukannya pinggir lobus tunggal. Kerja-kerja terdahulu ke dalam Formasi Temburong di SW Labuan mencadangkan cerun tengah ke tetapan lantai lembangan proksimal di mana selang lapisan nipis ditafsirkan sebagai berpotensi mewakili sama ada deposit tebing atau pinggir deposit lobus terkurung. Sebaliknya, Formasi Temburong di Kampung Bebuloh mempamerkan ciri persekitaran lobus yang tidak terkurung, mencadangkan perubahan evolusi dalam keadaan pemendapan dari semasa ke semasa.

Kata kunci: turbidit, endapan pinggir lob, analisa “bed type”, Analisa fasies, Formasi Temburong

ACKNOWLEDGEMENT

First and foremost, I would like to express my gratitude to ConocoPhillips Malaysia for providing scholarship to support my study. I would like to thank University of Malaya for providing the facilities and equipment I needed to complete my thesis.

I would like to express my sincere and greatest gratitude to my supervisor, Dr. Meor Hakif for his time and effort, continuous support, guidance, and patience. His valuable knowledge and experience have inspired me throughout my MSc journey and my professional career. I could not have imagined having a better advisor and mentor for my study.

To my mentor in Petronas, Joaquin Naar Escamilla, who is willingly devoted time in giving me guidance in deepwater clastic sedimentology, a big thank to you. Special thanks to my superior, Leonardo Humberto Piccoli, and my Sedi/Strat colleagues in Petronas, especially Chin, Hazwani, and Yusra, for all the guidance, moral support and feedback sessions. I would also like to extend my thanks to the lecturers and fellow postgrad students in Geology Department, especially Dr. Lin Chin Yik, Dr. Muhammad Hatta, Dr. Khairul Azlan, and Dr. Eva Mansor, for providing feedback, valuable input, and inspired me during these four years of my MSc study.

Lastly, words cannot express my gratitude to my family for all the support they have given me during these four years of distance learning. For my husband Azmi, thank you for being my field assistant, for taking care of our son and home whilst I wrote this thesis, and for all your patience and support, without which I would have stopped these studies a long time ago. Though it takes almost 5 years, but Alhamdulillah, I did it! :)

TABLE OF CONTENTS

ORIGINAL LITERACY WORK DECLARATION	II
ABSTRACT	III
ABSTRAK	V
ACKNOWLEDGEMENT	VII
TABLE OF CONTENTS	VIII
LIST OF FIGURES.....	XI
LIST OF TABLES.....	XVII
LIST OF ABBREVIATION.....	XVIII
CHAPTER 1: INTRODUCTION	1
1.1 OVERVIEW	1
1.2 OBJECTIVES	3
1.3 STUDY AREA	4
1.4 METHODOLOGY	6
1.4.1 DATA GATHERING.....	7
1.4.2 FACIES AND BED TYPE ANALYSIS	7
1.4.3 ICHNOLOGICAL ANALYSIS	9
CHAPTER 2: GEOLOGICAL SETTING	12
2.1 OVERVIEW	12
2.2 REGIONAL TECTONIC SETTING.....	13
2.3 LOCAL STRATIGRAPHIC FRAMEWORK	17
2.3.1 TEMBURONG FORMATION.....	21
2.3.2 BELAIT FORMATION.....	25
2.3.3 ABSENCE OF SETAP SHALE FORMATION IN LABUAN	30
CHAPTER 3: LITERATURE REVIEW.....	31
3.1 SUBAQUEOUS DENSITY FLOW	31
3.1.1 TURBIDITY CURRENTS.....	32
3.1.2 TURBIDITE CLASSIFICATION SCHEMES.....	36
3.1.3 HYBRID EVENT BEDS (HEBs).....	41
3.1.4 MASS TRANSPORT DEPOSIT (MTD).....	45
3.2 THIN-BEDDED TURBIDITES AND THEIR DEPOSITIONAL ENVIRONMENTS	48
3.2.1 THIN-BEDDED TURBIDITES IN CHANNEL-LEVEE SYSTEMS	50
3.2.2 THIN BEDDED TURBIDITES IN OUTER FAN LOBE SYSTEMS	55
CHAPTER 4: SEDIMENTARY FACIES AND BED TYPES OF THE EARLY MIOCENE TEMBURONG FORMATION.....	57
4.1 FACIES ANALYSIS	59
4.1.1 FACIES 1 (F1): STRUCTURELESS SANDSTONE.....	59
4.1.2 FACIES 2 (F2): PLANAR-LAMINATED SANDSTONE.....	60

4.1.3	<i>FACIES 3 (F3): RIPPLE CROSS-LAMINATED SANDSTONE</i>	61
4.1.4	<i>FACIES 4 (F4): PLANAR-LAMINATED SILTSTONE</i>	62
4.1.5	<i>FACIES 5 (F5): STRUCTURELESS TO FINELY PLANAR-LAMINATED MUDSTONE</i>	63
4.1.6	<i>FACIES 6 (F6): POORLY SORTED, ARGILLACEOUS SANDSTONE</i>	64
4.2	BED TYPE ANALYSIS	66
4.2.1	<i>BT1: THIN-BEDDED SANDSTONE</i>	68
4.2.2	<i>BT2: MEDIUM-BEDDED SANDSTONE</i>	71
4.2.3	<i>BT3: STRUCTURELESS TO FINELY LAMINATED MUDSTONE</i>	74
4.2.4	<i>BT4: HETEROLITHIC MUDSTONE</i>	76
4.2.5	<i>BT5: BIPARTITE / TRIPARTITE BEDS</i>	79
4.2.6	<i>BT6: UNGRADED SANDSTONE</i>	84
4.3	BED TYPE ASSOCIATION (BTA)	88
4.3.1	<i>BTA 1: LOBE-OFF AXIS</i>	92
4.3.2	<i>BTA 2: FRONTAL LOBE FRINGE</i>	94
4.3.3	<i>BTA3: LATERAL LOBE FRINGE</i>	96
4.3.4	<i>BTA 4: LOBE DISTAL FRINGE</i>	98
4.3.5	<i>BTA 5: SLUMP DEPOSITS</i>	100
4.3.6	<i>MUD-DOMINATED SUCCESSION</i>	104
4.4	DETAILED SEDIMENTARY LOGS	105
	CHAPTER 5: ICHNOLOGY ANALYSIS OF THE EARLY MIOCENE TEMBURONG FORMATION	111
5.1	OVERVIEW	111
5.2	DESCRIPTION OF TRACE FOSSILS	114
5.2.1	<i>COSMORHAPHE</i>	114
5.2.2	<i>DESMOGRAPTON</i>	115
5.2.3	<i>HELMINTHOPSIS</i>	116
5.2.4	<i>MEGAGRAPTON</i>	117
5.2.5	<i>NEREITES AND ASSOCIATED BIOTURBATED FABRIC</i>	118
5.2.6	<i>OPHIOMORPHA</i>	121
5.2.7	<i>PALAEOPHYCUS</i>	123
5.2.8	<i>PALEODICTYON</i>	124
5.2.9	<i>SCOLICIA</i>	126
5.2.10	<i>PROTOVIRGULARIA</i>	127
5.2.11	<i>TUBUTOMACULUM</i>	128
5.2.12	<i>OTHER TRACE FOSSILS OF RARE OCCURRENCE</i>	129
5.3	SIGNIFICANCE OF THE TRACE FOSSIL DISTRIBUTION TO DEPOSITIONAL ENVIRONMENT INTERPRETATION	131
5.3.1	<i>ETHOLOGY DISTRIBUTION</i>	133
5.3.2	<i>INTERPRETATION</i>	134
	CHAPTER 6: DISCUSSION	137
6.1	OVERVIEW	137

6.2	CHARACTERISTICS SHARED BY LEVEE AND LOBE FRINGE DEPOSITS	138
6.3	CRITERIA DIFFERENTIATING LEVEE AND LOBE FRINGE DEPOSITS	139
6.3.1	ASSOCIATION WITH OTHER THICK-BEDDED DEPOSITS.....	139
6.3.2	PRESENCE OF HYBRID EVENT BEDS (HEB)	140
6.3.3	LATERAL BED GEOMETRY AND VERTICAL BED THICKNESS TRENDS	141
6.4	CONCLUSIONS BASED ON INTEGRATED SEDIMENTARY AND ICHNOLOGICAL CHARACTERISTICS 142	
6.5	DEPOSITIONAL MODEL FOR THE EARLY MIOCENE TEMBURONG FORMATION AT KAMPUNG BEBULOH, LABUAN	146
6.6	THE KAMPUNG BEBULOH EXPOSURE IN RELATION TO OTHER EXPOSURES OF THE TEMBURONG FORMATION ON LABUAN ISLAND	148
6.7	PALEOGEOGRAPHIC RECONSTRUCTION OF EARLY MIOCENE NORTHWEST BORNEO	149
CHAPTER 7: SUMMARY		154
7.1	CONCLUSIONS	154
7.2	RECOMMENDATIONS FOR FUTURE WORK.....	155
REFERENCES		156

LIST OF FIGURES

Figure 1.1	:	(A) Map of Labuan Island. Red rectangle is the location of the study area. (B) Two outcrops were chosen for this study. (C) Outcrop A. Younging direction is towards SE. (D) Outcrop B. Younging direction is towards SE.....	5
Figure 1.2	:	Study workflow.....	6
Figure 1.3	:	Bed type consists of an assemblage of facies within a single bed. Assemblages of bed types with a repeating vertical pattern are grouped into Bed Type Associations.....	7
Figure 1.4	:	Schematic representation of the relationship between trace fossil assemblages, sedimentary facies and depth zones in the ocean. Taken from Seilacher (2007).....	9
Figure 1.5	:	Taphonomic classification system used in this study (after Martinsson, 1970, redrawn from Cumming and Hodgson, 2011).....	10
Figure 1.6	:	List of discussed ethological classification and typical ichnogenera assigned to these ethologies. Taken from Cumming and Hodgson (2011).....	11
Figure 2.1	:	Distribution of the Temburong Formation across Sabah and Labuan Island. Map redrawn from Lunt (2022).....	12
Figure 2.2	:	(A) Tectono-stratigraphic provinces of NW Sabah. Red circle is the location of Labuan island, which is located within the Inboard Belt structural zone of the NW Borneo continental margin. Redrawn from Hazebroek and Tan (1993). (B) E–W regional cross section showing an E–W fold and thrust belt underlying the Temburong, Setap Shale and younger deltaic sediments. Modified from Morley et. al. (2008).....	13
Figure 2.3	:	Schematic diagram of NW-SE sequential cross sections across NW Sabah. (A-B) Rifted continental crust due to the sea-floor spreading of South China Sea was moving towards NW Borneo. Deep water deposition occurred at the same time as SE-ward subduction of an ocean basin beneath NW Borneo margin. (C-D) Subduction ceased when the rifted continental crust collided with NW Borneo. Consequently, a major accretionary prism known as the West Crocker Group formed along the compressional zones. Modified from Tongkul, 1991.....	16
Figure 2.4	:	(A) Geological map of Labuan Island. Redrawn and modified based on Wilson and Wong (1964) and Som et. al. (2011) for the northern part of Labuan. Wilson and Wong (1964) reported the presence of Sabong Beds, mainly consisting of limestone, which they included in Temburong Formation but there is no recent study on the presence of this unit. (B) Stratigraphic chart of Labuan Island. Modified from Hennig-Brietfield et. al. (2019).....	17

Figure 2.5	:	Outcrop exposure in Tanjung Layang-Layangan (A) Heterolithic packages observed in Tanjung Layang-Layangan that represent the distal delta front deposits. (B) Hummocky cross-stratified sandstone observed within the Lower Belait. (C) Amalgamated, cross-bedded sandstone of Middle Belait. (D) Sharp contact between mud-dominated package, which represent the prodelta succession (based on biostratigraphic analysis done by Som et. al., 2011), sharply overlain by thick, amalgamated, cross-bedded sandstone with pebbly basal of Middle Belait.....	27
Figure 2.6	:	Outcrop photos of the Middle to Upper Belait Formation from Kubong Bluff to Bethune Head, northern Labuan. (A) Medium to coarse-grained, trough cross-bedded sandstone represent channel-fill deposits. (B) Presence of mud rip-up clast as channel lag, suggesting tidal influence. (C) Stack of amalgamated, coarse-grained cross-bedded sandstone. (D) Heterolithic succession with presence of swaley- and hummocky cross-stratification indicative of storm deposits in a lower shoreface environment. Supported by the presence of marine ichnofacies (i.e <i>Ophiomorpha</i>).....	29
Figure 3.1	:	Ideal deposit of a high-density turbidite showing S1 to S3 divisions, and an overlying late-stage low-density turbidite showing TB to TE divisions. Redrawn from Lowe (1982)....	34
Figure 3.2	:	The Mulder and Alexander (2001) classification scheme for turbidity currents.....	35
Figure 3.3	:	Classification scheme of turbidites from Bouma (1962), Lowe (1982) and Shanmugam (1997). Redrawn from Shanmugam (1997).....	36
Figure 3.4	:	A few similarities in the classification schemes of turbidite deposits from Mutti (1992) and Talling et. al. (2012), i.e., TB-3 is equivalent to F4. Redrawn from Talling et. al. (2012)....	39
Figure 3.5	:	'Ideal' internal division of HEBs based on the compilation of bed motifs from a wide range of systems, taken from Haughton et. al. (2009).....	41
Figure 3.6	:	Classification of HEBs by Fonnesu et. al. (2018).....	42
Figure 3.7	:	Simplified MTD classification.....	45
Figure 3.8	:	Depositional model for deep-water deposits, from slope to basin floor fan. Modified from Mutti (1977).....	49
Figure 3.9	:	Sub-environments within a channel-levee system. Terminology adopted from Kane and Hodgson (2011). Redrawn from Hansen et. al. (2017).....	50
Figure 3.10	:	(A) Simplified model displaying the various sub-environment in a lobe. (B) Plan-form view of the lobe hierarchy classification scheme: bed to bed set, lobe element, lobe, lobe complex, and lobe complex set (both diagrams were redrawn from Spsychala et. al., 2017).....	55

Figure 4.1	:	Measured section in the Early Miocene Temburong Formation from Kampung Bebuloh, Labuan, Malaysia.....	58
Figure 4.2	:	Bed types identified in the Early Miocene Temburong Formation in Kampung Bebuloh, Labuan. Bed thicknesses are not to scale.....	66
Figure 4.3	:	(A) Total bed type distribution based on number of beds observed. (B) Total bed type gross thickness.....	67
Figure 4.4	:	Examples of Bed Type 1. (A-C) Yellowish, very fine-grained sandstone with climbing and ripple cross-lamination (F3). Yellow arrows point to carbonaceous layers. (D) Yellowish brown, normal graded, thin-bedded sandstone that displays planar (F2) to cross ripple lamination (F3). Length of the scale is 13.5 cm.....	69
Figure 4.5	:	Examples of Bed Type 2. Normal graded sandstone. Yellowish brown, well sorted, fine to very fine-grained sandstone. Fining upward, this bed type predominantly consists of parallel lamination (F2) and thinner interval of cross ripple lamination (F3).....	73
Figure 4.6	:	Example of Bed Type 3: (A) Laminated mudstone. (B) Repetition of BT1 interbedding with BT4, which formed TCE sequence of Bouma. <i>Tubutomaculum</i> is observed within BT4 (yellow arrow).).....	75
Figure 4.7	:	Example of Bed Type 4: (A) Consists of intercalation of mudstone and thin siltstone. Sandstone layers are yellowish brown in color, only 1 to 2 cm thick, with sharp base and some show wavy to parallel lamination. (B) Siltstone layers within BT4. The top part has turned into siderite, but the lamination is still preserved. (C) BT4 shows thinning upwards trend where the thickness of sandstone reduces from 5 to less than 1 cm on the top. Sandstone is greyish brown in color, some displays wavy lamination).....	78
Figure 4.8	:	Sub-bed types of BT5.....	80
Figure 4.9	:	(A) Amalgamated hybrid event beds. Bipartite beds overlain by tripartite beds. Presence of soft deformation like convolute lamination and load casts with detached pseudo-nodules (yellow arrow_ between F6 and F2 of the bipartite bed, which is common in HEB due to differences in grain size. (B) Tripartite bed. Consist of planar-laminated sandstone in the lower interval, argillaceous sandstone with swirley/chaotic texture in the middle interval, and cross ripple laminated sandstone in the upper interval. (C) Amalgamated hybrid event beds. Bipartite beds overlain by tripartite beds. The thickest sandstone bed in the area, ca. 90cm. Argillaceous sandstone (F6) is identified based on its color, darker brown compared to below and above interval, swirley/chaotic appearance and presence of mud clasts. (D) Tripartite beds..	81

Figure 4.10	:	Examples of Bed Type 6. (A-B) Ungraded sequence. The beds display alternating F2 and F3 facies – T _{BCBC} sequence. (C) Yellowish brown, moderately sorted, fine- to very fine-grained sandstone. Consists of F1, overlain by F3. Flame structure can be observed on F1. Presence of cm-sized mud clasts. Missing parallel laminated sandstone (F2) may indicate a bypass surface. (D) This bed displays faint F3 at the bottom, then gradually overlain by F1 interval, and overlain by another F3 interval – T _{CAC} sequence.....	85
Figure 4.11	:	Schematic diagram showing the deposition of bed related to three individual sustained turbidity current events. (i) deposition during first flow under fluctuating velocity/discharge conditions; (ii) erosion associated with second flow and deposition of cobbles; (iii) deposition during second flow under fluctuating velocity/discharge conditions; (iv) erosion associated with third flow and deposition of cobbles; (v) waning of third flow and deposition of a fining-upwards, rippled upper interval. (Diagram on the right taken from Jackson and Johnson, 2009)).	87
Figure 4.12	:	Cross-plots of average sandstone proportion vs. average sandstone layer thickness in which four distinct trends were observed. BTA 1 has the highest sandstone proportion and average sandstone layer thickness. BTA 2 has 51% to 64% of sandstone proportion, while BTA 3 has 37% to 56%. BTA 4 has lowest sandstone proportion which is less than 35% (refer Table 4.3).....	89
Figure 4.13	:	Architectural hierarchy of lobe deposits ranging from beds, lobe elements and lobes. A lobe is bounded above and below by fine-grained units (BT4) and consists of several lobe elements.....	90
Figure 4.14	:	Distribution of bed types in each bed type association of the Early Miocene Temburong Formation at Kampung Bebuloh, Labuan	91
Figure 4.15	:	Example of BTA 1 from Outcrop B. Younging direction is towards SE direction.....	93
Figure 4.16	:	Example of BTA 2, BTA3 and BTA 5, from Outcrop A. Generally, BTA 2 has thicker sandstone beds, as compared to BTA 3. BTA 5 was identified based on its folded and heavily deformed strata. The thickness of BTA5 in outcrop A is about ~4 m and was gradually overlain by mud-dominated succession. The boundary between BTA 5 and mud-dominated succession is unclear. Younging direction towards SE direction.	97
Figure 4.17	:	Example of BTA 3, BTA 4 and BTA 5 from Outcrop B. BTA 4 is generally mud-dominated, with average of 29% sand proportion. BTA 5 was identified based on its deformed strata. Younging direction is towards SE direction.....	98

Figure 4.18	:	BTA 5 from Outcrop A. BTA 5 was identified based on its folded and heavily deformed strata. Younging direction towards SE direction.....	101
Figure 4.19	:	Example of BTA 5 from Outcrop A from plan view. The strata within BTA 5 is folded and there are deformed structures and siderite clasts. Red arrow is showing the younging direction.	103
Figure 4.20	:	Example of mud-dominated succession from outcrop A, Early Miocene Temburong Formation, Kampung Bebuloh, Labuan. Note that red lines represent faults.....	104
Figure 4.21	:	Detailed sedimentary logging for outcrop A. Total thickness logged is 47.21 m. Scale is in metre.....	105
Figure 4.22	:	Detailed sedimentary logging for outcrop B. Total thickness logged is 54.22 m. Scale is in metre.	108
Figure 5.1	:	Bioturbation observed on the sole of BT1. De = <i>Desmograption</i> , He = <i>Helminthopsis</i> , Pa = <i>Paleodictyon</i> , Op = <i>Ophiomorpha</i>	113
Figure 5.2	:	Examples of <i>Cosmorhaphie</i> . (A-B) <i>C. sinuous</i> displaying a random, complex meandering pattern. (C-D) <i>C. lobata</i> displaying 2-order meanders.	114
Figure 5.3	:	Examples of <i>Desmograption</i> in study area.	115
Figure 5.4	:	Examples of <i>Helminthopsis</i> in the study area. Note the difference in the meandering shapes. (A) <i>H. abeli</i> . (B) <i>H. tenuis</i>	116
Figure 5.5	:	Example of <i>Megagraption</i> in the study area. The arrow is showing single-connected network. The angle of branching is approximately at right angle.	117
Figure 5.6	:	Examples of <i>Nereites</i> in the study area. (A) Endichnial trace of <i>Nereites</i> . Presence of lighter halo around the dark coloured burrow. No 'bulging' appearance indicates that this is not a mud/carbonaceous clast. (B) Intensely bioturbated fabric (white box) due to the <i>Nereites</i> . Arrow is showing possible ? <i>Halopoa</i> burrow. (C) The bottom part of the bed has moderate bioturbated fabric due to <i>Nereites</i> . Co-occurred together with dwelling traces, which could be ? <i>Halopoa</i> . (D) is showing a close-up photo of the bioturbated fabric, where a complex muddy core (C) surrounded by sandy mantle (M) can be observed. (E) Bioturbated fabric within BT2 due to the colonization of <i>Nereites</i> and ? <i>Phycosiphoniform</i> . Co-occurred together with the ? <i>Ophiomorpha</i> burrow. (F) Epichnial trace of <i>N. Irregularis</i> , displaying irregular meandering pattern.	119
Figure 5.7	:	Examples of <i>Ophiomorpha</i> in the study area. (A – B) <i>O. annulata</i> , preserved as hypichnial furrow on the soles of BT1. Arrow in (B) is showing swelling at the sharp branching. (C – D) <i>Ophiomorpha</i> preserved as endichnial burrows.....	122

Figure 5.8	:	Examples of Palaeophycus traces in the study area. (A) Palaeophycus displaying slightly curve burrows. (B) Simple, straight, unbranched Palaeophycus burrows.	123
Figure 5.9	:	<i>Paleodictyon</i> ichnospecies observed at the base of BT1: (A) <i>P. latum</i> with mesh-size around 1 to 2 mm; (B) <i>P. miocenicum</i> with mesh-size around 4 mm; (C, D) <i>P. majus</i> with a mesh-size of 6 to 8 mm.	125
Figure 5.10	:	(A) <i>Scolicia prisca</i> observed on the top of BT1. (B) <i>Scolicia</i> preserved as endichnial traces on the vertical cross-section. Often observed at the top interval, within F3 or F4.....	126
Figure 5.11	:	Examples of <i>Protovirgularia</i> in the Early Miocene Temburong Formation, Kg, Bebuloh, Labuan.....	127
Figure 5.12	:	Examples of <i>Tubutomaculum</i> trace fossil.....	128
Figure 5.13	:	(A-B) Possible ? <i>Zoophycos</i> , based on its spreite structures with U-shaped protrusive burrows. Both traces were observed on the top of BT1. (C) Unknown, full-relief, sideritized burrow found within BT3. (D) Possible endichnial ? <i>Halopoa</i> burrows, often associated with <i>Nereites</i> and bioturbated fabric. (E) ? <i>Bergaueria</i> on the sole of BT1 (F) <i>Spirophycus</i> found on the sole of thin-bedded sandstone.....	129
Figure 5.14	:	Trace fossils distribution across all bed type associations in the Early Miocene Temburong Formation, Labuan.....	131
Figure 5.15	:	Distribution of ethological classification from the measured sections in the Early Miocene Temburong Formation, Kampung Bebuloh, Labuan.....	133
Figure 6.1	:	Decision tree diagram showing the criteria of levee deposits vs. lobe fringe deposits observed in the study area. Yellow box indicate the similarities between these two sub-environments, green box indicate characteristics that were observed in this study, while red box indicate characteristic that were not observed in this study.....	143
Figure 6.2	:	(A) Simplified plan view of a lobe, showing the distribution of lobe sub-environments and example logs for each sub-environment. (B) Turbidite lobe depositional model for the Early Miocene Temburong Formation at Kampung Bebuloh. The Temburong Formation at Kampung Bebuloh is interpreted as turbidite deposition at the fringes of lobe complexes (area marked by the red line). Both diagrams were modified from Spsychala et. al. (2017).....	147
Figure 6.3	:	Regional paleogeographic reconstruction for Early Miocene (~20 – 17 Ma, Burdigalian) proposed by Burley et. al. (2020) based on the on the tuff U-Pb dating results and previous literature reviews. The map is showing few palaeo-drainages from central Borneo supplying sediments for the Temburong Formation. Map is modified from Burley et. al. (2020). PCSC = proto South China Sea.....	149

LIST OF TABLES

Table 2.1	:	Lithostratigraphic schemes for Labuan Island as proposed by various authors. Note that in Wan Hasiah et. al. (2013), the unconformity (MMU/DRU) is not recognised in their study, but instead has been interpreted as a localised erosive surface of possibly a high energy short-lived event that formed the basal conglomerate and considered it to represent an intraformational unconformity. Abbreviations: Fm = Formation, DRU = Deep Regional Unconformity, MMU = Middle Miocene Unconformity, WCF = West Crocker Formation, TCU = Top Crocker Unconformity, BMU = Basal Miocene Unconformity. Modified from Wan Hasiah et. al. (2013)	19
Table 2.2	:	Sedimentary facies and depositional environment of Temburong Formation in Labuan and NW Sabah as discussed by various authors.....	20
Table 3.1	:	Summary of classification schemes from Mutti (1992).....	40
Table 3.2	:	Summary of HEBs type by Fonnesu et. al. (2017).....	44
Table 3.3	:	Definition and schematic cross sections of the common mass-transport deposits. Note that these processes form a continuum from very slow-moving creep (cm/yr) to very fast-moving debris flows (m/s). Taken from Posamentier and Martinsen (2010) and the citations herein.....	46
Table 3.4	:	Summary of difference between the thin-bedded turbidites in channel-levee system.....	54
Table 3.5	:	Summary of differences between the lateral and frontal lobe fringe.....	56
Table 4.1	:	Summary of the facies identified in the studied sections of the Early Miocene Temburong Formation, Labuan.....	57
Table 4.2	:	Summary of the statistical data for bed type distribution in the Early Miocene Temburong Formation, Labuan.....	68
Table 4.3	:	Summary of statistical data of bed type association.....	90
Table 5.1	:	List of ichnogenera and ichnospecies identified in the Temburong Formation, Kampung Bebuloh. Ethology classification is mainly taken from previous work, especially from Uchman (1998). Rare occurrence is defined by <5 traces observed.....	112
Table 5.2	:	Characteristics of sub-ichnofacies of Nereites ichnofacies based on Heard and Pickering (2008) and Cumming and Hodgson (2011).....	132

LIST OF ABBREVIATION

ca.	:	circa (approximately)
cm	:	centimeter
dm	:	decimeter
m	:	meter
Ma	:	mega annum (one-million years)
mm	:	millimeter

Universiti Malaya

CHAPTER 1: INTRODUCTION

1.1 OVERVIEW

Deep marine sandstones are important hydrocarbon reservoirs throughout the world, including in offshore NW Borneo. As oil fields mature and the easier reservoir targets are fully exploited, hydrocarbon exploration and production tends to shift toward more challenging reservoirs, including thin-bedded sandstones such as those observed in deep marine turbidite successions preserved offshore NW Borneo. However, optimal management and exploitation of such reservoirs require a good understanding of how the thin sandstone beds are arranged and connected to each other. Geophysical techniques such as well logging and seismic imaging are useful but insufficient in constructing depositional models for thin-bedded turbidite successions, because the individual layers of the reservoir are typically cm- to dm-thick, which is below the resolution of such techniques. Outcrop analogues, i.e., onshore exposures of sedimentary strata provide a detailed glimpse of the bed-scale features of the subsurface reservoir, including good 2- to 3-dimensional information regarding lateral extent and geometry of similar reservoir sandbodies. The Early Miocene Temburong Formation exposed in Labuan and Sabah is a good analogue for the deep marine hydrocarbon reservoirs of offshore NW Borneo. However, no detailed facies and bed-type analysis of the unit has been conducted previously. Recent quarrying activity at Kampung Bebuloh in the southern part of Labuan has exposed a more than 100 m thick succession of the unit. This has provided an opportunity to conduct a detailed sedimentological study for a better understanding of the Temburong Formation.

Previous sedimentological studies conducted on the Temburong Formation at Kampung Bebuloh interpreted a slope to deep marine depositional setting. Thin-bedded turbidites, with incomplete Bouma sequences, is the dominant facies, and are found intercalated with thick mudstone and slump intervals. However, there is still uncertainty regarding the large-scale geometry and nature of the Kampung Bebuloh succession, in particular, whether the thin-bedded strata represent channel-associated levee deposits or lobe / fan fringe deposits. This has important implications for the characterization of deepwater hydrocarbon reservoirs, as different types of turbidite sandbodies will have different reservoir properties, sandbody geometries and distributions. The identification of geological criteria for the differentiation between lobe- and channel-associated thin beds will be very useful in deepwater hydrocarbon exploration and field development. This project proposes to resolve this uncertainty in interpretation using a combination of facies and bed type analysis, as well as ichnology.

1.2 OBJECTIVES

The main aim for this study is to produce a detailed facies description and interpretation of the depositional setting of the Early Miocene Temburong Formation on Labuan Island, NW Borneo. This study is conducted with the following objectives:

- i. To describe and interpret the sedimentary facies of the Early Miocene Temburong Formation at Kampung Bebuloh, Labuan.
- ii. To describe the trace fossil assemblages present in the beds of the Early Miocene Temburong Formation at Kampung Bebuloh, Labuan.
- iii. To construct a depositional model for the Early Miocene Temburong Formation on Labuan, based on an integrated analysis of the sedimentary facies and ichnology.
- iv. To document the dimensions, geometry and stratal arrangement of thin-bedded turbidites of the Early Miocene Temburong Formation at Kampung Bebuloh, Labuan.

1.3 STUDY AREA

The study area is an abandoned quarry located at Kampung Bebuloh, along the Jalan Bebuloh Road, in the southern region of Labuan island (latitude 5°16'45.43" N and longitude 115°11'23.13" E). Labuan island is located 15 km off the south-western coast of Sabah, NW Borneo. The study area (**Figure 1.1**) is relatively wide (around 60,000 m²) and exposes a thick succession of steeply dipping (70 ° – 80°), thin-bedded turbidites of the Early Miocene Temburong Formation.. Recent housing development area has exposed 2 fresh outcrops (referred to as outcrop A and B) which preserve exquisite sedimentary features and trace fossils, hence providing the opportunity to conduct detailed sedimentary logging. Strata of both outcrops A and B dip steeply (70 ° – 80°) towards the NE, with a younging direction towards SE. The geology of the study area will be discussed in the next chapter.



Figure 1.1 (A) Map of Labuan Island. Red rectangle is the location of the study area. (B) Two outcrops were chosen for this study. (C) Outcrop A. Younging direction is towards SE. (D) Outcrop B. Younging direction is towards SE.

1.4 METHODOLOGY

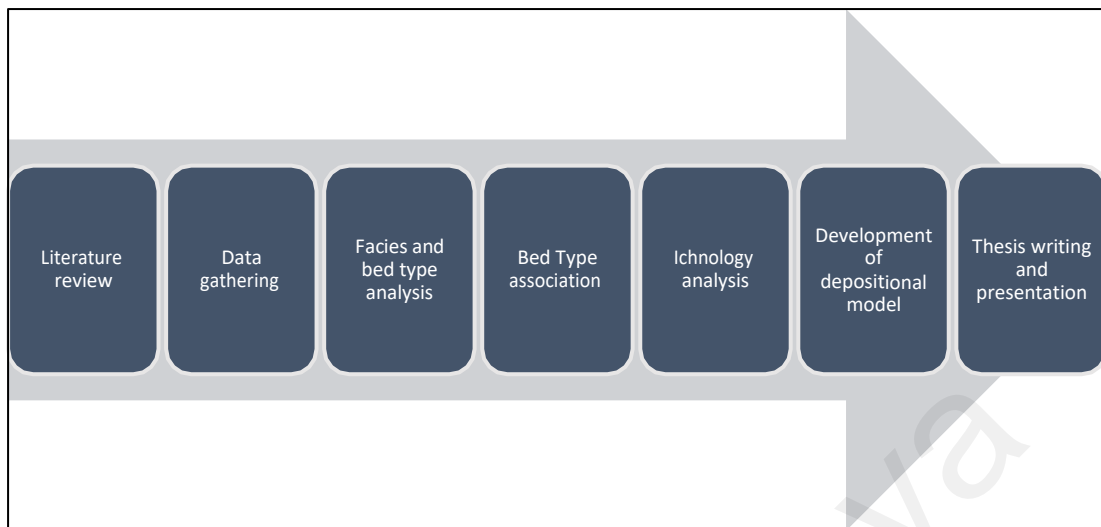


Figure 1.2 Study workflow.

A total of **756 beds** with a total thickness of **97.7 m** have been described and logged in this study. Two outcrops (A and B) in Kampung Bebuloh, Labuan were chosen for detailed sedimentological analysis. This study integrated facies and ichnological analyses in order to determine the sedimentary characteristics and interpret the depositional setting of the Temburong Formation in Kampung Bebuloh, Labuan. Facies in Temburong Formation are described and classified based on lithology, textural characteristics and sedimentary structures. Density flow classification schemes from several authors were used in this study to aid the facies classification (e.g., Talling et. al., 2012; Baas et. al., 2009; 2016; Haughton et. al., 2009; Lowe, 1982; Mulder and Alexander, 2001). Then, the assemblages of facies within individual beds are identified and described as bed types (BT), which are interpreted as indicative of specific depositional processes and flow types. Bed types will then be grouped together into larger-scale, repeatable vertical bed type trends, or bed type associations (BTA). Each bed type association must contain at least two bed types, and will be used to construct a depositional model for the Temburong Formation.

1.4.1 DATA GATHERING

Fieldwork was conducted for a total of 12 days during two separate trips to collect data and samples. As the exposures are dominated by thin-bedded strata, the outcrops were separately logged in centimetres with scale of 1:10 using a Jacob's staff with attached compass-clinometer for more accurate bed strike and dip measurement. The focus was on collection of data on bed thickness, grain size, sedimentary structures and trace fossils. Grain size was assessed visually in the field with the use of a grain size comparator chart and hand lens. Field and aerial drone photographs, and sketches were also used to complement the sedimentary log descriptions.

1.4.2 FACIES AND BED TYPE ANALYSIS

This study uses a sedimentological analysis approach to describe the characteristics of facies, bed type and bed type association. Each identified facies are used to interpret and understand the depositional process. Bed types, which comprise an assemblage of facies, are used to interpret depositional events and flow evolution, while bed type associations are used to interpret depositional elements and depositional environments.

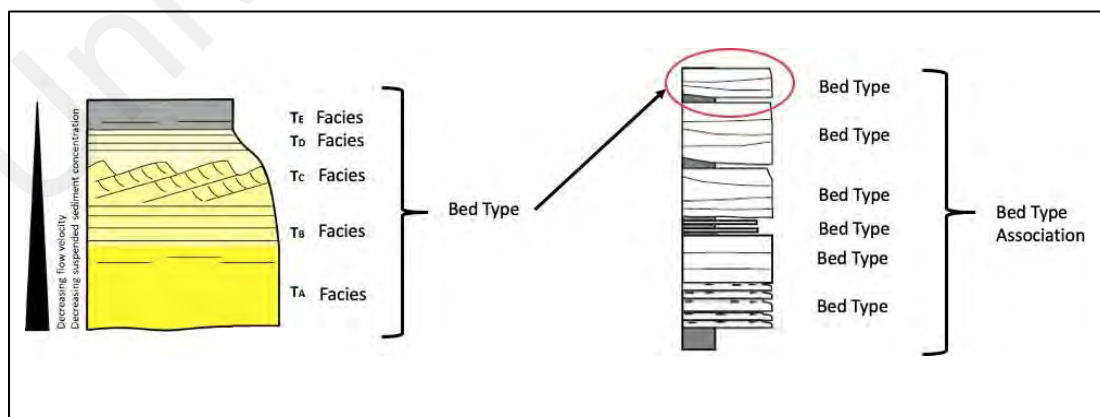


Figure 1.3 Bed type consists of an assemblage of facies within a single bed. Assemblages of bed types with a repeating vertical pattern are grouped into Bed Type Associations.

BED TYPES

This study adopts a bed type method for facies analysis (see Talling et. al., 2007; Mueller et. al., 2017; Kuswandaru et. al., 2019; Mansor and Amir Hassan, 2021). Merely describing facies does not work well with turbidites as individual gravity flow event beds can be composed of multiple facies, and each facies tends to be thin (i.e., cm- or dm-scale).

Bed type analysis is more systematic when describing facies in gravity flow beds as it allows interpretation of flow evolution through time. Below is the method for bed type analysis:

- i. Identify each facies within individual beds. Make observation of each facies characteristics such as thickness, colour, grain size, sediment textures, diagenetic features and presence of trace fossils in the outcrop. Deduce the processes responsible for each facies. Several density flow classification schemes were used to aid the facies classification (see Chapter 3).
- ii. Beds with similar facies composition and arrangement are classified together as a “Bed Type”. Beds are defined as conformable, genetically-related sequences of facies which are bounded by sharp erosional surfaces, and represent specific depositional processes and flow types.
- iii. Assemblages of bed types with a repeating vertical patterns are classified into “Bed Type Associations”. Each bed type association must contain at least two bed types, and it is an indicative of a specific depositional environment (i.e., lobe fringe, outer levee, depositional terrace)

1.4.3 ICHNOLOGICAL ANALYSIS

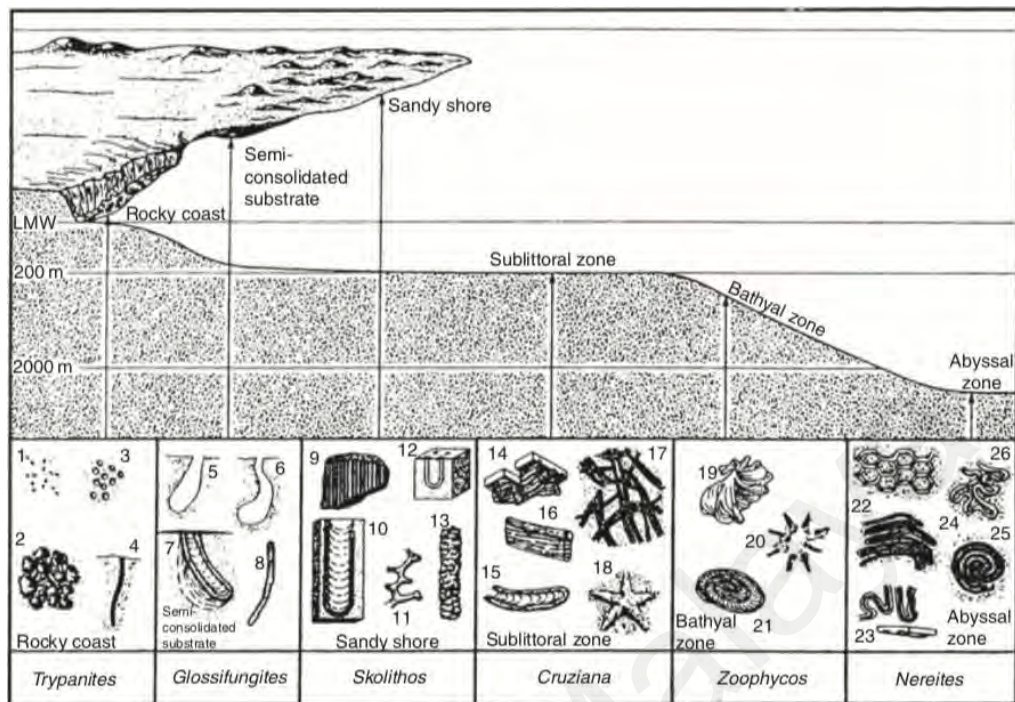


Figure 1.4 Schematic representation of the relationship between trace fossil assemblages, sedimentary facies and depth zones in the ocean. Taken from Seilacher (2007).

Ichnology is the study of trace fossils, which preserve the activity of animals as recorded by their tracks, trails, burrows and borings. These traces can be used to provide information about an animal's behaviour in response to its environment, as they are almost always found *in situ* and commonly specific to a particular suite of environmental conditions (McIlroy, 2004).

An increasing number of workers have started to place ichnological observation within a detailed turbidite facies architectural context as this data can aid to construct more detailed deep marine depositional models (e.g., Heard and Pickering, 2008; Monaco et. al., 2010; Cumming and Hodgson, 2011; Callow et. al., 2012). For example, ichnological analysis has helped to distinguish between proximal (coarse-grained) and distal (fine-grained) turbidites on broad spatial scales. This has shown that the distribution of trace fossils in deep water settings is strongly facies controlled.

METHODOLOGY

Visible trace fossils in the Kampung Bebuloh section were analysed on well-exposed bedding planes. The data were then recorded on sedimentary logs and the Excel spreadsheet for statistical analysis. Trace fossils were analysed on ~22% of all bedding planes (including bed soles and top), and some on the vertical cross sections. The potential diversity of burrow mottling in mudstone facies (BT3 and BT4) were not fully captured in this study as it was difficult to discern due to strong weathering.

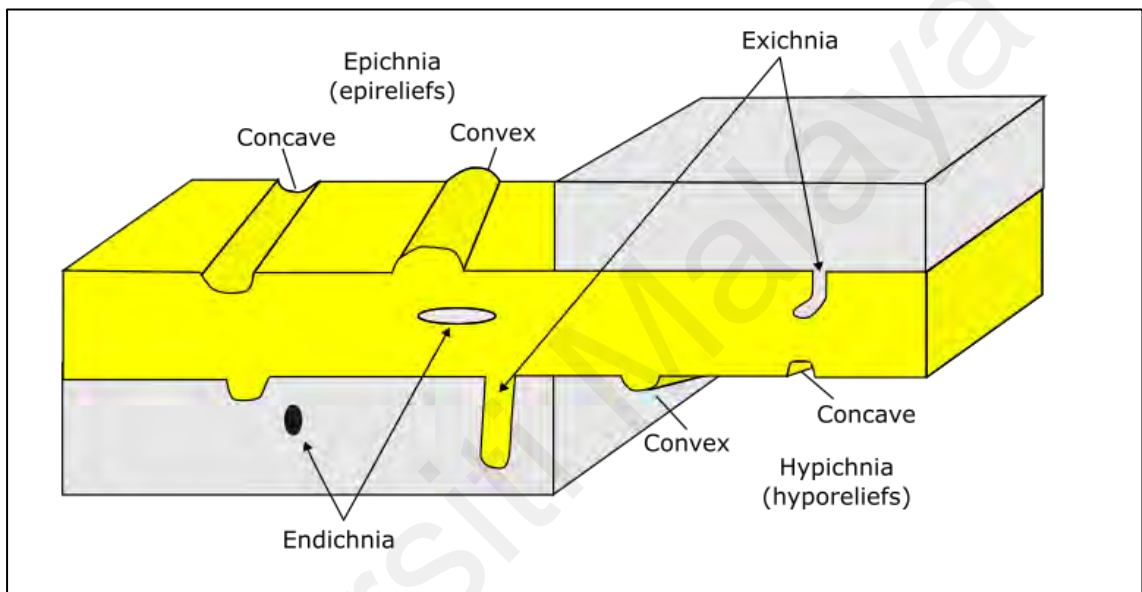


Figure 1.5 Taphonomic classification system used in this study (after Martinsson, 1970, redrawn from Cumming and Hodgson, 2011).

The morphology of the trace fossils were described and their taphonomy (mode of preservation) was recorded using Martinsson's (1970) classification (**Figure 1.5**). The trace fossils were later identified to ichnospecies level using Uchman's (1998) taxonomic classification system and Fan's et. al. (2018) topological characteristics for graphoglytid trace fossils. Even so, most of the endichnial trace fossils were only identified at the ichnogeneric level due to the difficulties in comparing and identifying ichnospecies in vertical cross-section. This is because there is a lack of well-defined representation of normal ichnospecies taxobases in vertical cross-sections from the literature (see Callow and McIlroy, 2011).

Each identified ichnogenus or ichnospecies will then be classified based on their behaviour (ethology) to further understand the significance of these traces to the environment of deposition (**Figure 1.6**). The interpretation of ethology is mostly taken from published work (e.g., Uchman, 1998; Buano and Mangano, 2011, Knaust, 2017). However, the bioturbation intensity of each bed was not recorded and calculated for this study due to constraint of data.

The trace fossil analysis was then combined with the bed type analysis to aid in constructing a depositional model for the Early Miocene Temburong Formation at Kampung Bebuloh, Labuan.










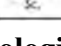

Ethology	Description	Typical genera	Legend:
Agrichnia	Microbial farming/ gardening traces	 Pa.  Me.  Sp.	Agrichnia Pa=Paleodictyon Me = Megagraption Sp = Spirorhaphe.
Chemichnia	Chemosymbiotic feeding traces	 Ch.	Chemichnia Ch = Chondrites
Cubichnia	Resting traces	 Ca.  Be.	Cubichnia Ca = Cardioichnus Be = Bergaueria.
Domichnia	Dwelling traces	 Oph.	Domichnia Oph = Ophiomorpha
Fodinichnia	Feeding traces	 Th.  Zoo.	Fodinichnia Th = Thalassinoides Zoo=Zoophycos.
Pascichnia	Grazing traces	 Sc.  Ne.	Pascichnia Sc=Scolicia Ne=Nereites.

Figure 1.6 List of discussed ethological classification and typical ichnogenera assigned to these ethologies. Taken from Cumming and Hodgson (2011).

CHAPTER 2: GEOLOGICAL SETTING

2.1 OVERVIEW

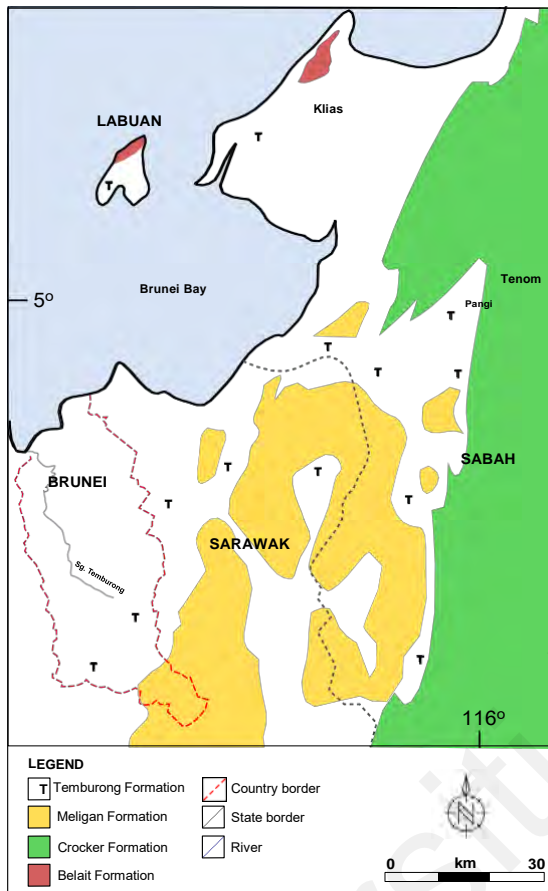


Figure 2.1 Distribution of the Temburong Formation across Sabah and Labuan Island. Map redrawn from Lunt (2022).

The Temburong Formation consists of steeply dipping, thin- to medium-bedded sandstone-mudstone alternations, with evidence of deformation, and interpreted as deep marine turbidites (Brondjik, 1962b; Wilson and Wong, 1964; Hennig-Brietfield et. al., 2019). It extends northwards from the Sarawak border to southwest Sabah, mainly exposed in Sipitang, Tenom, Padas Valley, and Klias Peninsula area, and also in the southwest of Labuan island (**Figure 2.1**). The part of this formation exposed on Labuan is considered as the correlative deep-marine facies of the Early Miocene Setap Shale and Nyalau formations in Sarawak, and may represent the earliest deposits of the Sabah Basin (Cullen, 2010).

2.2 REGIONAL TECTONIC SETTING

Labuan is located within the Inboard Belt province of the NW Sabah continental margin (**Figure 2.2**). This province is characterised by narrow NNE-SSW trending anticlines with steep flanks and strongly faulted crests separated by wide synclines (Bol and van Hoorn, 1980; Madon, 1999b; Hutchison, 2005; Hazebroek and Tan, 1993). Labuan Island is the geomorphological expression of one of these narrow anticlines that strikes along the centre of the island. Structurally, the Temburong Formation in Kampung Bebuloh is located on the steeply dipping (up to 80°) south-eastern limb of this anticline.

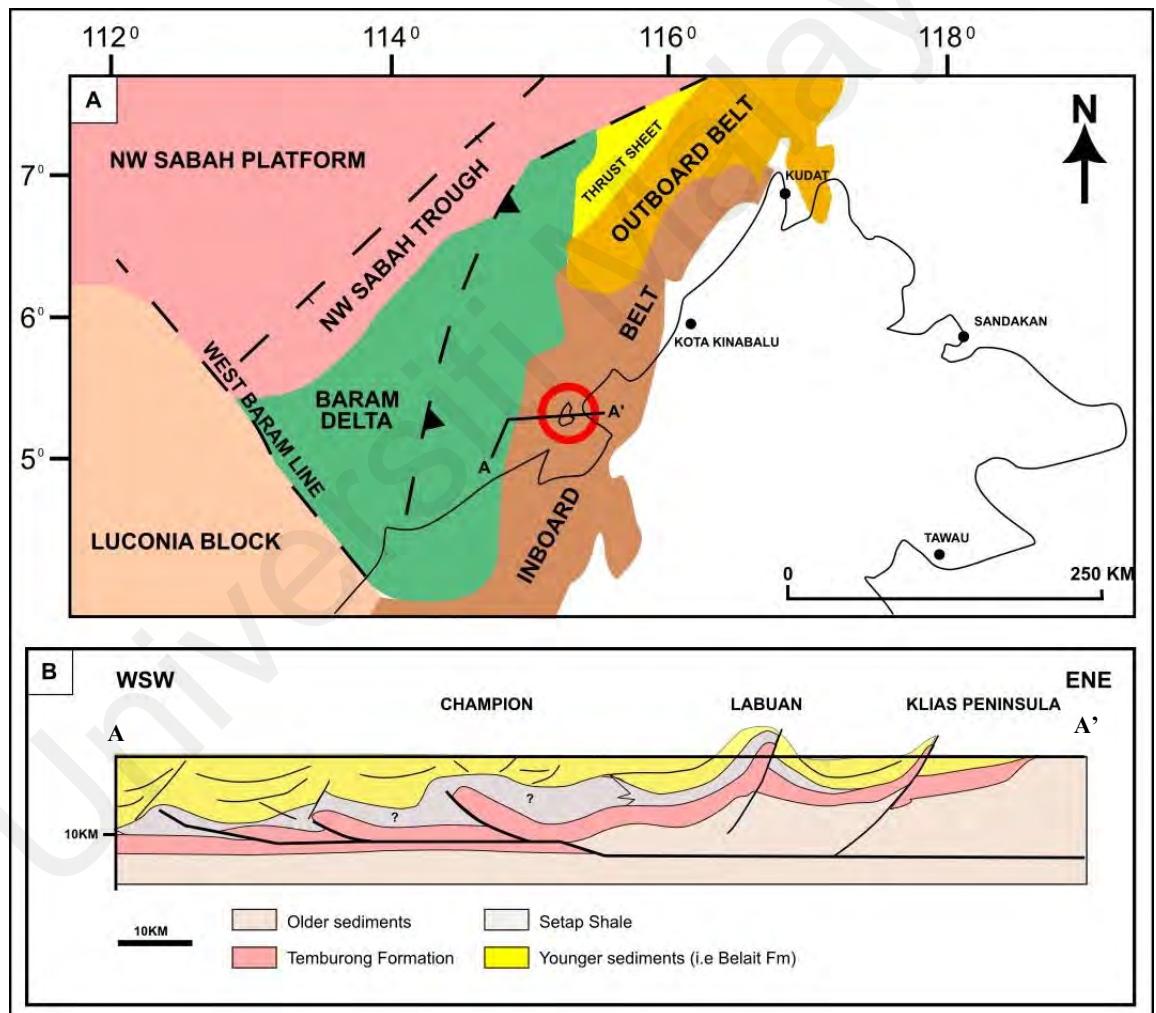


Figure 2.2 (A) Tectono-stratigraphic provinces of NW Sabah. Red circle is the location of Labuan island, which is located within the Inboard Belt structural zone of the NW Borneo continental margin. Redrawn from Hazebroek and Tan (1993). (B) E–W regional cross section showing an E–W fold and thrust belt underlying the Temburong, Setap Shale and younger deltaic sediments. Modified from Morley et. al. (2008).

The Inboard belt province was subjected to a strong compressional event in response to collision between the Reed Bank-Dangerous Grounds continental fragment and North West Borneo (Hutchinson, 2005; Madon, 1999b). It was initiated in the Late Oligocene but was continuously active through to the Middle Miocene. This event was associated with Late Eocene to Early Miocene regional extension which resulted subsequently in seafloor spreading in the South China Sea (Cullen, 2010). Deepwater sedimentation occurred in the basin during the Oligocene – Early Miocene, preserved today as the West Crocker and Temburong formations, as well as age-equivalent Stage III deposits in the present day offshore (Taylor and Hayes, 1980).

Deepwater sedimentation in NW Sabah is interpreted to have continued until the early Miocene, and completely ceased when the Dangerous Grounds collided with Borneo, marking the end of subduction and closure of Proto-South China Sea (PSCS) (Hutchison et al., 2000; Balaguru and Lukie, 2012; Hall, 2013; Burley et. al., 2020). This event is referred as the Sabah Orogeny by Hutchison (1996), where much of Sabah was uplifted and deformed, and produced a major regional unconformity. Some authors call this unconformity the Base Miocene Unconformity (BMU) (e.g., Jackson et. al., 2009; Balaguru and Lukie, 2012), while some call it the Top Crocker Unconformity (TCU) (e.g., van Hattum et. al., 2006; Hall, 2013, Hennig Brietfield et. al., 2019; Burley et. al., 2020). Hall (2013) interpreted the age of the TCU as between 19-20 Ma, older than the well-known Deep Regional Unconformity (DRU) in offshore Sabah (Bol and van Hoorn, 1980; Levell, 1987) and its approximate equivalent, the Middle Miocene Unconformity (MMU), in offshore Sarawak (Madon, 1999a).

The TCU is considered as one of the major tectonic events in NW Sabah as it marks abrupt change in depositional environment from deep-marine turbidites of the Temburong Formation to a shallow deltaic setting of the Lower Belait Formation on Labuan Island (The Lower Belait is sometimes referred in older literature as the Setap Shale, see Brondijk, 1962; Balaguru and Lukie, 2012, but has also been referred to as the Layang-Layangan Beds, see Lee, 1977).

Universiti Malaysia

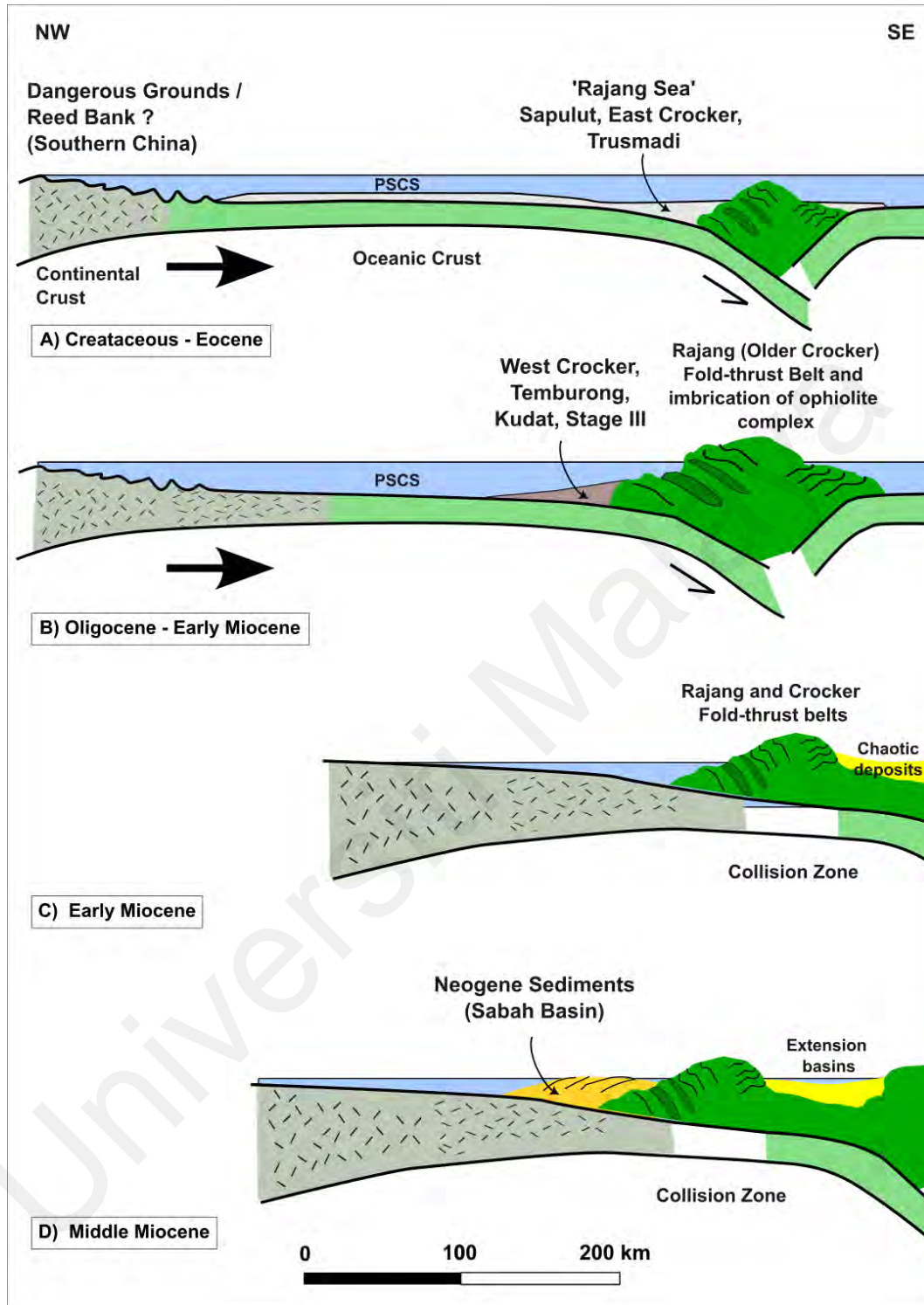


Figure 2.3 Schematic diagram of NW-SE sequential cross sections across NW Sabah. (A-B) Rifted continental crust due to the sea-floor spreading of South China Sea was moving towards NW Borneo. Deep water deposition occurred at the same time as SE-ward subduction of an ocean basin beneath NW Borneo margin. (C-D) Subduction ceased when the rifted continental crust collided with NW Borneo. Consequently, a major accretionary prism known as the West Crocker Group formed along the compressional zones. Modified from Tongkul, 1991.

2.3 LOCAL STRATIGRAPHIC FRAMEWORK

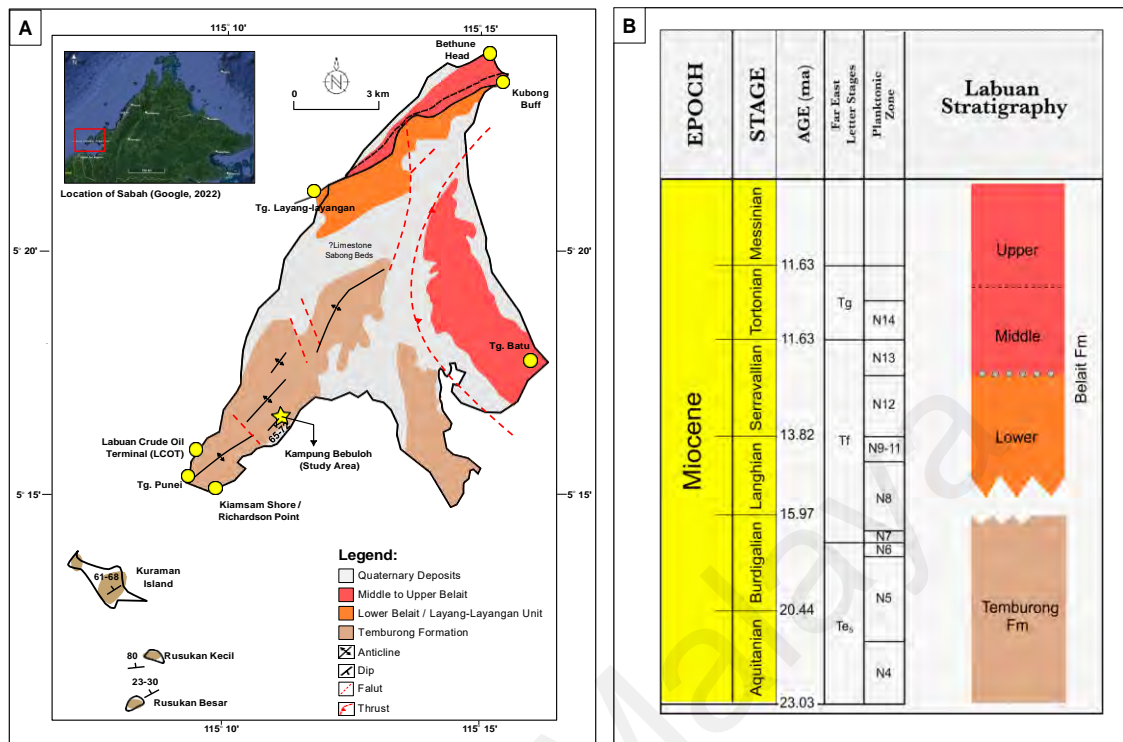


Figure 2.4 (A) Geological map of Labuan Island. Redrawn and modified based on Wilson and Wong (1964) and Som et. al. (2011) for the northern part of Labuan. Wilson and Wong (1964) reported the presence of Sabong Beds, mainly consisting of limestone, which they included in Temburong Formation but there is no recent study on the presence of this unit. (B) Stratigraphic chart of Labuan Island. Modified from Hennig-Briefeld et. al. (2019).

The stratigraphy of Labuan is somewhat controversial and has been debated by many authors (e.g., Liechti et. al., 1960; Wilson and Wong, 1964; Lee, 1977, Madon, 1994; Balaguru and Lukie, 2012; Wan Hasiah et. al, 2013; Hennig-Briefeld et. al., 2019, Burley et. al., 2020; **Table 2.1**). Labuan is mainly underlain by sedimentary rocks and the strata can be divided into two major groups (Levell, 1987; Madon, 1997; Wan Hasiah et. al., 2013); an older deep-marine succession which is commonly accepted to be made up of the Temburong Formation and West Crocker Formation, and a younger unit consisting of the Belait Formation.

One of the earliest works on the stratigraphy of Labuan is by Wilson and Wong (1964) who identified three rock units: Temburong Formation, Setap Shale Formation, and Belait Formation. They assigned the southwest of Labuan to the Temburong/Crocker Formation, while the Northern and Eastern part of Labuan as Belait Formation. Though they did not map the contact between Setap Shale and Temburong Formation due to poor exposure, they implied the weathered mudstone of Setap Shale Formation was observed below the Belait Formation outcrop nearby the Layang-layangan Road. Most authors supported this stratigraphic scheme, though Madon (1994) and Henning-Brietfield et. al. (2019) believed that the Setap Shale Formation is absent on Labuan Island.

Contrary to Madon (1994; 1997), Balaguru and Lukie (2012) believe that the Temburong Formation is absent in Labuan. They consider the strata below the conglomeratic ridge of Belait Formation at Tanjung Layang-layangan as equivalent to the Early Miocene Stage III Meligan and Setap Shale Formations, which underlie the mainland of NW Borneo. The conglomeratic sandstone at the base of the Belait Formation reflects Stage IVA lowstand fluvial deposits cutting into the underlying Stage III Setap/Meligan formation. They interpret the sequence of deep water turbidites and debrites observed in the southwestern part of Labuan as the distal expression of the Meligan Delta System. Wan Hasiah et. al. (2013) who studied the geochemistry of coal-bearing strata in Labuan did not agree with Balaguru and Lukie (2012) as they did not recognise the Meligan Formation in their study, and interpreted the sand-rich sequences as the middle member of the fluvial-deltaic to intertidal facies of the Belait Formation. They also reassigned East Kiamsam of Lee (1977) as Setap Shale Formation based on similar Vitrinite reflectance values with other Setap Shale exposures on the island.

Table 2.1 Lithostratigraphic schemes for Labuan Island as proposed by various authors. Note that in Wan Hasiah et. al. (2013), the unconformity (MMU/DRU) is not recognised in their study, but instead has been interpreted as a localised erosive surface of possibly a high energy short-lived event that formed the basal conglomerate and considered it to represent an intraformational unconformity. Abbreviations: Fm = Formation, DRU = Deep Regional Unconformity, MMU = Middle Miocene Unconformity, WCF = West Crocker Formation, TCU = Top Crocker Unconformity, BMU = Basal Miocene Unconformity. Modified from Wan Hasiah et. al. (2013)

Age	Geological age		Wilson (1964)	Lee (1977)	Mazlan (1994)	Cullen (2010)	Balaguru & Lukie (2012)	Wan Hasiah et. al. (2013)	Hennig-Brietfeld (2019)
5.3	Miocene	Late	Belait Fm	Belait Fm	Belait Fm	Belait Fm	Belait Fm	Upper Belait Fm	Belait Formation
11.6		Middle				Setap Fm		Middle Belait Fm	
16.0		Early	Setap Shale Fm	Layang - Layangan Unit	Layang - Layangan Unit	DRU Tmb Fm Meligan Fm	DRU / MMU	Lower Belait	Lower Belait
23.0	Oligocene		? ? ?			?BMU			
		Late		Setap Shale Fm	Temburong Fm	Temburong (Tmb) Fm	Setap / Meligan Fm	Setap Shale Fm Temburong Fm	Temburong Fm
28.1		Early	Temburong Fm	Temburong Fm					
33.9								WCF	West Crocker Fm

Table 2.2 Sedimentary facies and depositional environment of Temburong Formation in Labuan and NW Sabah as discussed by various authors.

Authors, Year	Location	Type of Analysis	Observation	Depositional Environment	Age
Madon (1994, 1997)	Tg. Layang-Layangan	Sedimentology	Hummocky cross-stratification (HCS) intercalated with mudstone	Deposition under a regressive environment in a shelfal regime (prodelta environment passing upwards into shallower marine)	N/A
Jackson & Johnson (2009)	Southwest of Tg. Kiamsam, SW of Labuan	Sedimentology	Presence of both debrites and turbidite facies	Lower-slope to proximal basin floor setting	Early Miocene
Asis et. al. (2015)	Tenom area, Sabah	Biostratigraphy (Planktic foraminifera)	2 biozones: <ul style="list-style-type: none"> <i>Globorotalia ciperoensis</i> Zone (P22) of Chattian age <i>Catapsydrax dissimilis</i>-<i>Preaorbulina sicana</i> Zone (N7) of late Burdigalian 	Distal part of a deep sea on a basin plain	Late Oligocene (Chattian) - Late Early Miocene (Burdigalian)
Bakar et. al. (2017)	Kg. Bebuloh, Labuan	Biostratigraphy (Benthic foraminiferal)	Presence of deep-marine agglutinated foraminifers assemblages (i.e <i>Bolivina</i> sp., <i>Ammosphaeroidina</i> sp.)	Bathyal to abyssal	N/A
Asis et. al (2018)	Menumbok, Klias Peninsula, Sabah	Biostratigraphy (Planktic foraminifera)	2 biozones: <ul style="list-style-type: none"> <i>Globigerinoides primordius</i> Zone (N4 zone) <i>Globoquadrina dehiscens</i> - <i>Globoquadrina praedehiscens</i> Zone (N5 zone) 	Distal part of deep-sea fan	Late upper Oligocene to lower Miocene
Jasin & Firdaus (2019)	Kg. Bebuloh, Labuan & Klias, Sabah	Ichnology	2 sub-ichnofacies of <i>Nereites</i> : <ul style="list-style-type: none"> <i>Paleodictyon</i> sub-ichnofacies in Kg. Bebuloh indicate distal lobe <i>Ophiomorpha rudis</i> subichnofacies in Klias indicate channels or proximal lobes	Submarine fan, from proximal lobes/channels to distal lobe	N/A
Burley et. al. (2020)	Southern Labuan, including 3 islands	Sedimentology, biostratigraphy & mineralogy (XRF, XRD)	<ul style="list-style-type: none"> Presences of MTDs and turbidites 	Slope setting, from slope channels to distal lobe or low relief levees adjacent to deep water turbidite feeder channels.	Early Miocene (19-20 ma, Burdigalian), based on foraminifera, nannofossils and zircon dating

2.3.1 TEMBURONG FORMATION

DEFINITION OF THE TEMBURONG FORMATION

The term Setap Shale Formation was used by Liechti et. al. (1960) to generally refer to all argillaceous successions underlying the Belait, Miri and Lambir Formations, but overlying the Belaga, Mulu and Kelalan Formation in NW Borneo. However, Brondjik (1962a) observed a difference in structural fold style within this unit in north Sarawak (Tate, 1994). He proposed that the Setap Shale Formation should be restricted to the dominant argillaceous rocks occurring above Te₅ unconformity, and introduced the name Temburong Formation for the highly folded rocks occurring below the unconformity. The type locality of Temburong Formation is at the headwaters of Temburong River in Brunei where the formation was described as a monotonous series of black and dark grey shale, usually having a satin sheen on fractured surfaces, with sandstones and quartzite occurring in stringers, lenses and continuous bands (Wilson and Wong, 1964). This formation was interpreted as the deposits of a deepwater, marine environment based on the presence of planktonic foraminifera and occurrence of turbidites (Brondjik, 1962b; Tate, 1994).

TEMBURONG FORMATION IN LABUAN

There is still a disagreements regarding the stratigraphic nomenclature for Labuan, which is mainly due to historical lithostratigraphic assignment and more recent information on the biostratigraphy and chronostratigraphy of the unit. The same stratigraphic nomenclature described in the previous has also been used on Labuan, with the Temburong Formation referring to the thick argillaceous, deep marine succession underlying the Belait Formation (e.g., Brondjik, 1962b; Jackson and Johnson, 2009). The unit underlies a large area of southern Labuan. Several authors consider the Temburong Formation as the distal, muddier equivalent of the West Crocker Formation in Sabah,

which is also dominated by turbidites (Zakaria et. al., 2013; Jamil et. al., 2020). However, Hutchison (2005) lumps the Temburong Formation in Labuan into the West Crocker Formation in Sabah, with both units merely representing lateral variations in facies. There is some justification to this assignment, given that there are sandier turbidite successions in southwestern of Labuan i.e., at Tanjung Punei, which Wilson and Wong (1964) originally referred to as West Crocker Formation. Wan Hasiah et. al. (2013) also agreed that the sandier unit in Tanjung Punei is a part of the West Crocker Formation based on its similarity in vitrinite reflectance to well-establish West Crocker Formation exposed in mainland Sabah.

Despite this, it should be noted that some workers still prefer to use the term Setap Shale Formation for this unit (e.g., Tongkul, 2001). Biostratigraphic and radiometric work on the unit indicates an Early Miocene age, which is equivalent to the Setap Shale Formation of NW Borneo, thus providing justification for maintaining usage of the term Setap Shale Formation here (Burley et. al., 2020). In this scheme, the turbiditic succession of southern Labuan, encompassing the studied area at Kampung Bebuloh, will be a sandier and more turbidite-dominated facies of the Setap Shale Formation.

A thorough re-assessment of the stratigraphy of Labuan is beyond the scope of this study. Therefore, for simplicity and complying to lithostratigraphy, I retain the usage of the term Temburong Formation here for the succession at Kampung Bebuloh, but add in the prefix “Early Miocene” at the front so that the age discrepancy with mainland Borneo Temburong Formation is recognized.

The Early Miocene Temburong Formation is the oldest rock formation in Labuan Island and consists mainly of deepwater argillaceous deposits, representing a shelf to basin slope environment (Brondijk, 1962b; Jackson and Johnson, 2009). This formation is mostly exposed at Tanjung Punei, coast near Labuan Crude Oil Terminal (LCOT), Kiamsam Shore / Richardson Point, and along Jalan Bebuloh. Jackson and Johnson (2009) conducted a detailed sedimentological analysis of the Early Miocene Temburong Formation around Tanjung Punei and recorded the presence of channelised turbidite sandstones on the top of slump-derived debrite deposits, in which they interpreted both debrites and turbidites deposited within a lower-slope to proximal basin floor succession. The presence of the debrites and widespread soft sediment deformation also suggested that there was active slope failure and contemporary periodic growth of the Labuan Anticline during deposition of the Temburong Formation (Madon, 1994; Jackson and Johnson, 2009).

Lee (1977) subdivided the Early Miocene Temburong Formation on Labuan into two units; (i) a Proximal Unit comprising thick, sandy and conglomeratic turbidites, debrites and slumps, exposed at the SW of Tanjung Kiamsam, and (ii) a Distal Unit comprising argillaceous succession of thin-bedded turbidites, exposed at South of Tanjung Kiamsam / Kiamsam Shore (nearby Richardson Point). The sand to mud ratio in this Distal Unit is around 60:40 and the bed thickness varies from less than 15 cm to 50 cm. Burley et. al. (2020) also identified a smectite-rich clay beds within a thick sequence of mudstones and siltstone beds exposed in Kiamsam Shore, which are interpreted as tuff deposits.

Burley et. al. (2020) also did a sedimentological analysis of the three islands located south from the main Labuan Island (Rusukan Besar, Rusukan Kecil and Kuraman). These three localities were dominated by thin-bedded, fine-grained sandstone beds, sometimes attaining medium-grain size, dominantly in the range of ca 5–20 cm thick, interbedded with mudstones which contain continuous bands and nodules of siderite.

Hutchinson (2005) reported the presence of limestone in Upper Sabong Formation, which is composed of nodular claystone with thin sandstone and some limestone layers at the centre of Labuan island, just below the Layang-layangan beds (refer Figure 130, pg. 353). Wilson and Wong (1964) includes it within the Temburong Formation, however no detailed sedimentological analysis has been conducted on this formation previously.

AGE AND DEPOSITIONAL ENVIRONMENT OF TEMBURONG FORMATION IN LABUAN

The age of Temburong Formation ranges from Oligocene to Early Miocene based on planktonic foraminifera and palynological data from NW Sabah and Labuan (Wilson and Wong, 1964, Jackson and Johnson, 2009; Asis et. al., 2015; 2018). Recent analysis of a tuff bed found in southern Labuan using detrital zircon U–Pb geochronology has confidently put the age of Temburong Formation in Labuan between 19 and 21 Ma (Early Miocene) (Burley et. al., 2020). The age indicates that deep water sedimentation in NW Borneo continued into the Burdigalian, suggesting the subduction trench of the Proto-South China Sea was active into the Early Miocene, beneath the depocentre of the Temburong turbidite fan. They also studied the mineralogy of the Temburong Formation sandstone, which yielded abundant Cretaceous-age zircons. This result indicates a switch in source provenance during the early Miocene since the Crocker Formation is mainly characterised by Permian-Triassic zircons. They concluded that the Temburong

Formation was sourced by reworking of the uplifted Rajang Group, Sapulut or Trusmadi formations, thus indicating the initial phase of uplift in the early Miocene before the onshore depositional system changed to shallow marine-fluvial deposition of the Belait Formation.

Benthic foraminifera assemblages from previous works (e.g., Wilson and Wong, 1964; Madon, 1997; Bakar et. al., 2017; Burley et. al., 2020) have established that the Temburong Formation was deposited in a middle bathyal environment, between 500 to 1000 m water depth. More recent foraminiferal assemblage analysis conducted by Burley et. al. (2020) also suggest that Temburong Formation had a continuous supply of fine-grained sediment in successive turbidite flows, which was transported from a shallow marine setting with brackish influence, such as a delta front setting.

2.3.2 BELAIT FORMATION

The Belait Formation is the youngest formation on the island and mainly exposed at the northern part of Labuan island, from Tanjung Layang-Layangan to Bethune Head and in the Eastern part of Labuan Island (in the town area to Tanjung Batu). Wilson and Wong (1964) and Madon (1994) described the Belait Formation as being composed of conglomerate, cross-bedded sandstone, and interbedded sandstone and mudstone. Wan Hasiah et. al. (2013) further classified the Belait Formation into a Lower, Middle and Upper Unit. Foraminifera are sparse, but Hutchison (2005) reported a Middle to Late Miocene age.

LAYANG-LAYANGAN UNIT AS A PART OF THE LOWER BELAIT FORMATION

The Layang-Layangan Unit exposed in Tanjung Layang-Layangan in NW Labuan, was first described by Lee (1977), as being composed of mud-dominated heterolithic deposits, with presence of lenticular, hummocky cross-bedded sandstone and wavy ripple laminated sandy heterolithics. This stratigraphic placement of this unit has been debated by several authors; Madon (1994) included this unit as a part of Temburong Formation as he observed the unit is more strongly deformed than the Belait Formation. Balaguru and Lukie (2012) did not agree as based on the biostratigraphic analysis, and observed that this unit more resembles the shallow marine-deltaic Early Miocene Setap and Meligan Formation. However, Albaghdady et. al. (2003) proposed that this Unit to be grouped within the Belait Formation as it has similar thermal maturation and vitrinite reflectance characteristics. This interpretation was further supported by Wan Hasiah et. al. (2013) and Hennig-Breitfield et. al. (2019), where they assigned this unit as Lower Belait. Biostratigraphic analysis conducted by Som et. al. (2011) suggested that this formation was deposited under shallow marine condition (inner neritic to upper bathyal), hence more suitable if it is regrouped within the Belait Formation, rather than Temburong Formation.

In this study, I characterized the Lower Belait as a unit that is unconformably overlain by a thick succession of conglomerate and pebbly sandstone, where its sharp contact can be observed at a few localities such as in Tanjung Layang-Layangan and Kampung Ganggarak (**Figure 2.5D**; Lee, 1977; Som et. al., 2011; Wan Hasiah et. al., 2013; Hennig-Breitfield et. al., 2019). The sharp contact is interpreted as possible sequence boundary as it reflects an reflects the incision of the lowstand fluvial deposits cutting into the underlying marine deposits (Som et. al., 2011; Balaguru and Lukie, 2012). It is interpreted as shelf edge prodelta to upper slope with the progradation of thicker sand beds that

suggest a distal delta front environment, with probable intervening tidal flats deposits based on the sedimentary structures such as hummocky cross-bedded and wavy ripple lamination, also the dominance of finer grained strata (Lee, 1977; Albaghdady et. al., 2003; Som et. al., 2011; Balaguru and Lukie, 2012; Heinnig-Breitfeld et. al., 2019).

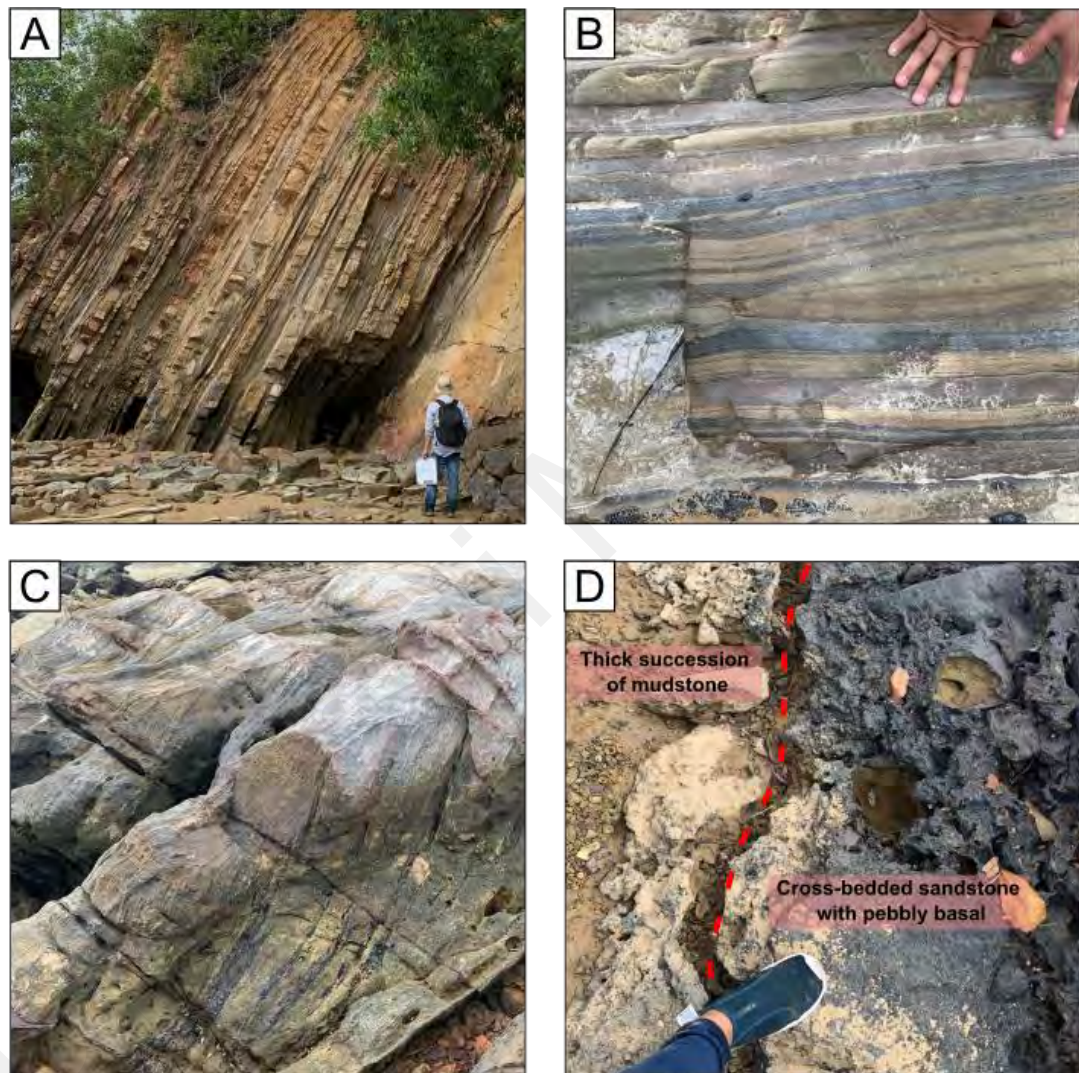


Figure 2.5 Outcrop exposure in Tanjung Layang-Layangan (A) Heterolithic packages observed in Tanjung Layang-Layangan that represent the distal delta front deposits. (B) Hummocky cross-stratified sandstone observed within the Lower Belait. (C) Amalgamated, cross-bedded sandstone of Middle Belait. (D) Sharp contact between mud-dominated package, which represent the prodelta succession (based on biostratigraphic analysis done by Som et. al., 2011), sharply overlain by thick, amalgamated, cross-bedded sandstone with pebbly basal of Middle Belait.

MIDDLE AND UPPER BELAIT FORMATION

The Middle Belait forms a distinct NE-SW trending ridge across northern Labuan, which can be traced from Tanjung Layang-Layangan to Kubong Bluff. This unit displays a thick succession of amalgamated, medium- to coarse-grained, cross-bedded sandstone with pebbly, poorly sorted conglomerate at the base. Based on the biostratigraphic analysis conducted by Som et. al. (2011), Middle Belait was deposited within a lower coastal plain depositional setting, hence supporting its previous interpretation as fluvial deposits (Wilson and Wong, 1964; Madon, 1997). The basal conglomeratic sandstone may represent lowstand fluvial deposits unconformably overlying Lower Belait, and the sharp contact can be considered as a sequence boundary as it reflects a basinward shift in facies that separates distal shallow marine deposit of the Lower Belait from the overlying fluvial to estuarine strata of the Middle Belait Formation (Balaguru and Lukie, 2012; Som et. al., 2011).

Wilson and Wong (1964) reported the age of this formation to be T_{f1} (~23Ma), based on the presence of *Globigerinoides* foramenifera. This suggests that the unconformity may be of T_{e5} age and can be related to the same orogenic event that folded the West Crocker Formation, which may correlate with the Deep Regional Unconformity (DRU) in the offshore Sabah basin (Madon, 1994).

Lastly, the Upper Belait Formation is characterized by shallow marine deposits with tidal influence, mainly consisting of amalgamated, cross-bedded sandstone, and hummocky- and swaley cross-stratified sandstone, interbedded with medium- to thin-bedded grey mudstone and heterolithic deposits (Hennig-Brietfield et. al., 2019). Lenticular and wavy bedding, rhythmic beds and mud drapes on top of foresets were also observed and indicate possible tidal influence. Presence of hummocky- and swalley-

cross-stratified sandstone, together with the occurrence of escape-like trace fossil, is indicative of the storm beds in the lower shoreface environment. Overall, the Upper Belait is interpreted as a shallow marine succession coarsening-upward from offshore shales to shoreface sandstones (Madon, 1997; Som et. al., 2011).



Figure 2.6 Outcrop photos of the Middle to Upper Belait Formation from Kubong Bluff to Bethune Head, northern Labuan. (A) Medium to coarse-grained, trough cross-bedded sandstone represent channel-fill deposits. (B) Presence of mud rip-up clast as channel lag, suggesting tidal influence. (C) Stack of amalgamated, coarse-grained cross-bedded sandstone. (D) Heterolithic succession with presence of swaley- and hummocky cross-stratification indicative of storm deposits in a lower shoreface environment. Supported by the presence of marine ichnofacies (i.e *Ophiomorpha*).

2.3.3. ABSENCE OF SETAP SHALE FORMATION IN LABUAN

Liechti et. al. (1960) defined the Setap Shale Formation as a thick, extensive and monotonous succession of shale with subordinate thin sandstone beds and a few thin lenses of limestone argillaceous succession. In Labuan, Wilson and Wong (1964) reported that a grey mudstone, referred to as the Setap Shale, occurred consistently below the Belait Formation, and also locally exposed in small streams, but it was poorly preserved. Based on the pelagic foraminifera, the age of this formation was Te_{1-4} to Te_5 (Upper Oligocene to Lower Miocene), however Brondijk (1962) observed Te_5 unconformity within Setap Shale and restricted that the term 'Setap Shale Formation' to a formation above that unconformity. A few authors such as Madon (1994) and Hutchison (2005) are of the opinion that the Setap Shale is absent in Labuan, and Lower Miocene Temburong Formation is unconformably overlain by Middle-Upper Miocene Belait Formation. Similarly, Hennig-Breitfield et. al. (2019) also proposed that Setap Shale Formation is only limited to inner to middle neritic equivalents of the Nyalau Formation and considered all steeply dipping sandstone-mudstone alternations in Labuan island as Temburong Formation, with the Temburong Formation being the deep marine extension of the Nyalau and Setap Shale formations. Therefore, they suggested that the Belait Formation in Labuan Island lies directly and unconformably above the turbiditic Early Miocene Temburong Formation.

CHAPTER 3: LITERATURE REVIEW

3.1 SUBAQUEOUS DENSITY FLOW

Recent studies by many authors have considered that turbidite deposition involves a more complex process-response framework, as opposed to being the product of a simple, single process flow. Our understanding of the dynamics of density flows have greatly evolved with the inclusion of many types of processes ranging from dilute turbulent flows up to cohesive debris flows, through a series of transitional flows.

Information on the type of density flows and their classification schemes gathered from theoretical considerations, laboratory experiments, evidence from modern deep-sea fans, and outcrop observation from ancient turbidite sediments, have been compiled and summarized in numerous papers including Middleton and Hampton (1973), Lowe (1982), Mutti et. al. (1992, 2003), Shanmugam (1997), Kneller and Branney (1995), Mulder and Alexander (2001), Talling et. al. (2004, 2012), Talling (2012), Haughton et. al. (2009), and Fonnesu et. al. (2017).

Several processes associated with subaqueous density flow sedimentology, including turbidity currents, debris flows and hybrid flows will be discussed further in the following sections.

3.1.1 TURBIDITY CURRENTS

Turbidity currents are sediment gravity flows in which the sediment is supported mainly by the upward component of fluid turbulence (Middleton and Hampton, 1973; Mulder and Alexander, 2001). The origin of this flow is varied, but it is often thought that many flows form through the down-current transformation of a precursor slide or slump which may pass through an intervening debris-flow phase (see Jackson and Johnson, 2009). Turbidity currents deposit turbidite beds, which fine-upward and display a distinct vertical succession of sedimentary structures.

In this chapter, I will discuss on the low-density and high-density turbidity currents, as well as surge, surge-like and quasi-steady turbidity currents of the Mulder and Alexander (2001) classification scheme (see also Lowe, 1982; Mutti, 1992; Mulder and Alexander, 2001, Talling et. al., 2012).

LOW-DENSITY TURBIDITY CURRENT

The term low-density turbidity current refers to low concentration (<10% volume), fully turbulent flows that can only transport clay, silt and fine- to medium-grained sand sediments in suspension (Lowe, 1982; Mutti, 1992; Talling et. al., 2012). The deposition of this flow often forms a Bouma sequences comprising divisions T_B to T_E. The flows lack the energy to carry coarser sediments as the flow decelerates down-dip, and sediment transport evolves from suspended to bed load, and subsequent deposition by traction sedimentation to form the Bouma T_B and T_C divisions. The overlying T_D is deposited by direct suspension sedimentation but with some traction or near-bed effects before or during deposition to produce fine lamination, while the T_E division is a product of direct suspension of the finest sediments.

HIGH-DENSITY TURBIDITY CURRENT

The term high-density turbidity current refers to turbidity currents with higher sediment concentrations (6-44% volume) (see Lowe, 1982; Middleton and Hampton, 1973; Pickering et. al., 1989; Talling et al., 2012). High density turbidites tend to be coarse-grained, massive sandstones, i.e., the T_A division of the classical Bouma sequence (Lowe, 1982; Mutti, 1992; Kneller and Branney, 1995; Talling et. al., 2012).

Lowe (1982) divides the process of deposition from a high-density turbidity current into three stages through time, from S₁ to S₃ (**Figure 3.1**):

- i) S₁: traction sedimentation stage where the flow is slightly unsteady but fully turbulent. The deposits often show traction-sedimentation structures i.e., planar lamination or cross stratification;
- ii) S₂: traction-carpet stage where the flow unsteadiness increases and the suspended sediment load starts to become concentrated towards the bed. The deposits are commonly described to have lamination/stratification at the bottom interval, well-developed but discontinuous inverse grading in the middle interval, and upper interval of ungraded granule conglomerate;
- iii) S₃: suspension stage, where suspended-load fallout rates are higher as there is insufficient time for development of either bed-load layer or an organized traction carpet. Hence, deposition is dominated by direct suspension sedimentation. The deposits are often massive or show size grading, and most of the time display dewatering structures (i.e., dish and pillar structures) that developed during mass settling.

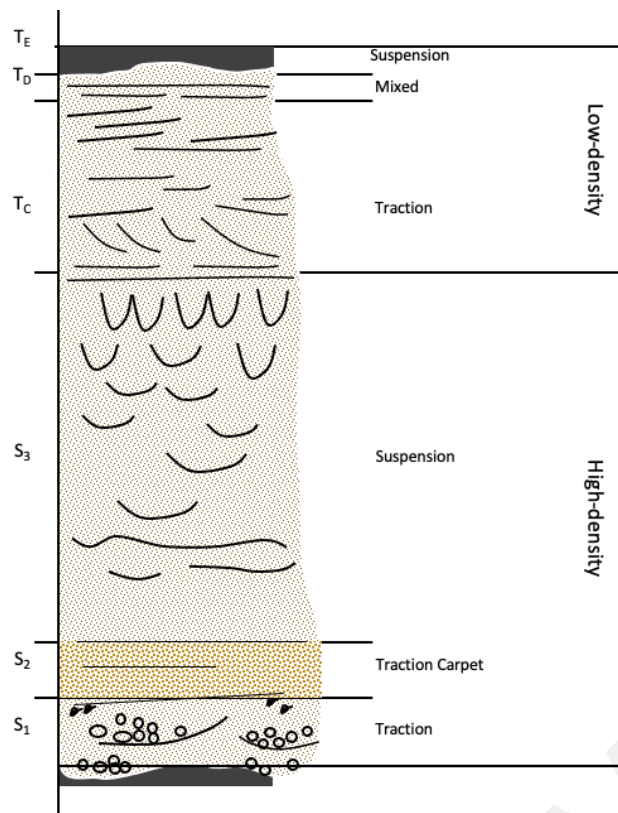


Figure 3.1 Ideal deposit of a high-density turbidite showing S_1 to S_3 divisions, and an overlying late-stage low-density turbidite showing T_B to T_E divisions. Redrawn from Lowe (1982).

SURGE, SURGE-LIKE AND QUASI-STEADY TURBIDITY CURRENTS

Mulder and Alexander (2001) classified turbidity currents into 3 types, based on the flow behaviour: (i) surge flows; (ii) surge-like flows, and; (iii) quasi-steady flows. Surge flows are very-short-duration flow events that travel in the form of isolated flow heads. This type of flow only deposits thin, fine beds (sometimes laminae) and may not be easily recognized as they are difficult to distinguish from other pelagic and hemipelagic deposits. These thin beds can also be homogenized by bioturbation or even be completely eroded later. In contrast, surge-like flows run longer than surge flows, and the flow may include a short flow body following the head. These flows commonly deposit well-developed Bouma T_{B-D} facies.

Lastly, quasi-steady flows (or sustained turbidity flows, *sensu* Jackson and Johnson, 2009) have a longer duration (hours to months). Kneller and Branney (1995) proposed that massive sandstone in turbidite successions were deposited by this type of flow. A

major difference between quasi-steady flows and surge-like flows is the duration of the phenomena relative to its magnitude. Quasi-steady turbidites typically have a coarsening-up basal unit, followed by a fining-up unit with a sharp erosional base (**Figure 3.2**).

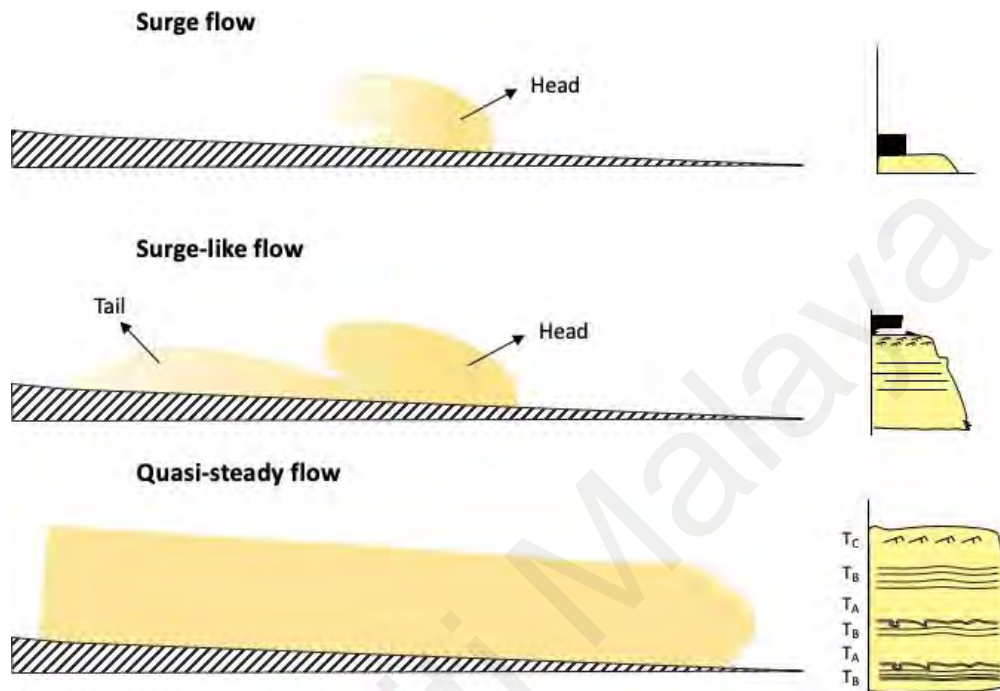
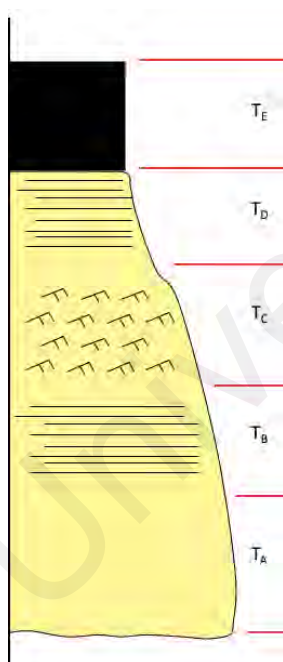


Figure 3.2 The Mulder and Alexander (2001) classification scheme for turbidity currents.

3.1.2 TURBIDITE CLASSIFICATION SCHEMES

The ideal Bouma sequence (Bouma, 1962) is often used as a guide to interpret facies arrangement in turbidites. Each division within a Bouma sequence represents deposition from different processes of formation within a single turbidity current. A complete Bouma sequence comprises several divisions, which grade upwards in the following order; massive and structureless sandstone (T_A); parallel laminated sandstone (T_B); ripple cross laminated sandstone (T_C); parallel laminated siltstone (T_D) and a topmost nearly structureless mudstone division (T_E). However in reality, many Bouma sequences can be incomplete, with sequences being truncated at the top due to erosion/bypass, or the turbidites probably started to be deposited under conditions incapable of forming underlying parts of the succession.



	Bouma's Sequence (1962)	Lowe (1982)	Shanmugam (1997)
T_E	Laminated to structureless	Pelagic and hemipelagic deposits	Pelagic and hemipelagic deposits
T_D	Upper parallel laminae (silty to very fine-grained)	Low-density turbidity current	Bottom-current reworking
T_C	Ripples, wavy or convolute laminae		
T_B	Plane parallel laminae		
T_A	Massive, graded	High-density turbidity current	Sandy debris flow

Figure 3.3 Classification scheme of turbidites from Bouma (1962), Lowe (1982) and Shanmugam (1997). Redrawn from Shanmugam (1997).

Lowe (1982) interpreted the Bouma sequence as representing the evolution of a flow from high density to low density turbidity current, with the T_A division representing a high-density turbidite, while the other divisions (T_B, T_C and T_D) were deposited by a low-density turbidity current.

Shanmugam (1997) did not agree with the use of the term “high-density turbidity current” as this term was used to represent plastic flows and proposed that it should be replaced with the term “sandy debris flow”. The presence of floating mud clasts within T_A division also suggests *en masse* freezing of sediments of the denser portion of turbidity currents (Mutti and Nilsen, 1981), hence showing a characteristic of plastic flow rather than fluidal flows. Shanmugam (1997) also suggested that the T_B, T_C and T_D divisions were the results from bottom current reworking, rather than the deposition from low-density turbidity current.

Talling et. al. (2012), on the other hand, proposed different criteria to identify clean-sand debrites and did not support the conclusion made by Shanmugam (1997). They concluded that chaotically distributed clasts are a distinctive feature of some debrites, while clasts tend to be aligned along distinct horizons in high-density turbidites. However, clasts are not always present in either debrites or high-density turbidites. They concluded that a distinctive feature of a massive clean debrite sandstone is to have a patchy grain-size distribution (swirly fabric), as observed in the Marnoso-arenacea Formation, Italian Apennines (Talling et. al., 2007; Talling et. al., 2012a). The external shape of a sandstone layer can also help to distinguish whether the deposits were formed by debris flow or high-density turbidity current. Debris flows produce deposits that pinch out abruptly in areas of low relief sea floor, while incremental deposition by turbidity

current produces deposits that taper and thin more gradually. Even so, it is difficult to observe the shape of sandstone beds in most outcrop and core studies.

A robust facies classification scheme for turbidites was published by Mutti (1992). In this scheme, several facies were found to be characteristic of turbidites, which can be separated into 3 main groups: (1) Very Coarse Grained Facies (F1 – F3), (2) Coarse Grained Facies (F4 – F6), and (3) Fine Grained Facies (F7 – F9). The description and interpretation of each facies are shown in **Table 3.1**. This scheme shows the basic and most common deposits produced by gravity flow, with different facies being progressively deposited during the different stages of development of gravity flow during its downslope motion. In the same publication, they provided some remarks concerning the classical Bouma Sequence. They observed that the T_A divisions from the Annot Sandstone in the Appennines (described by Bouma, 1962) are not structureless as predicted by the model, but is a more coarse-grained, internally stratified facies (refer plate 39A and 40 from Mutti, 1992). They suggested that if the Bouma Sequence model has to be maintained, the T_A division should be defined as a basal, coarse-grained division, rather than a “structureless sandstone”. This means that the T_A division can be either internally stratified or unstratified, graded or ungraded, and capped by the finer grained deposits (T_B to T_E).

Talling et. al. (2012) provided a review of turbidite classification schemes, where they proposed subdivisions of T_B and T_E based on flow type and sediment support mechanism. They summarized each process of density flows and their resultant deposits, and also discussed and compared their proposed deposit-based classification schemes with previous widely used schemes e.g. Lowe (1982), Mutti (1992), Mutti et. al., (2003, 2009), Kneller and Branney (1995), Shanmugam (1997), and Mulder and Alexander (2001). The summary of this new classification scheme is shown in **Figure 3.4** below. This study will

adapt the nomenclature from the classification scheme of Bouma (1962) and Talling et. al. (2012),but will also consider other classification scheme models and the processes when describing the Temburong Formation facies.

Mutti et. al., 1992		Talling et. al., 2012	
Fine Grained Facies Product of low-density, subcritical turbidity current F7 intervals formed from relatively dense near-bed layers in which sediment was sorted by traction		Hemipelagic mud T_{E-3}	Settling of suspension Laminar En masse consolidation and abrupt freezing
		Debris flow Matrix (gel) strength and excess pore pressure T_{E-2} T_{E-1}	Laminar En masse consolidation and abrupt freezing
		Mud density flow (Densite mud) Fluid turbulence T_C	Turbulent Size-segregating settling and layer-by-layer deposition
		Low density turbidite Fluid turbulence (with grains reworked as bedload) T_{B-1}	Turbulent Size-segregating settling and layer-by-layer deposition
		High density turbidite Turbulence damped and settling of grains hindered. Grain support via combination of damped turbulence, grain to grain interactions, and to a lesser extent excess pore pressure. Grains can be reworked in denser near bed traction carpet. T_{B-2} T_A T_{B-3}	Damped Turbulent Size-segregating settling and layer-by-layer deposition
Coarse Grained Facies Product of gravelly, high density turbidity currents	F5 F4		

Figure 3.4 A few similarities in the classification schemes of turbidite deposits from Mutti (1992) and Talling et. al. (2012), i.e., TB-3 is equivalent to F4. Redrawn from Talling et. al. (2012).

Table 3.1 Summary of classification schemes from Mutti (1992)

Facies	Description	Process
F1	(1) Lack of significant basal scours, (2) larger clasts floating in the matrix, which is muddier and may show features related to plastic flow, (3) the tendency for the largest clasts to concentrate towards the top of the bed	Product of cohesive debris flows
F2	(1) Occurrence of deep basal scours and large rip-up mudstone clasts, (2) the larger clasts float in a fully mixed, occasionally crudely graded matrix composed of mud, sand and gravel, (3) largest clasts show a clear tendency to occur in the lower part of the bed	Product of hyperconcentrated flows that result from the downslope transformation of a cohesive debris flow through progressive mixing with ambient fluid
F3	Clast-supported conglomerate forming beds and bedsets commonly bounded by basal erosional surfaces. The internal organization of this facies is variable and is often unstratified and inversely graded deposit.	Debris flow deposits or pebbly sandstone (i) Left behind by a residual hyperconcentrated flow that has been transformed into a gravelly, high density turbidity current, (ii) overlain by the sediment resulting from the freezing of the overlying residual flow
F4	Thick and coarse grained traction carpets	Product of gravelly, high density turbidity currents
F5	Devoid of internal stratification fluid escape features. Often poorly sorted	Product of gravelly, high density turbidity currents
F6	Coarse grained and internally stratified deposits. Well sorted and characterized by the common lack of grading. Presence of (1) plane-bed horizontal stratification, (2) small scale cross stratification, (3) megaripple bedform/antidunes (?)	Product of hydraulic jump that transform a supercritical high-density current into a subcritical, low-density turbidity current. Vertical succession shows that these beds formed through tractional processes associated with waning, unidirectional flow
F7	Thin and relatively coarse grained. Horizontal laminae that can be easily mistaken for traction carpets (F4) or Tb of F9 beds	Product of low-density, subcritical turbidity current. This two facies were interpreted to form by sediment reconcentration after hydraulic jump, followed by sedimentation by thin traction carpets (F7) and suspension (F8).
F8	True division of Bouma Ta. Structureless to, medium to fine sand. Grading may or may not be present. Better sorted than F5.	Product of low-density, subcritical turbidity current. F8 can be correlated over long distances in depositional lobes and basin plain settings can only be explained through shearing of a loosely packed high-density layer applied by an overlying, thick and low-density residual flow.
F9	Base-missing Bouma Sequence (Tb – Te). Very fine to coarse siltstone. (1) F9a: Tb – Te, (2) F9b: Typically have higher sand-to-shale ratio, internally less organized.	Product of low-density, subcritical turbidity current. F9 is deposited by traction, plus fallout process produced by waning, low-density turbidity current. Main factors that control facies spectrum of F9: (i) the number of suspended fines carried by the flow, (ii) turbulence decay rate.

3.1.3 HYBRID EVENT BEDS (HEBs)

Recently, many workers have noticed that density flows can show spatial and temporal evidence of flow transformation. Such transitional or co-genetic flows can display vertical and lateral changes from non-cohesive to cohesive transport. Beds deposited by such flows are known as hybrid event beds or HEBs (*sensu* Haughton et. al., 2009), and were recognized as a key element of deep-water systems across a wide range of scales and tectonic settings (e.g., Hodgson et. al., 2009; Talling et. al., 2004, 2012; Amy and Talling, 2006; Kane and Ponten, 2012; Mueller et. al., 2017; Fonnesu et. al., 2017; Kuswandar et. al., 2018; Mansor and Amir Hassan, 2021).

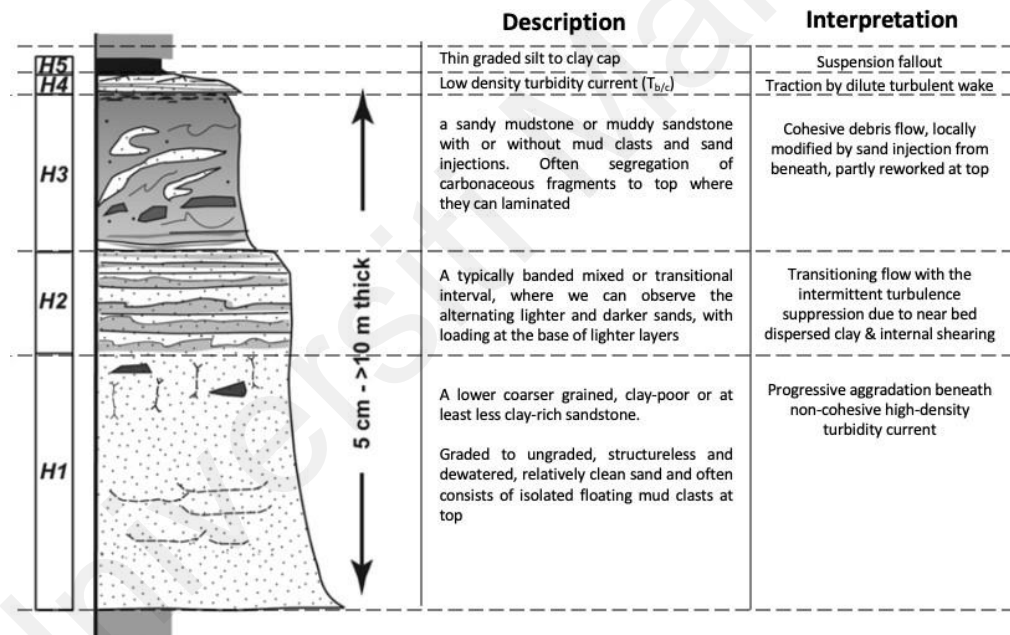


Figure 3.5 ‘Ideal’ internal division of HEBs based on the compilation of bed motifs from a wide range of systems, taken from Haughton et. al. (2009)

HEBs are commonly associated with unchannellized distal fan, basin-floor or basin-plain depositional settings, and these beds are usually concentrated at the base of prograding lobe packages in vertical one-dimensional successions as fringes to lobe bodies deposited further upslope (Talling et. al., 2004; Haughton et al., 2003; Hodgson, 2009; Kane and Ponten, 2012; Kane et al., 2017; Sychala et al., 2017). One of the mechanisms that formed this type of bed is by down-dip flow transformation from a

turbidity current to an increasingly cohesive flow (Haughton et. al, 2009). Their occurrence can indicate the progressive deceleration of clay-enriched flows in which the turbulence was suppressed as flow energy dissipated on flatter and more distal fan sectors (Talling et al., 2004; Fonnesu et. al., 2017).

Overall, HEBs are often characterized by a vertical association of a clean, well to moderate sorted and structureless to faintly laminated sandstone (H1), and a poorly sorted and argillaceous sandstone with a chaotic appearance (H3). Other divisions such as banded sandstone (H2), a low density T_B/T_C turbidite (H4), and a silty mudstone cap (H5) can also be found but are not always present (Talling, 2013; Fonnesu et. al., 2017). The order of each division is displayed as per **Figure 3.5** and never observed in an inverse or different order.



Figure 3.6 Classification of HEBs by Fonnesu et. al. (2018)

Fonnesu et. al. (2018) subdivided HEBs into six bed types, named HEB-1 to HEB-6, based on: (i) the texture of the H3 division, and the size and shape of the clasts within it, (ii) bed thickness, (iii) presence of other divisions like H2 and H4, and (iv) type of sole structures. The characteristics of each HEB type are shown in **Figure 3.6** and **Table 3.2**. They also classified these HEB bed types into **two groups**: (i) mudstone-clasts-rich HEB (HEB 1 to HEB 4), and clast poor HEB (HEB 5 and HEB 6). The two groups of HEBs are found in different deep marine sub-environments, where their deposition is influenced by palaeogeographic location.

Table 3. 2 Summary of HEBs type by Fonnesu et. al. (2018)

HEBs	Thickness	Characteristic of H3 division	Other division
HEB-1	0.6 – 6.8 m, average 3.32 m	Presence of large and relatively undeformed substrate rafts. These rafts are supported by a poorly sorted, coarse to fine-grained sandstone matrix including mudstone chips, mud-poor sand patches and sand injections.	The H4 and H5 divisions are usually well-developed; H4 is characterized by a fine-grained laminated and/or rippled sandstone division (typically about 35 cm thick) with a very irregular base and flat top.
HEB-2	0.4 to 9.57 m; average 2.37 m	Heterogeneous, chaotic and made up of folded pieces of thin-bedded sand, or by a complex sand injection network set in a mud-rich matrix.	Presence of well-developed, typically about 35 cm thick, laminated and graded H4 division, loading and sometimes foundering into the underlying mud-rich H3 division.
HEB-3	0.3 to 5.3 m; average 1.77 m	Composed of densely packed mudstone clasts. The average size of the clast is above 5 cm and surrounded by a dirty sandstone rich in mm- to cm-sized mudstone clasts, clean sandy patches and sand injections.	Uppermost H4 division is developed in most cases (87%) and typically is about 25 cm thick; it commonly has tabular boundaries, but local m-scale wavelength load casts can also occur.
HEB-4	0.2 to 3.2 m; average 0.92 m	Abundant cm-sized mudstone clasts (typically about 2 to 5 cm across) set in a dirty, medium to fine-grained sandstone matrix	H4 division is commonly present (82%) but is usually thin (typically about 15 cm), normally graded and planar laminated.
HEB-5	0.05 - 2.4 m, average 0.44 m	A well-mixed argillaceous sandstone with scattered mudstone clasts.	A few beds show H2 division in the form of dark clay-prone sandy layers alternating with lighter fine-grained cleaner sandy intervals. H4 is present, it forms a thin planar or ripple-laminated unit capping.
HEB-6	0.12 – 0.75 m, average 0.2 m	No H3 division	The basal division is a fine-grained parallel or ripple-laminated sandstone (H4) overlain by a weakly graded fine-sandstone to clay-enriched fine-grained sandstone (H5)

3.1.4 MASS TRANSPORT DEPOSIT (MTD)

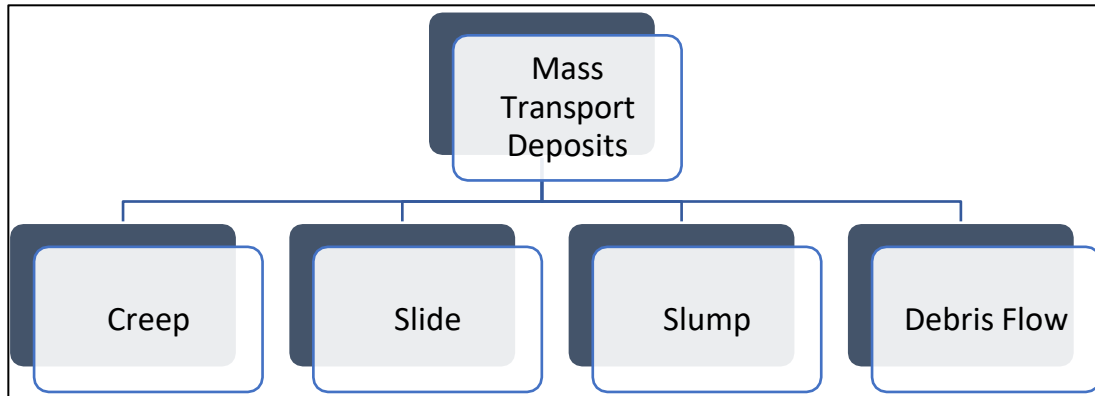
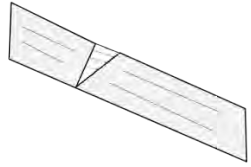
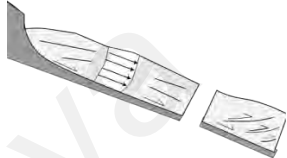
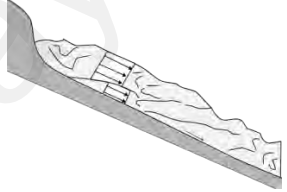
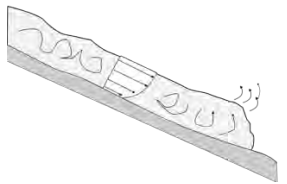


Figure 3.7 Simplified MTD classification.

A mass-transport deposit (MTD) is an *en masse* (or mass movement) deposit derived from slope failure, which includes creep, slide, slump, and debris flow (Figure 3.7, Zhu et. al., 2011; Posamentier and Martinsen, 2010). These processes form a process continuum and are intergradational. Turbidity currents and their deposits are excluded from MTDs as the main grain support mechanisms in MTDs is not fluid turbulence (Posamentier and Martinsen, 2010). However, turbidity currents can transition into mass-transport processes such as debris flows (see Haughton et. al., 2009)

Many authors have established classifications for mass-movement processes, mainly based on process and rheology, product, climate, type of material moved, local geology, and triggering mechanisms (Posamentier and Martinsen, 2010 and citations herein). This study will only discuss the most common MTD; creep, slide, slump and debris flow (Table 3.3).

Table 3.3 Definition and schematic cross sections of the common mass-transport deposits. Note that these processes form a continuum from very slow-moving creep (cm/yr) to very fast-moving debris flows (m/s). Taken from Posamentier and Martinsen (2010) and the citations herein.

Mass-transport deposits	Definition	Example
Creep	Slow intergranular frictional sliding with quasi-static grain contacts	
Slide	Involve mass movement of sediments with little or no internal deformation and often overlies a distinct shear surface	
Slump	Characterized by significant internal distortion of bedding, above a basal shear surface	
Debris Flow	Cohesive to noncohesive laminar flows that transport unsorted and disaggregated debris that can travel across extremely low-gradient slopes.	

Creep is rarely identified as compared to other MTDs and often occurs at the initial stage of the slope failure before transition into slumps or slides (Posamentier and Martinsen, 2010). It is believed that these deposits often occurred on steep slopes ($>20^\circ$), when more than 30 m of sediments were deposited (Silva and Booth, 1984).

Unlike creep, slides can be recognized in high-resolution seismic data based on the presence of listric faults in the head region. However, the central region is often undeformed, hence it would be difficult to be recognized in both seismic and outcrop (Posamentier and Martinsen, 2010).

Slumps can be easily recognized in both outcrop and seismic based on the significant internal distortion of bedding above a basal shear surface (Martinsen, 1989; Martinsen and Bakken, 1990). In outcrops, slumps can be recognized by the presence of deformation structures such as folds, faults and internal shear structures (Posamentier and Walker, 2006; Martinsen, 1994)

Meanwhile, debrites are characterized by a matrix-supported texture, are often ungraded and are poorly sorted, with the largest clasts occurring at the top or base of the debrite (Posamentier and Martinsen, 2010; Talling et. al., 2012). Talling et. al. (2012) further subdivided debris flows into three types: (i) cohesive debris flows with a mud-rich sand matrix, (ii) poorly cohesive debris flows with a poorly sorted clean-sand matrix, and (iii) end-member non-cohesive debris flows comprising only clean sand with no cohesive mud.

3.2 THIN-BEDDED TURBIDITES AND THEIR DEPOSITIONAL ENVIRONMENTS

Thin-bedded turbidites are defined as turbidite beds that are less than 10 cm thick and commonly displaying the upper divisions of the Bouma sequence ($T_C - T_E$) (Mutti, 1977; Kane et. al., 2007; Hansen et. al., 2015). Many authors have established that thin-bedded turbidites can be found in variety of deep-marine depositional environments, and are not simply confined to the basin plains or depositional sites located most distant from the source (Mutti, 1977).

Thin-bedded turbidites are important elements of channel-levee systems, where they can be deposited within (i) outer external levees (Kane et. al., 2007; Kane and Hodgson, 2011), (ii) internal levees (Kane et. al., 2009; Khan and Arnott, 2011), and (iii) depositional terraces (Hansen et. al., 2017) or inter-channels (Mutti, 1977).

Thin-bedded turbidites are also commonly deposited in outer fan lobe systems, within the basin plain, fan fringe, lobe fringe, and lobe distal fringe environment (see Mutti, 1977; Spychala et. al., 2017; Prelat et. al., 2009; Zhang et. al., 2015; Zakaria et. al., 2013; So et. al., 2013; Kuswandaru et. al., 2018; Mansor and Amir Hassan, 2021). Note that the difference between fan fringe and lobe fringe is its association with other thick-bedded deposits. Lobe fringe is often found interbedded with sandstone lobe deposits (lobe axis and lobe off-axis), while fan fringe develops in the absence of intercalations of sandstone lobe deposits (Mutti, 1977).

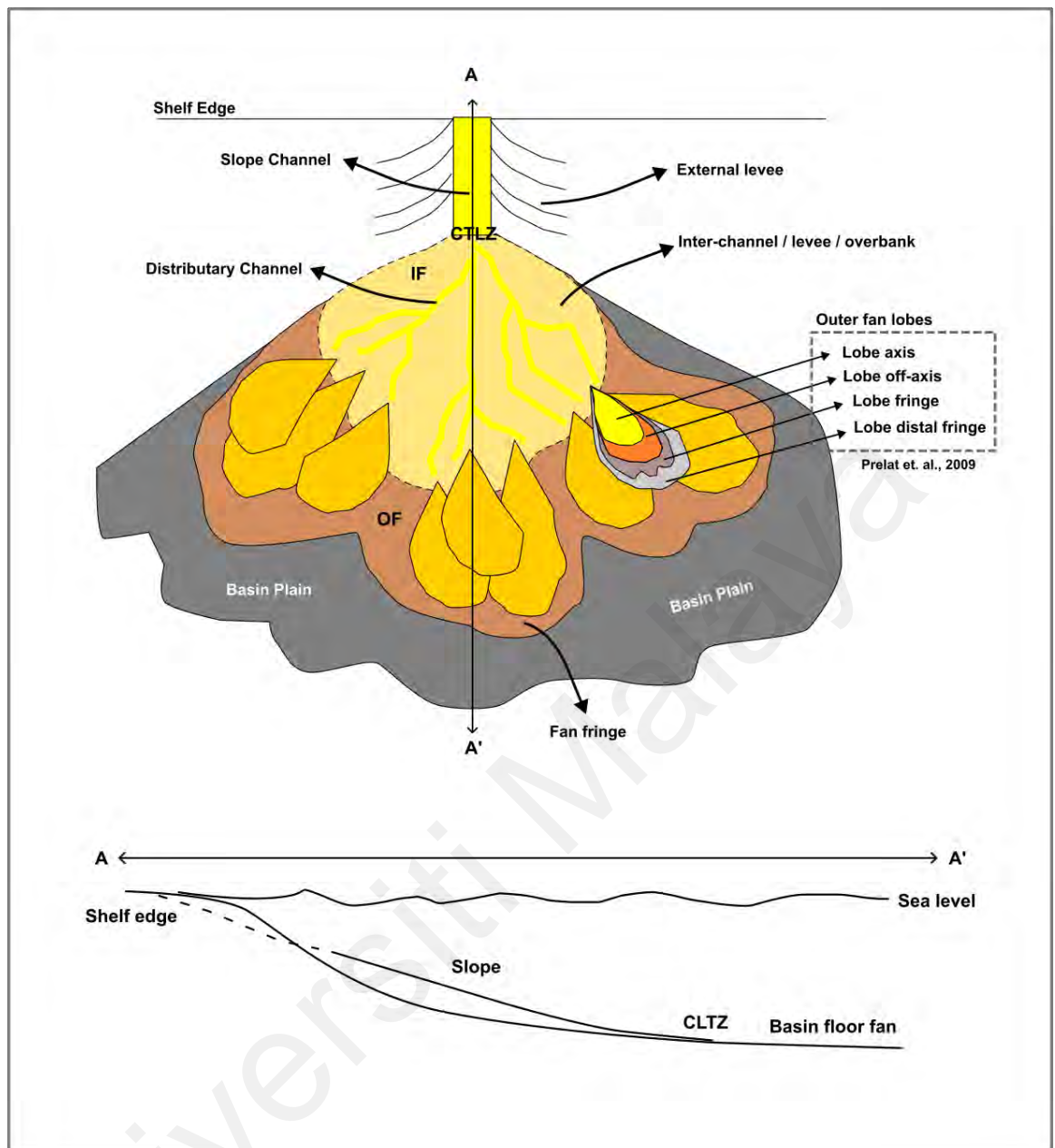


Figure 3.8 Depositional model for deep-water deposits, from slope to basin floor fan. Modified from Mutti (1977).

CTLZ = channel lobe transition zone, IF = inner fan, OF = outer fan

3.2.1 THIN-BEDDED TURBIDITES IN CHANNEL-LEVEE SYSTEMS

A channel-levee system refers to channels with their associated levees, which are commonly deposited in the middle slope to inner fan of a basin floor fan. Thin-bedded turbidites within channel-levee systems form elements of external levees, internal levees, depositional terraces and channel abandonment (e.g., Mutti, 1977; Deptuck et. al., 2003; Khan and Arnott, 2011; Kane et. al., 2007; Kane and Hodgson, 2011; Hansen et. al., 2015, 2017).

Sedimentological characteristics such as sand bed thickness trends and sedimentary structures can be used to distinguish between external levee, internal levee and depositional terrace deposits. The trace fossil assemblage associated with thin-bedded turbidite deposits may also vary between different settings, for example, channel-proximal deposits such as proximal external levees, internal levees and depositional terraces can have much higher biodiversity compared to sand-rich channel axes and more mud-dominated outer external levees (Callow et. al., 2012; Hansen et. al., 2015).

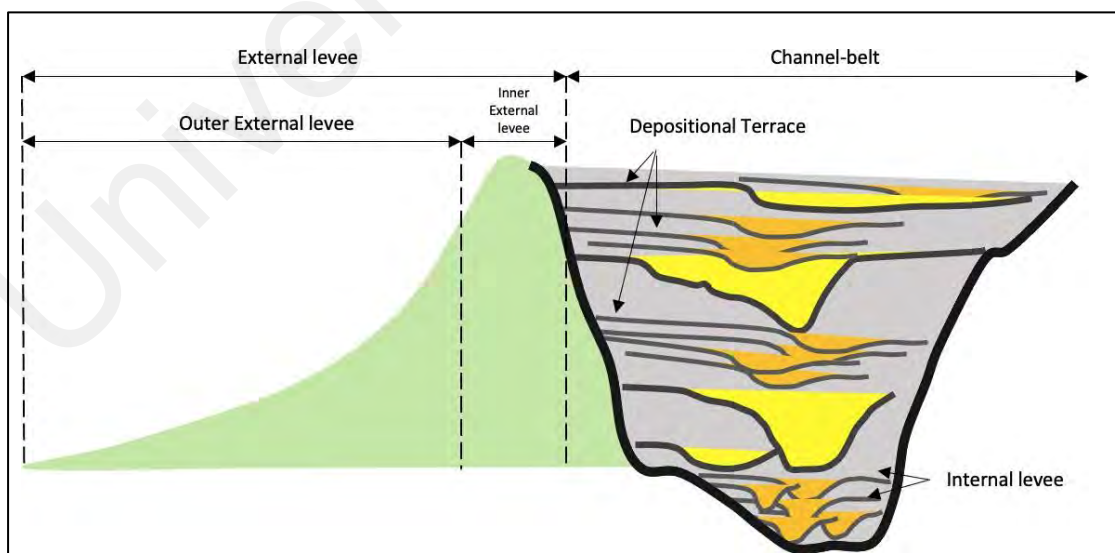


Figure 3.9 Sub-environments within a channel-levee system. Terminology adopted from Kane and Hodgson (2011). Redrawn from Hansen et. al. (2017).

EXTERNAL AND INTERNAL LEVEES

Kane and Hodgson (2011) conducted outcrop studies on the Cretaceous Rosario Formation in Baja California, Mexico, and also Permian Fort Brown Formation, Karoo Basin, South Africa to differentiate submarine channel-levee system sub-environments. They proposed a definition and comparison between external and internal levee sub-environments and morphologies. First, they defined the terminology of these sub-environments. External levee is defined as a depositional body forming a constructional wedge of sediment that thins perpendicularly away from a channel-belt, while internal levees are constructional features fed by flows that spilled out of channelised confinement, but were largely unable to escape the confinement of the channel-belt (**Figure 3.9**).

They concluded that outer external levees are characterised by: (i) laterally extensive beds that taper, fine, and change facies gradually away from the channel; (ii) large-scale thinning or thickening upward trends superimposed by smaller-scale thickness trends, (iii) bed thickness becomes less variable and better organised with stratigraphic height; (iv) sedimentary structures indicating waning flow conditions of relatively simple surges; (v) palaeocurrents which suggest progressive flow evolution; and (vi) very few erosional structures where the large-scale deformation can be observed at the channel-belt margin while smaller (metre-scale) features within the channel-distal areas.

In contrast, internal levees are characterised by: (i) variable lateral extent of beds, locally with sudden pinching out; (ii) poorly-defined vertical bed thickness trends but with some small-scale trends of thickening or thinning; (iii) sedimentary structures indicative of complex unsteady overspill, multiple fining upward sequences and erosion surfaces within individual beds; (iv) palaeocurrents are often complicated and suggestive

of overspill from different points of the channel and recombination of older and younger overspill; (v) erosional structures are much more common, sometimes leading to bed amalgamation; and (vi) deformation is restricted to small slumps and slides.

However, these characteristic is only based on the work of Kane and Hodgson (2011) and there is still some disagreement regarding these characteristics being diagnostic of levees (see Khan and Arnott, 2010; Khan et al., 2011; Cunningham and Arnott, 2021; Bergen et. al., 2022; Sylvester et. al., 2011).

DEPOSITIONAL TERRACE

Depositional terrace is defined as flat deposits occurring adjacent to the active channel within the channel belt (Hansen et. al., 2015). It can be differentiated from the internal levees using the geometry of the deposits; internal levees display a wedge-shape geometry while terraces are often observed as a flat deposit. A depositional terrace is formed when the over-spilling flow extends across the entire space between the confining surfaces on each side of the channel-belt.

Hansen et. al. (2015) also reviewed most of the previous studies conducted by different authors that mistakenly interpreted terraces as other deposits such as inner levees (Deptuck et. al., 2003), flat lying features resulting from channel entrenchment (Deptuck et al., 2003; Babonneau et al., 2010), over-bank, channel margin, and inner external levee (Morris et al., 2014). Mutti (1977) also described thin-bedded turbidite deposited from dilute turbidity currents that overflowed from the adjacent active channels as inter-channels. We concluded that these inter-channels are similar to depositional terraces as both have similar processes and bed geometry.

Table 3.4 summarizes the differences between external levee, internal levee, and depositional terrace based on the studies done by Kane et. al. (2007), Kane and Hogdson (2011), Hansen et. al. (2015; 2017), and ichnology analysis done by Callow et. al. (2012) at the Rosario Formation, Mexico.

Universiti Malaya

Table 3.4 Summary of difference between the thin-bedded turbidites in channel-levee system

Characteristics	Outer external levee (Kane and Hodgson, 2011)	Depositional Terrace (Hansen et. al., 2015; 2017)	Internal levee (Kane and Hogdson, 2011)
Lateral Variation	<ul style="list-style-type: none"> A fining and thinning of beds away from an adjacent channel-belt A divergence of paleo-currents from the related channel-belt 	<ul style="list-style-type: none"> Poorly defined vertical bed thickness trends. Variation in sand bed thickness is usually large compared with external levees. 	Decrease in sandstone proportion or average sandstone layer thickness away from the channel-belt axis.
Average sandstone proportion (Hansen et. al., 2017)	Proximal: 50% Distal: 15%	49%	15%
Bed thickness analysis (Hansen et. al., 2017)	Mean: 5.5 cm Stdev: 4.5 cm Min: <i>no data</i> Max: 20 cm	Mean: 5 cm Stdev: 11 cm Min: 0.5 cm Max: 20 cm	Mean: 2 cm Stdev: 4 cm Min: 0.5 cm Max: 33 cm
Sedimentary structures	Indicative of simple, episodic, steady to waning flow of individual currents. Sedimentary structures vary with grain size of system	Indicative of complex unsteady over-spill	Indicative of complex unsteady over-spill
Ichnology (Callow et. al., 2013)	Low intensity and biodiversity, decreasing away from the channel <i>Phycosiphon</i> and <i>Nereites</i> dominant	High intensity and biodiversity compared to the external levee <i>Scolicia</i> dominant	High intensity and biodiversity compared to the external levee. <i>Phycosiphon</i> and <i>Nereites</i> dominant
Geometry	Depositional body forming a constructional wedge of sediment that thins perpendicularly away from a channel-belt	Form flat bench-like areas adjacent to the channels within the channel-belt	May form distinct wedges of sediment where enough space is available. However, if the space is limited, overspill deposits may appear superficially similar to terrace deposits.

3.2.2 THIN BEDDED TURBIDITES IN OUTER FAN LOBE SYSTEMS

Heterolithic deposits dominated by thin-bedded turbidites are also common elements of lobe-fringe environments within lobe systems (**Figure 3.10**; Mutti, 1977; Talling et al., 2004, 2012; Amy and Talling, 2006; Hodgson, 2009; Kane and Ponten, 2012; Fonnesu et al. 2015; Kane et. al., 2017; Zhang et. al., 2015; Spychala et. al., 2017; Kuswandaru et. al., 2018; Claussman et. al., 2021; Mansor and Amir Hassan, 2021).

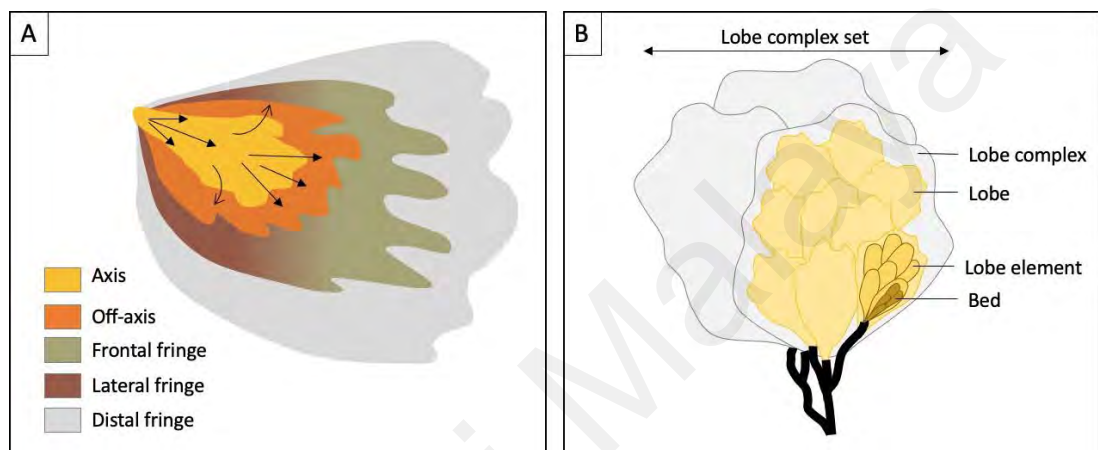


Figure 3.10 (A) Simplified model displaying the various sub-environment in a lobe. (B) Plan-form view of the lobe hierarchy classification scheme: bed to bed set, lobe element, lobe, lobe complex, and lobe complex set (both diagrams were redrawn from Spychala et. al., 2017 and not to scale).

Prelat et. al., (2009) referred to extensive thin-bedded, heterolithic, very fine-grained turbidites between thick-bedded sand-rich deposits as “interlobes”, which can be a good stratigraphic marker to identify a lobe. Later, Prelat and Hodgson (2013) interpreted that these interlobes represent the fringes of lobe complexes. Spychala et. al. (2017) further investigated the lobe fringe environments, where they differentiated between down-dip (frontal) and across-strike (lateral) lobe-fringe environments. They concluded that these two lobe-fringe sub-environments are different in terms of thickness and grain-size trends, facies distribution, and depositional geometries of the deposits, which are summarized in **Table 3.5** below.

HIERARCHICAL ARRANGEMENT OF LOBE DEPOSITIONAL COMPONENTS

A common hierarchy of depositional elements of lobe system was proposed by Prelat et. al. (2009) which consists of four components from higher to lower order: (i) bed to bed set – representing a single depositional event, (ii) lobe elements – represents stacks of beds, which are radial to elongated sandy bodies up to 5 km in diameter and a few meters thick, (iii) lobe – represents stacks of several lobe elements that are divided by thin siltstone intervals, and (iv) lobe complex – stacking one or more lobes. Later, Spychala et. al. (2017) added a lower order “lobe-complex set”, which is formed by the stacking of one of more related lobe complexes within the same lowstand systems tract.

Table 3.5 Summary of differences between the lateral and frontal lobe fringe

	Lobe Fringes (Spychala et. al., 2017)	
	Lateral Lobe Fringe	Frontal Lobe Fringe
Bed type / Facies	<ul style="list-style-type: none"> • Dominated by thin-bedded (> 20 m) heterolithic deposits of structureless or planar-laminated siltstone, and wavy, ripple, and climbing-ripple laminated very fine-grained sandstone. • 20-50% sandstones • 60–80% silt • Rare hybrid beds 	<ul style="list-style-type: none"> • Comprised of dewatered, structureless, or planar-laminated fine-grained sandstones associated with hybrid beds and rare thick debrites. • Percentage of structureless sandstone is around 10-50% • 25–45% silt • Common hybrid beds
Bed Thickness	Highly variable; 0.1–1.5 m	0.05–0.2 m
Process	lateral fringes are dominated by deposits from low-density turbidity currents that are prone to tractional reworking.	deposits of the highest-energy parts of turbidity currents that passed through the axis of the lobe, and maintained the highest momentum
Architecture / geomorphology Extension	<ul style="list-style-type: none"> • Gradually pinch-out, occurs over several km through thinning and fining of the deposits. • commonly show tabular geometries at the scale of observation. • fine and thin as they taper away from lobe-axis environments 	<ul style="list-style-type: none"> • They can exhibit elongated finger-like shapes with abrupt sandstone pinch-out • Presence of depositional pinch-and-swell geometries, which are underlain by siltstones but without any basal truncation • The dimensions of these fingers are 200–300 m in strike width and 1.5 to 2.0 km in dip length.

CHAPTER 4: SEDIMENTARY FACIES AND BED TYPES OF THE EARLY MIOCENE TEMBURONG FORMATION

Two sections of the Early Miocene Temburong Formation exposed in Kampung Bebuloh, Labuan were vertically logged, with a total thickness of 97.7 m (**Figure 4.1**). Both outcrops predominantly comprise thin-bedded turbidites, with occasional chaotic deposits. This chapter will focus on the sedimentological description and interpretation of these sections using a facies and bed type analysis approach. Detailed sedimentary logs for both sections can be found at the end of the chapter (**Figure 4.21 and Figure 4.22**).

Table 4.1 Summary of the facies identified in the studied sections of the Early Miocene

FACIES CODE	FACIES	PROCESS INTERPRETATION
F1	Structureless Sandstone	Deposition by suspension from a high-density turbidity current.
F2	Planar-laminated Sandstone	Deposition by either: (i) low-density turbidity current – traction sedimentation due to migration of bedload sheets , or (ii) high-density turbidity current – repeated collapse of laminar shear layers due to rapid sediment fall out.
F3	Ripple cross-laminated Sandstone	Deposition from a relatively dilute and fully turbulent suspension, with relatively low rates of sediment fallout, resulting in bedload reworking
F4	Planar-laminated Siltstone	Represents T _D division of the Bouma sequence, formed by a waning dilute low-density current.
F5	Structureless To Planar-laminated Mudstone	Either: (i) a turbidite mud, or (ii) a hemipelagic mud.
F6	Poorly Sorted, Argillaceous Sandstone	linked-debrite formed by abrupt <i>en masse</i> deposition in which coarser and finer grains in the matrix tend not to segregate.

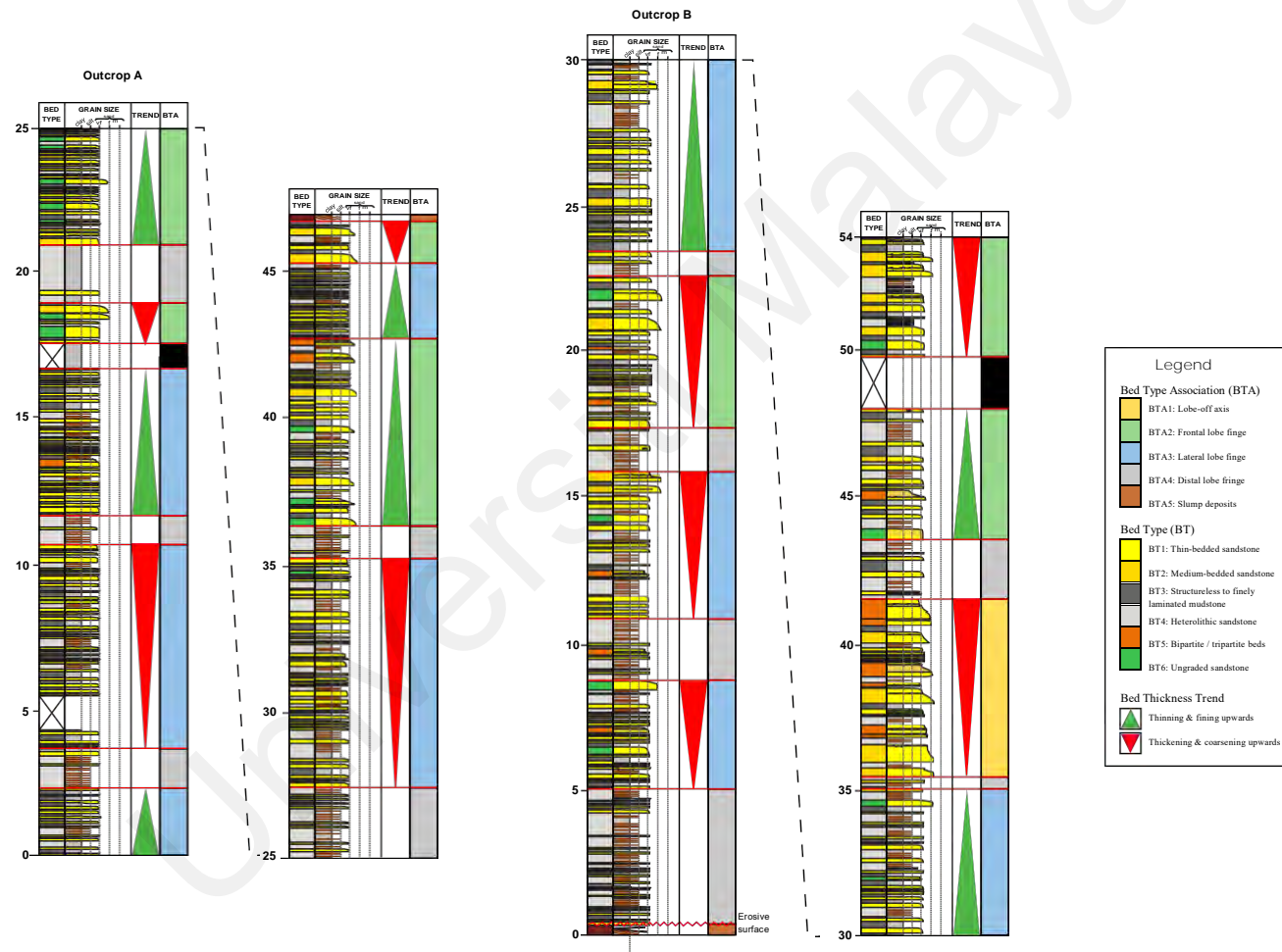


Figure 4.1 Measured section in the Early Miocene Temburong Formation from Kampung Bebuloh, Labuan, Malaysia.

4.1 FACIES ANALYSIS

Six facies were identified in the studied section of the Temburong Formation at Kampung Bebuloh: (i) F1: structureless sandstone, (ii) F2: planar-laminated sandstone, (iii) F3: ripple cross-laminated sandstone, (iv) F4: planar-laminated siltstone, (v) F5: structureless to finely planar-laminated mudstone, and (vi) F6: poorly sorted, argillaceous sandstone (See **Table 4.1** for summary). Each facies are described and interpreted with their possible process of deposition as below.

4.1.1 FACIES 1 (F1): STRUCTURELESS SANDSTONE

DESCRIPTION

F1 is light brown coloured, medium- to fine-grained, well sorted sandstone. The thickness ranges from 5 to 54 cm. Soft-sediment deformation structures such as flame structures within beds are common, while mud or carbonaceous clasts are rarely observed. The facies is sharp-based and slightly erosional. F1 is often gradually overlain by F2 or F3, or sometimes overlain sharply by F6.

PROCESS INTERPRETATION

F1 represents the classic T_A division of Bouma (1962), S₃ division of Lowe (1982) or F8 facies of Mutti et. al. (1992). The generally structureless nature indicates deposition by suspension from a sandy high-density turbidity current (Mutti, 1992; Lowe, 1982; Kneller and Branney, 1995; Talling et. al., 2012). The suspended-load fallout rates were high during deposition and there was insufficient time for development of either a bed-load layer or an organized traction carpet (Lowe, 1982). Presence of flame structures also indicate rapid deposition, where they develop due to sinking of rapidly deposited sand layers onto an underlying unconsolidated mud (Middleton, 1978).

4.1.2 FACIES 2 (F2): PLANAR-LAMINATED SANDSTONE

DESCRIPTION

F2 is light brown coloured, medium- to very fine-grained, moderate to well sorted sandstone. It displays rhythmic planar lamination, and sometimes the individual laminae are lined by carbonaceous material. Bioturbation (i.e., *Nereites*, *Ophiomorpha* and *Scolicia*), mud clasts and carbonaceous/plant fragments can be observed within this facies. F2 is sharp-based and slightly erosional, and is usually overlain gradually by F3.

Process Interpretation:

Facies F2 is interpreted to have been deposited by low-density turbidity current (Bouma, 1962; Talling et. al., 2012). F2 represents the Bouma T_B division or T_{B-1} from Talling et. al. (2012) facies classification.

Deposition from high-density turbidity current is also possible where it can be formed by repeated collapse of laminar shear layers due to rapid sediment fall out. When the flow unsteadiness increases due to rapid sediment fall out, the suspended sediment load becomes progressively concentrated toward the bed and forms high concentration near-bed layers, or traction carpets (Hiscott and Middleton, 1980; Lowe, 1982, Talling et. al., 2012). This deposit represents the S₂ division of Lowe's classification or T_{B-2} from Talling et. al. (2012) facies classification. However, it is difficult to differentiate facies deposited from low-density and high-density turbidity flow from the internal texture of the fine laminations alone. Further investigation i.e., grain size analysis and thickness of beds are needed to determine the possible process of deposition for this facies (Talling et. al., 2012).

4.1.3 FACIES 3 (F3): RIPPLE CROSS-LAMINATED SANDSTONE

DESCRIPTION

F3 comprises greyish to yellowish brown coloured, very fine-grained, well to moderately sorted sandstone. The individual bed thickness ranges from 10 to 33 cm. F3 displays sedimentary structures such as climbing ripples and starved ripples, which occur as discrete ripple trains over a few metres (see Kane et. al., 2007). Similar to F2, in some beds, individual laminae are lined by carbonaceous material, and presence of carbonaceous/mud clasts can be observed. F3 is commonly overlain sharply by F6.

PROCESS INTERPRETATION

F3 represents the T_c division of the Bouma sequence and is interpreted as deposition from a relatively dilute and fully turbulent suspension, with relatively low rates of sediment fallout (Amy and Talling, 2006; Talling et. al., 2012 and the citations hereinafter). The starved or climbing ripples indicate varying amounts of sand available from the suspension flows (Mutti, 1977). Climbing ripples indicate relatively rapid sediment deposition (Kane and Hodgson, 2010; Jobe et al., 2012; Talling et. al., 2012), while starved ripples occurring in trains are commonly preserved in the distal sandstones, where it may be a result primarily from bedload reworking by muddy flow that contained little sand (Kane et. al., 2007; Talling et al., 2007; 2012).

4.1.4 FACIES 4 (F4): PLANAR-LAMINATED SILTSTONE

DESCRIPTION

F4 is light brown coloured siltstone displaying planar lamination. The thickness of F4 is less than 10 cm. Top and base of this facies is planar and sharp. Facies F4 tends to be deeply weathered. Some beds are reddish in colour due to siderite cementation. The sideritized beds tend not to display any sedimentary structures.

PROCESS INTERPRETATION

F4 represents the T_D division of the Bouma sequence. This facies was formed by waning dilute low-density current (Lowe, 1982). The parallel lamination indicates the presence of tractional forces (Bouma, 1962; Amy and Talling, 2006). Based on flume experiments conducted by Bass et. al. (2011), silt-sized sediment can be segregated from the clay suspension only in a turbulent flow, while in other types of flows, the silt-sized sediments tend to mix with the suspended clay. F4 observed in Temburong Formation did not seem to be mixed with the suspended clay, hence further support that this facies was most likely formed by turbulent flow.

4.1.5 FACIES 5 (F5): STRUCTURELESS TO FINELY PLANAR-LAMINATED MUDSTONE

DESCRIPTION

F5 is greyish-coloured mudstone, ranging in thickness from 1 to 30 cm, with average thickness of 7 cm. The majority of beds are structureless, but there are a few beds which display faint silt lamination. Bioturbation is common, predominantly in the form of thick, elongated *Tubutomaculum*. These trace fossils are easily recognized from their lateral tapering offshoot and pellet-covered exterior wall surface. Rare, small coal fragments are observed in some beds. Similar to F4, detailed observation for this facies type is difficult due to weathering

PROCESS INTERPRETATION

F5 represents the T_E division of the Bouma sequence (Bouma, 1962). It can be interpreted as either: (1) a turbidite mud, where it was deposited from a dilute muddy turbidity current (Stow and Piper, 1984; Talling et. al., 2012), or; (2) a hemipelagic mud, where it was formed by settling of sediment particles from the ocean in the time period between density flow events (Stow and Piper, 1984; Talling et al., 2012; Stow and Smillie, 2020).

4.1.6 FACIES 6 (F6): POORLY SORTED, ARGILLACEOUS SANDSTONE

DESCRIPTION

F6 consists of greyish brown coloured, silty to very fine-grained, poorly sorted, argillaceous sandstone. Thickness of this facies ranges from 2 cm up to 19 cm. This interval has a more recessively weathered appearance in the field, relative to other sandstone facies. This facies displays a chaotic, swirly appearance with no obvious internal structures. Scattered mud clasts are present throughout the interval, but not abundant and they are typically smooth-edged, elongate (up to tens of centimetres long), and oriented parallel to bedding. This facies is sometimes sharply overlain by F3, where soft sediment deformation structures such as load casts and pseudo-nodules are observed at the top of F6.

PROCESS INTERPRETATION

Facies F6 may have been formed by abrupt *en masse* deposition in which coarser and finer grains in the matrix tend not to segregate (Talling et. al., 2012). F6 displays characteristics of deposition by low strength cohesive debris flow as the thickness is quite thin (average 4 to 5 cm) and mud clasts are not abundant, which is similar to facies DM₁ described by Talling et. al. (2012). The rare occurrence of mud clasts indicates insufficient energy flow to support large (more than a few millimetres) clasts. The greyish brown-colour may due to mud content exceeding 20% volume within the facies. The soft sediment deformation observed may due to the difference in the grain-size with the overlying interval (Tinterri et. al., 2016).

F6 is interpreted as a linked-debrite as it often found overlying F1 or F2, and/or overlain by F3. Presence of the soft sediment deformation also supports this interpretation as it shows that F6 was still wet and actively dewatering when the overlying sand overrode it, hence making it genetically “linked” (Haughton et. al., 2009). The term ‘linked debrite’ was introduced by Haughton et. al. (2003) to describe hybrid beds of turbidite sandstone overlain by a clast-rich debrite, where the upper clast-rich divisions formed as a part of the same event with the underlying and overlying sandstones, and not as ‘stand-alone’ debrites. The origin of F6 will be further discussed in the bed type section.

4.2 BED TYPE ANALYSIS

Bed types are defined based on the facies assemblage and arrangement in individual beds, where each bed type records the temporal evolution of a single flow event (e.g., Mutti, 1992; Talling et. al., 2007; Mueller et. al., 2017; Kuswandaru et. al., 2019; Mansor and Amir Hassan, 2021). A total of 6 bed types (BT) are identified in the Early Miocene Temburong Formation logged at Kampung Bebuloh: (i) BT1: thin-bedded sandstone, (ii) BT2: medium-bedded sandstone, (iii) BT3: structureless to finely laminated mudstone, (iv) BT4: heterolithic mudstone, (iv) BT5: bipartite or tripartite beds, and (vi) BT6: ungraded sandstone.

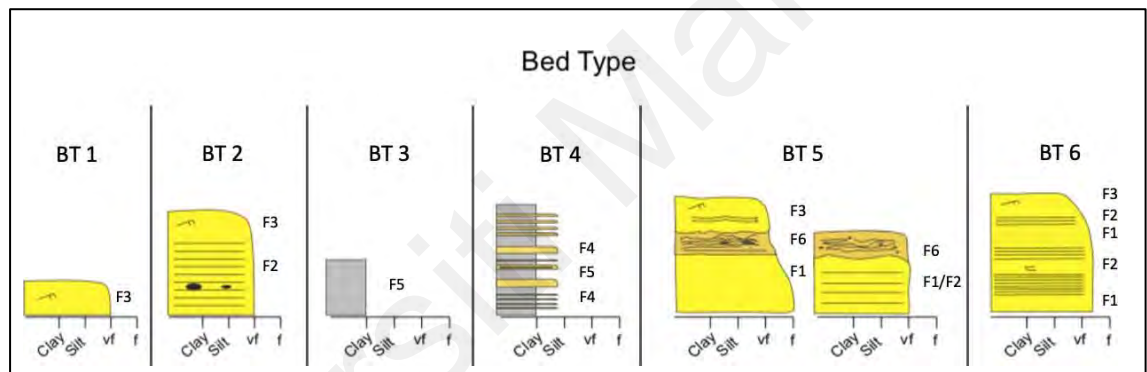


Figure 4.2 Bed types identified in the Early Miocene Temburong Formation in Kampung Bebuloh, Labuan. Bed thicknesses are not to scale.

Overall, the Early Miocene Temburong Formation is dominated by BT1 (42%) interbedded with BT3 (39%). Rare medium-bedded sandstone (BT2), hybrid event beds (BT5) and ungraded sandstone (BT6) were also observed. A statistical summary of the bed types is provided in **Figure 4.3** and **Table 4.2** as below.

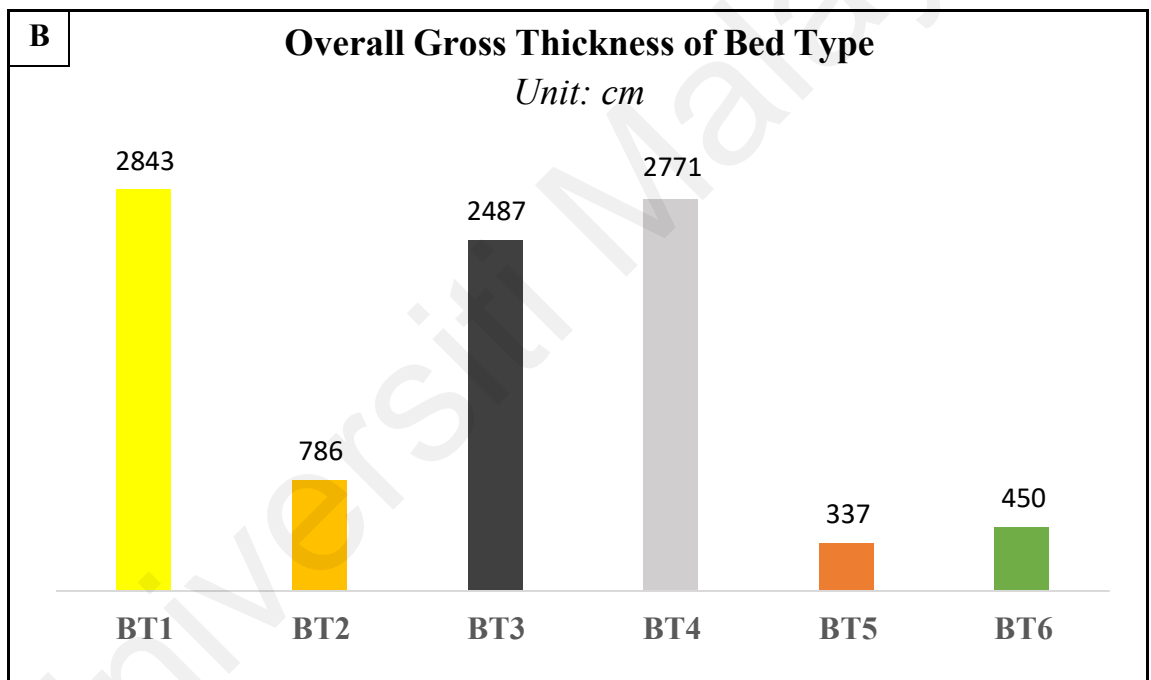
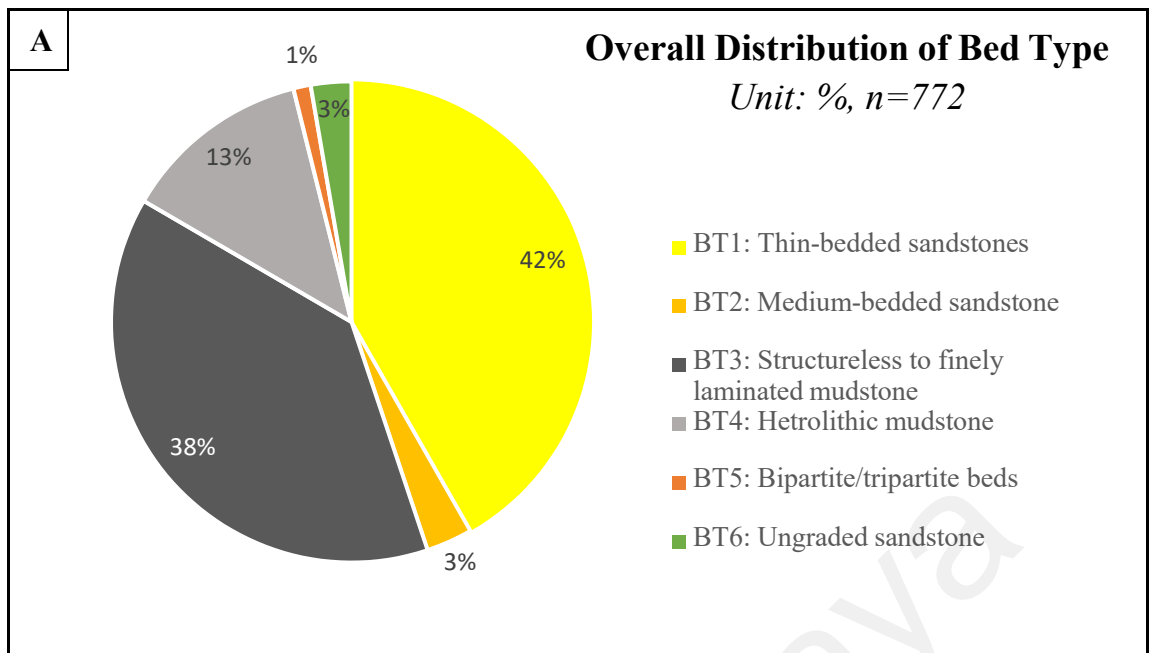


Figure 4.3 (A) Total bed type distribution based on number of beds observed. (B) Total bed type gross thickness.

Table 4.2 Summary of the statistical data for bed type distribution in the Early Miocene Temburong Formation, Labuan.

Bed Type (BT)	Num. of Beds	Total Thickness (cm)	Min. Thickness (cm)	Max. Thickness (cm)	Average of Thickness (cm)	Distribution of BT (%)
BT1: Thin-bedded sandstone	322	2843	3	20	9	42%
BT2: Medium-bedded sandstone	24	786	21	60	33	3%
BT3: Structureless to finely laminated mudstone	297	2487	1	49	8	39%
BT4: Heterolithic mudstone	98	2771	6	155	28	13%
BT5: Bipartite/tripartite beds	9	337	15	90	37	1%
BT6: Ungraded sandstone	21	450	6	41	21	3%
Total	771	9674				

4.2.1 BT1: THIN-BEDDED SANDSTONE

DESCRIPTION

Overall, BT1 comprises 3 to 20 cm thick beds, with average thickness of 9 cm, and make up 42% from the total number of beds observed. It is predominantly characterised by current-ripple and climbing-ripple laminated sandstone (F3). Beds are sharp-based and often show a vertical grain size break with the overlying mudstone of BT3 and BT4. Some of the beds contain parallel laminated sandstone (F2) and show normal grading. Some of the beds are also associated with reddish-coloured clasts, possibly siderite, and carbonaceous clasts/wood fragments ranging from 1 to >15 cm in diameter.

Sole marks such as flute casts, groove casts and cm-thick scour-like features are rarely associated with BT1 beds (only 26% of beds have them). Groove casts are rare and mostly occurred at the base of beds more than 10 cm thick. Siderite layers and clasts can also be observed within a few beds.

Only 30% of BT1 show evidence of bioturbation, which predominantly consists of graphoglyptids at the base of the beds. This trace fossil assemblage is representative of the *Nereites* Ichnofacies and includes *Paleodictyon*, *Megagraption*, *Cosmorhappe*, *Unihelminthoida*, *Scolicia*, and *Ophiomorpha*. A few undifferentiated vertical burrows can also be observed in cross sections of the beds.

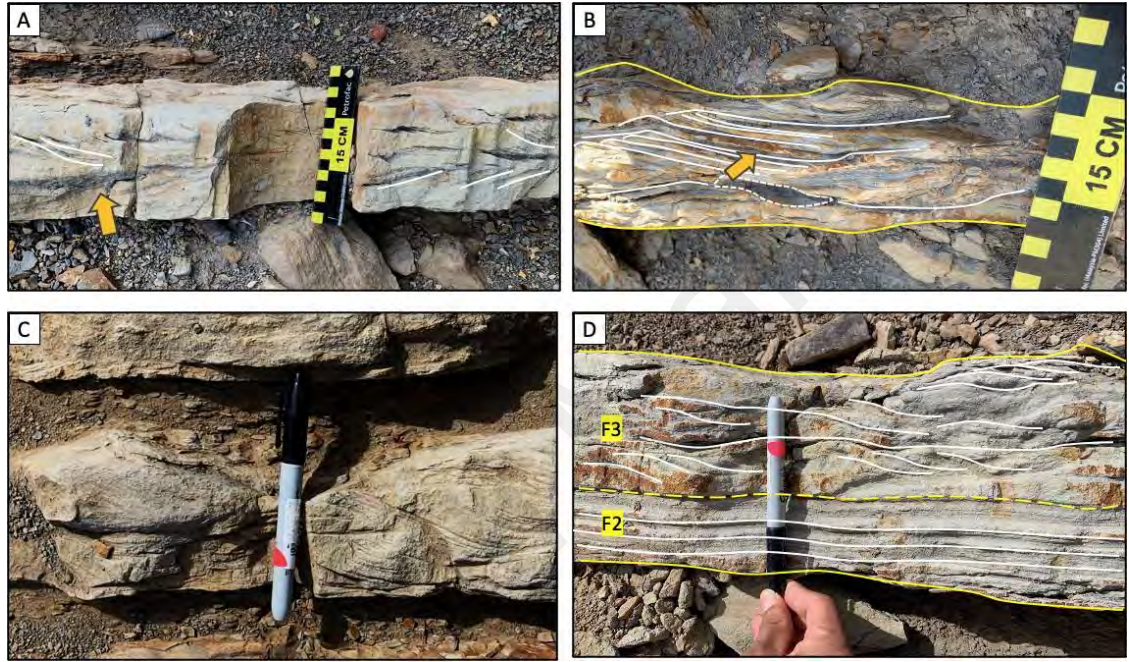


Figure 4.4 Examples of Bed Type 1. (A-C) Yellowish, very fine-grained sandstone with climbing and ripple cross-lamination (F3). Yellow arrows point to carbonaceous layers. (D) Yellowish brown, normal graded, thin-bedded sandstone that displays planar (F2) to cross ripple lamination (F3). Length of the scale is 13.5 cm.

INTERPRETATION

BT1 is interpreted as the deposits of dilute, fine-grained turbidity currents. The facies arrangements observed in the beds display T_c (Bouma, 1962) and T_{B-3} (*sensu* Talling et.al., 2012) divisions. The presence of ripples is consistent with this interpretation, because they do not form in flows where the turbulence is strongly damped by cohesive mud (Talling et. al., 2012).

As the velocity further decreased, at certain moments it is sufficiently low that current ripples (T_c) started to form. The presence of climbing ripple cross lamination suggests that the sedimentation rates were relatively high, enabling the current ripple bedforms to aggrade (Khan and Arnott, 2011, Talling et. al., 2012). The common occurrence of BT1 being overlain by mudstone of BT3 further supports the interpretation of deposition from a waning dilute flow (Talling et al. 2012).

Presence of flute casts indicate deposition from a turbulent flow, meanwhile presence of groove casts may indicate deposition by laminar plug flow, which is commonly associated with debris flow deposits (Peakall et. al., 2020). However, as groove casts are very rare in this bed type, this erosional feature may not be genetically linked to the overlying BT1 beds and it was probably formed by an older bypassing debris flow event (Peakall et. al., 2020).

4.2.2 BT2: MEDIUM-BEDDED SANDSTONE

DESCRIPTION

BT2 typically displays normal grading, changing upwards from parallel laminated sandstone (F2) into ripple and climbing ripple cross laminated sandstone (F3). Carbonaceous clasts and wood fragments (up to 15 cm long), siderite layers and siderite clasts are common in BT2. Soft sediment deformation structures such as convolute lamination and load structures can also be observed in a few beds.

The base of BT2 beds are planar, sharp and erosional, with 47% of the beds having flute casts and scours. Individual bed thickness ranges from 21 cm to 60 cm, with average thickness of 33 cm. BT2 makes up 3% of the total number of beds logged at Kampung Bebuloh.

76% of the logged BT2 beds display bioturbation. The trace fossils at the base of beds are mostly represented by a low diversity *Nereites* Ichnofacies assemblage i.e. *Paleodictyon*, and *Megagraption*. The trace fossils *Ophiomorpha* and *Scolicia* are also observed in cross sections of beds.

INTERPRETATION

BT2 is interpreted as low-density turbidites. The sharp, fluted bases, and the fining-upwards grain size profiles within BT2 are characteristic of the deposits of turbidity currents. The parallel and cross-ripple laminated intervals are representative of the T_B and T_C divisions, respectively, of a Bouma sequence. These are typically associated with deposition of gradual waning, surge-like, turbulent gravity flows (e.g., Mulder and Alexander, 2001; Jackson and Johnson, 2009).

The T_B division in BT2 most likely represents the T_{B-1} subdivision of Talling et. al. (2012) which is deposited by low-density turbidity current because it is finer grained, and no alternating inversely graded traction-carpet layers can be observed. Convolute lamination observed within the parallel lamination suggests rapid deposition where it caused dewatering to occur (Talling et. al., 2012), while load structures were due to unstable density contrasts (density loading) or lateral variations in load (uneven loading) when sediment becomes liquidized (Owen, 2003; Tinterri et. al., 2016). Load structures that formed within a more or less uniform lithology can be gradational to the convolute laminations and occur especially within T_{BCD} Bouma divisions (Tinterri et. al., 2016).

Similarly as in BT1, T_C divisions formed at the top of the bed when the flow velocity was further decreased, indicating the final stage of the waning flow. Overall, BT2 predominantly shows the attributes of sediments deposited by low-density turbidity currents but with higher energy or more proximal location from the source of sedimentation relative to BT1. This interpretation is supported by the fine-grained texture of BT2 and the internal sedimentary structures (parallel and cross ripple lamination) that suggests traction sedimentation which often deposited by low density turbidity flow (Lowe, 1982; Mutti, 1992; Mutti et. al., 2003).

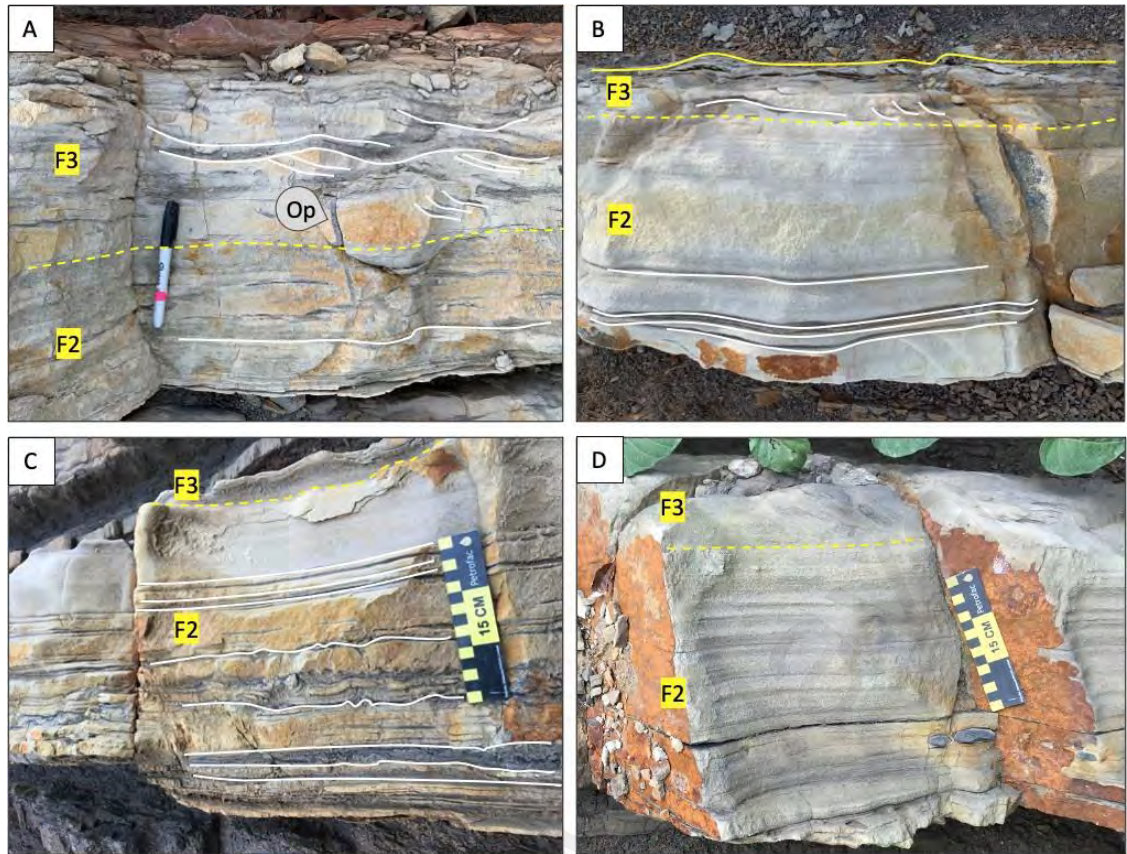


Figure 4.5 Examples of Bed Type 2. Normal graded sandstone. Yellowish brown, well sorted, fine to very fine-grained sandstone. Fining upward, this bed type predominantly consists of parallel lamination (F2) and thinner interval of cross ripple lamination (F3).

4.2.3 BT3: STRUCTURELESS TO FINELY LAMINATED MUDSTONE

DESCRIPTION

BT3 mainly comprises thin- to medium-bedded, greyish mudstone (F5). The thickness ranges from 1 to 49 cm, with average thickness of 8 cm, and making up 39% from the total beds logged. Most of beds are structureless, but there are a few beds which display faint silt lamination. Bioturbation in the form of elongated *Tubutomaculum* is common, however the potential diversity of burrow mottling in this facies were not fully captured as it was difficult to discern due to the effect of weathering. Rare, small coal fragments are observed in some beds. Note that detailed observation for this facies type is difficult to obtain due to the superficial weathering

INTERPRETATION

BT3 represents the T_E division of the Bouma sequence (Bouma, 1962). It can be interpreted as either: (1) a turbidite mud, where it was deposited from a dilute muddy turbidity current (Stow and Piper, 1984; Talling et. al., 2012), or; (2) a hemipelagic mud, where it was formed by settling of sediment particles from the ocean in the time period between density flow events (Stow and Piper, 1984; Talling et al., 2012; Stow and Smillie, 2020).

BT3 may also be the combined product of both processes. Beds that show silt lamination may represent turbidite mud, T_{E-1} (Piper, 1978), or in greater detail, T₄ to T₅ (Stow and Piper, 1984; Stow and Smillie, 2020). T_{E-1} is usually less than 10 cm to 25 cm thick and consists of 0.1 to <2mm thick lamination. The stratification of silt and mud layers is thought to result from the depositional segregation of silt particles due to increased shear within the lower boundary layer, separating them from clay flocs (Stow & Bowen, 1980; Talling et. al., 2012). T_{E-1} is often developed in more proximal locations (Talling et. al., 2012). However, the majority of the beds are thin and structureless, which

may represent the hemipelagic mud which settled during quiescence. Presence of bioturbation also suggests a quiet environment between flow events. The only way to differentiate between turbidite and hemipelagic mudstone is by comparing them under thin section. Hemipelagic mudstone contains widely dispersed remains of calcareous organisms, e.g., foraminifera, while dense typically has a higher organic carbon content and most of the components were originally terrigenous (see Stow and Piper, 1984; Talling et. al., 2012; Stow and Smillie, 2020).

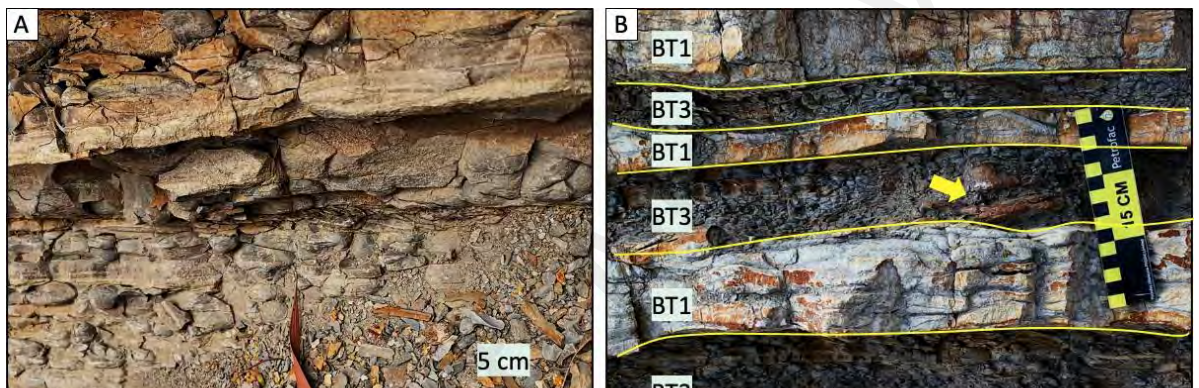


Figure 4.6 Example of Bed Type 3: (A) Laminated mudstone. (B) Repetition of BT1 interbedding with BT3, which formed T_{CE} sequence of Bouma. *Tubutomaculum* is observed within BT3 (yellow arrow).

4.2.4 BT4: HETEROLITHIC MUDSTONE

DESCRIPTION

BT4 predominantly consists of medium-bedded, light to dark grey mudstones (F5), interbedded with thin-bedded siltstone (F4) and very fine-grained sandstone beds (F3). Thickness of this bed type ranges from 6 to 155 cm, with average thickness of 28 cm. BT4 makes up 17% of the total number of beds logged. Some BT4 display a thinning upwards trend (**Figure 4.7c**).

This bed type normally consists of 3 to 6 interbedded layers of thin-bedded, sharp-based F4 and sometime F3, with the thickness ranging from 2 to 5 cm (refer to detailed sedimentary logs, **Figure 4.21** and **Figure 4.22**). However, thicker beds of BT4 (more than 45 cm) can comprise more than 6 interbedded layers. Some of the layers may have been sideritized as the color has turned reddish and a few beds still preserve the parallel lamination, but mostly no longer display any internal sedimentary structures.

Reddish-colored clasts, carbonaceous nodules, and trace fossils, in form of *Tubutomaculum*, are commonly present within BT4. Note that detailed description of this facies type is difficult because of intense weathering. This is due to the mudstone's soft nature that makes it easy to be eroded.

INTERPRETATION

BT4 is interpreted as a deposit of dilute, low density turbidity currents. BT4 reflects more direct suspension sedimentation but with pulses of traction sedimentation which produced the fine lamination of F4 and F5 (Lowe, 1982). Presence of the trace fossil *Tubutomaculum* indicates a low rate of sedimentation setting (Gracia-Ramos et. al., 2014), which explains why thicknesses of F3 and F4 are relatively very thin.

Overall, the dominance of mudstone facies of F4 and F5 and low rate of sedimentation in BT4 indicate a deposition of dilute, low-density turbidity current at more distal location from the sediment source compared to BT1 and BT2.

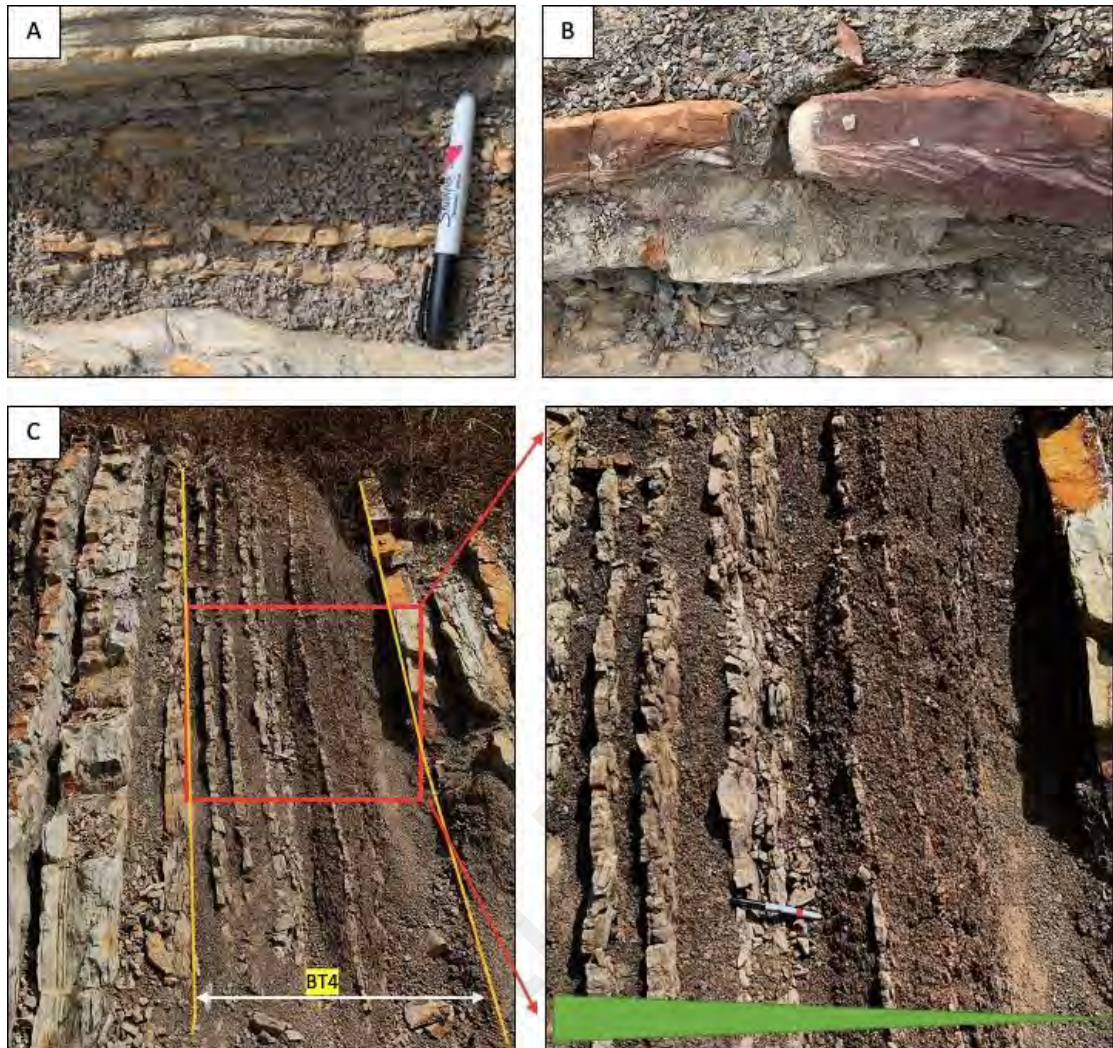


Figure 4.7 Example of Bed Type 4: (A) Consists of intercalation of mudstone and thin siltstone. Sandstone layers are yellowish brown in color, only 1 to 2 cm thick, with sharp base and some show wavy to parallel lamination. (B) Siltstone layers within BT4. The top part has turned into siderite, but the lamination is still preserved. (C) BT4 shows thinning upwards trend where the thickness of sandstone reduces from 5 to less than 1 cm on the top. Sandstone is greyish brown in color, some displays wavy lamination.

4.2.5 BT5: BIPARTITE / TRIPARTITE BEDS

DESCRIPTION

BT5 is characterized by a well-sorted, structureless to faintly laminated sandstone, overlain by a chaotic, poorly sorted, argillaceous sandstone. The thickness ranges from 11 to 90 cm, with average thickness of 32 cm. BT5 makes up only 2% of the total beds logged. Most BT5 beds comprise 3 intervals: (i) a lower interval composed of structureless to faintly parallel laminated sandstone (F1/F2); (ii) a middle interval of poorly sorted, argillaceous sandstone (F6), and; (iii) an upper interval of parallel to ripple cross laminated sandstone (F2/F3).

The lower interval sandstone is light brown in colour, well sorted and rarely has any associated clasts within it. This interval is predominantly structureless (F1) and displays dewatering sheets and flame structures. However, some intervals exhibit a weak normal grading (F2). The base of the lower interval is slightly erosive, where the presence of scour, flute and groove casts can be observed.

The middle interval consists of argillaceous sandstone (F6) with a chaotic, swirly appearance. Scattered mud clasts are present throughout the interval, but not abundant and they are typically smooth-edged, elongate (up to tens of centimetres long), and oriented parallel to bedding. Carbonaceous layers can also be observed in a few beds within this interval. Contact between the middle and lower interval is sharp.

The top interval comprises light brown coloured, moderate to well sorted, very fine-grained sandstone. It mostly displays parallel and/or ripple cross lamination and rarely contains mud clasts (F2 and F3). The contact between the top and middle intervals is

gradual to sharp, and soft deformation structures such as load, ball-and-pillow structures and pseudonodules can be observed.

BT5 in the Temburong Formation can be subdivided into three sub-bed types, as listed below:

- (i) BT5a: tripartite beds, consisting of all intervals described above
- (ii) BT5b: bipartite beds, with missing upper interval
- (iii) BT5c: bipartite beds, with missing lower interval

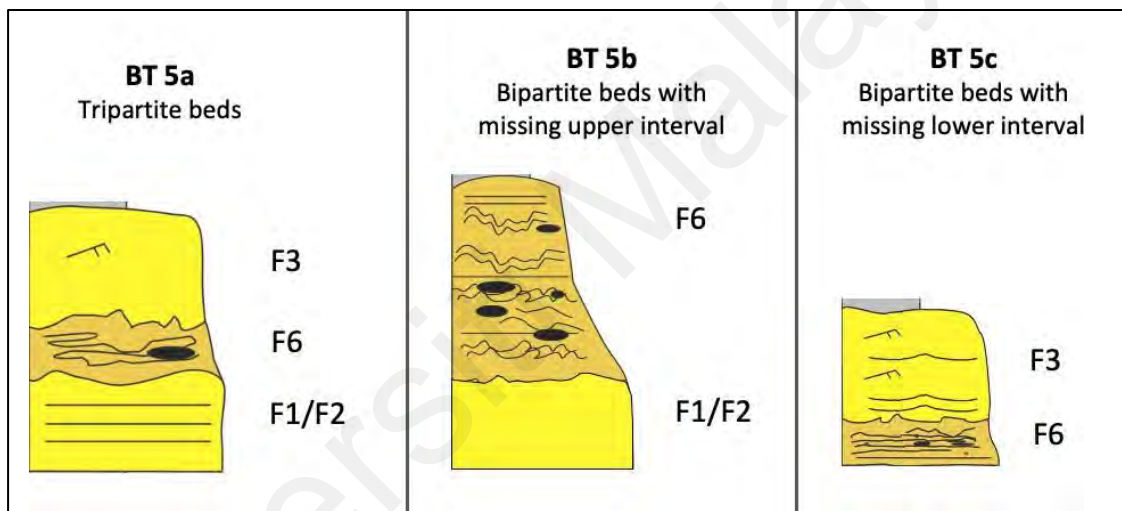


Figure 4.8 Sub-bed types of BT5.

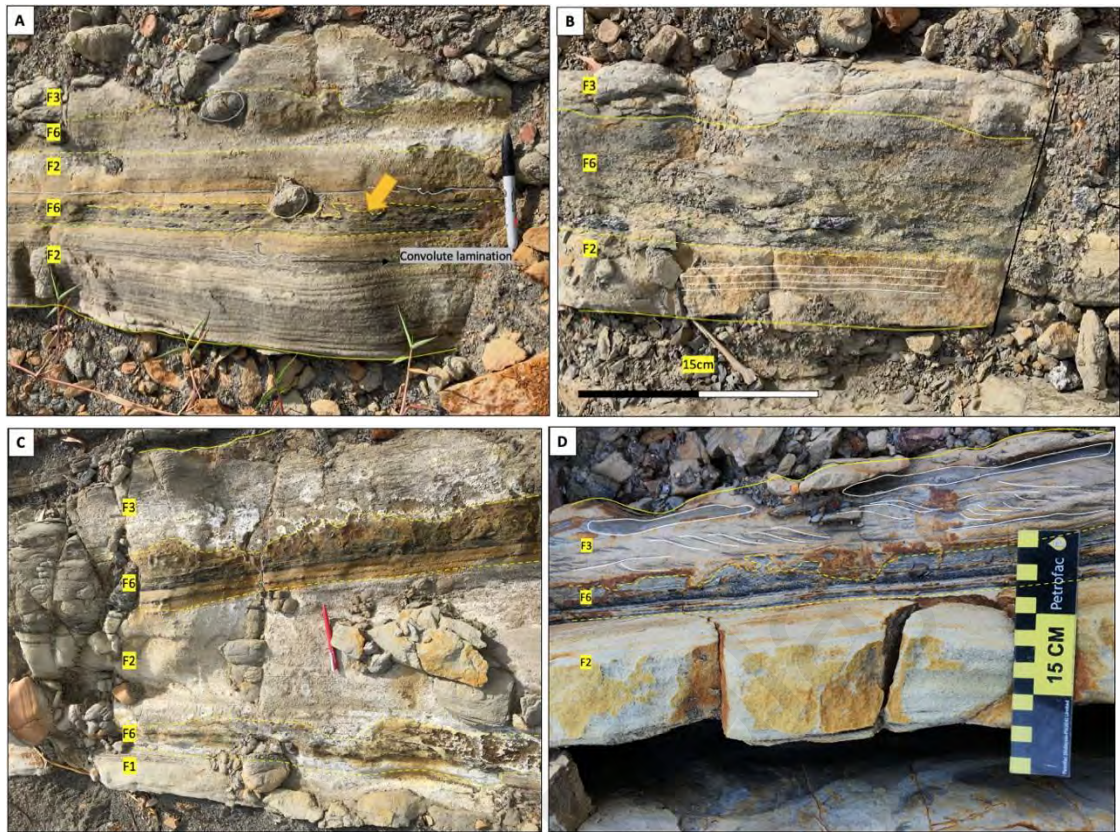


Figure 4.9 (A) Amalgamated hybrid event beds. Bipartite beds overlain by tripartite beds. Presence of soft deformation like convolute lamination and load casts with detached pseudo-nodules (yellow arrow_ between F6 and F2 of the bipartite bed, which is common in HEB due to differences in grain size. (B) Tripartite bed. Consist of planar-laminated sandstone in the lower interval, argillaceous sandstone with swirly/chaotic texture in the middle interval, and cross ripple laminated sandstone in the upper interval. (C) Amalgamated hybrid event beds. Bipartite beds overlain by tripartite beds. The thickest sandstone bed in the area, ca. 90cm. Argillaceous sandstone (F6) is identified based on its color, darker brown compared to below and above interval, swirly/chaotic appearance and presence of mud clasts. (D) Tripartite beds

F1: structureless sandstone, F2: planar-laminated sandstone, F3: cross ripple-laminated sandstone, F6: argillaceous sandstone.

INTERPRETATION

Overall, BT5 is interpreted as hybrid event beds deposited from a **transitional or co-genetic flow** (Talling et. al., 2004; Haughton et. al., 2003; 2009; Hodgson et. al., 2009; Talling et. al., 2012; Mueller et. al., 2017; Kuswandaru et. al, 2018). The intervals of BT5 are interpreted as divisions within the hybrid event bed classification scheme of Haughton et al. (2008).

The lower interval of BT5 is interpreted as the H1 division of Haughton et. al. (2009). This interval was deposited by a sandy high-concentration turbidity current where it has a high rate of sedimentation fallout, hence producing the dewatering structures. The argillaceous sandstone in the middle interval is interpreted as division H3, where its chaotic, argillaceous matrix indicates inefficient sorting and *en masse* deposition from a cohesive flow (Talling et. al, 2004; Hodgson et. al., 2009). Lastly, the upper interval is interpreted as the H4 division, deposited from a low-density turbidity current. This interval comprising a low density T_C turbidite, was deposited from a trailing and waning turbulent cloud, which marks a return to non-cohesive behaviour of the flow (Haughton et. al., 2009; Fonnesu et. al., 2018; Kuswandaru et. al., 2018).

Based on the thickness range, the texture of the H3 division, and presence of flute and groove casts, BT5 resembles the HEB-5 type *sensu* Fonnesu et. al. (2018). The H3 division in BT5 does not have mega mudstone clasts and the clasts that are present are often scattered throughout the facies (no clast-to-clast contacts observed such as those in the HEB-4 type). Fonnesu et. al. (2018) also observed a missing lower interval in HEB-5 type, which is similar to BT5c. The absence of the H1 division, as observed in BT5c, is not uncommon as H1 division tends to be thin and pinches out in distal and lateral locations (Haughton et al., 2003; Amy and Talling, 2006).

Haughton et. al. (2003; 2009) explained a few mechanisms on the origin of hybrid event beds, among those are (1) transformation of debris flow downslope into a turbidity current, which moves faster than the debris flow developed up-dip due to slope failure, is partially transformed downslope into a turbidity current. The tail-end debris flow then catches up and overlies the forerunner turbidity current; or (2) down-dip transformation from non-cohesive to more cohesive flow driven by incorporation of clay via erosion.

Universiti Malaya

4.2.6 BT6: UNGRADED SANDSTONE

DESCRIPTION

BT6 is characterized by yellowish to greyish brown coloured beds of well to moderately sorted, very fine- to fine-grained sandstone. The thickness ranges from 6 to 41 cm, with average thickness of 21 cm. BT6 makes up 3% of the total beds logged.

This bed type is somewhat similar to BT2 in terms of grain size and internal structures as it consists of parallel and cross ripple laminated F2 and F3 sandstone. The differences between BT6 and BT2 are in the vertical organization of the internal structures and the presence of structureless sandstone (F1). Unlike BT2, BT6 displays alternating parallel lamination (F2) with cross ripple lamination (F3) and/or structureless (F1) intervals (T_{BCBC}/A_{BCBC} sequence, Fig. 9). Some beds comprise structured F1 intervals, overlain by ripple cross-laminated intervals of F3. Flame structures can also be observed within a few beds.

Bioturbation is common in this bed type, with 60% of the beds being bioturbated. Sole marks such as flute casts and cm-thick scour-like features are present in roughly 60% of the beds.

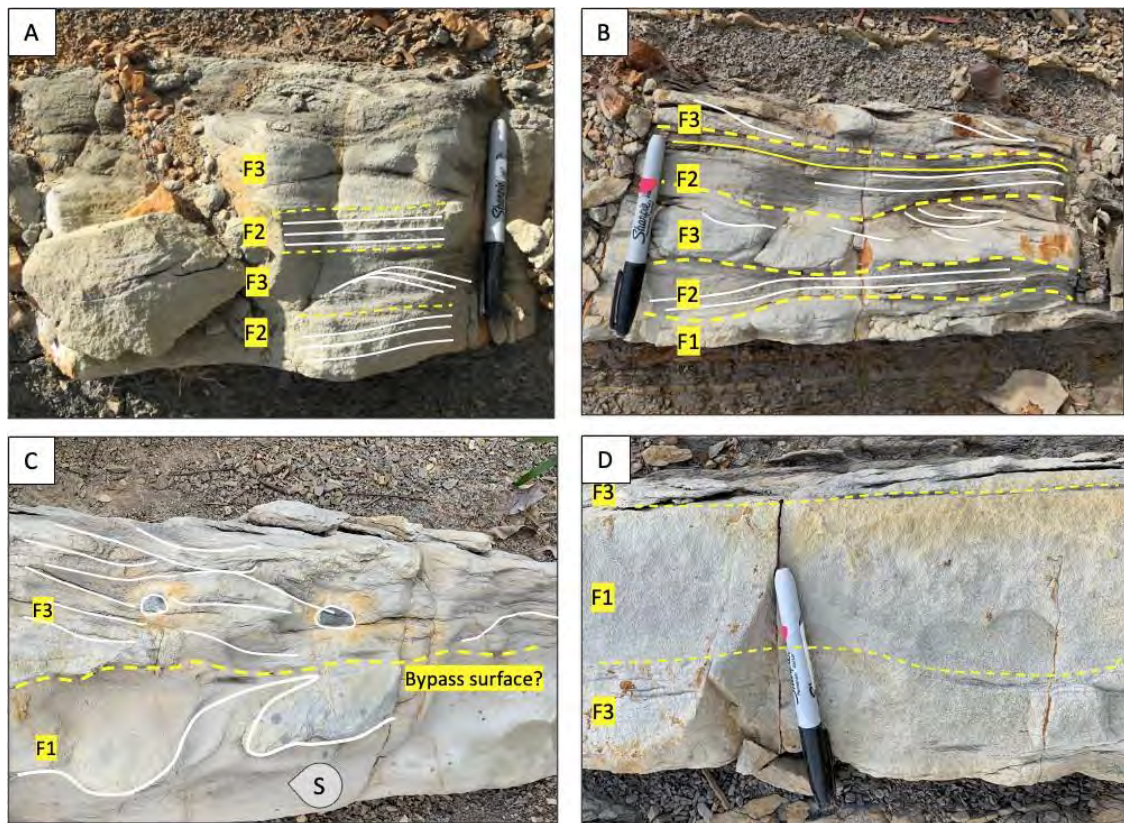


Figure 4.10 Examples of Bed Type 6. (A-B) Ungraded sequence. The beds display alternating F2 and F3 facies – T_{BCBC} sequence. (C) Yellowish brown, moderately sorted, fine- to very fine-grained sandstone. Consists of F1, overlain by F3. Flame structure can be observed on F1. Presence of cm-sized mud clasts. Missing parallel laminated sandstone (F2) may indicate a bypass surface. (D) This bed displays faint F3 at the bottom, then gradually overlain by F1 interval, and overlain by another F3 interval – T_{CAC} sequence.

F1: structureless sandstone, F2: planar-laminated sandstone, F3: cross ripple-laminated sandstone

INTERPRETATION

The vertical arrangement for BT6 indicates deposition from “quasi-steady” (*sensu* Kneller and Branney, 1995; Mulder and Alexander, 2001) or sustained (Jackson and Johnson, 2009) turbidity currents. The vertical variations in the internal structures may be formed due to the fluctuations in the velocity flow, which resulted in the alternations between structureless sands and stratified tractional layers (**Figure 4.11**).

Jackson and Johnson (2009) also observed bed with similar features in the Temburong Formation outcrops at Tanjung Kiamsam (5 km southwest of Kampung Bebuloh). They interpreted that the fluctuation of velocity flow can originate either from (i) hyperpycnal flow, which explains the abundance of carbonaceous clasts / coalified wood fragments, or (ii) collapse of sand-rich mouth bars, resulting in several pulses of flow to occur.

Meanwhile, beds that display structureless sandstone (F1) overlain by cross ripple-laminated sandstone (F3) are indicative of a bypass surface. This bypass of sediment may have occurred during the transition from dense to dilute flow (Mutti et. al., 2003; Tinterri et. al., 2003). As the thickness of the T_A division in this bed type is thin, it may indicate briefer periods when sediment fallout from the flow was sufficiently high that a distinct interface could not form between the deposited bed and the associated flow. As a result, tractional sediment transport and the formation of bedforms could not occur (Mutti, 1992; Talling et. al., 2012)

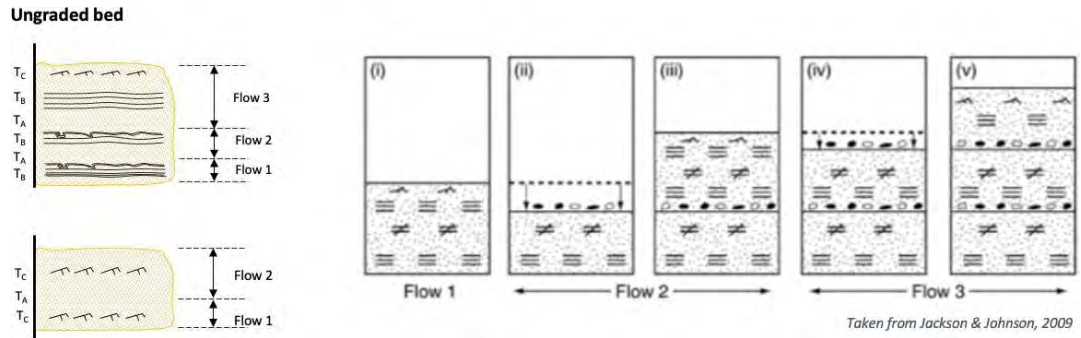


Figure 4.11 Schematic diagram showing the deposition of bed related to three individual sustained turbidity current events. (i) deposition during first flow under fluctuating velocity/discharge conditions; (ii) erosion associated with second flow and deposition of cobbles; (iii) deposition during second flow under fluctuating velocity/discharge conditions; (iv) erosion associated with third flow and deposition of cobbles; (v) waning of third flow and deposition of a fining-upwards, rippled upper interval. (Diagram on the right taken from Jackson and Johnson, 2009)

4.3 BED TYPE ASSOCIATION (BTA)

Based on the bed types observed, overall bed geometry and common presence of muddy heterolithic BT4, it is likely that Temburong Formation in Kampung Bebuloh represents a lobe depositional setting rather than levee-associated environment (see Kane et. al., 2007; Prelat et. al., 2009; Spychala et. al., 2017; Starek and Fuksi, 2017; Kuswandaru et. al., 2018; Shan et. al., 2020).

Bed type associations in this study are identified based on observed vertical assemblages of bed types and the quantitative analysis of the bed thickness distribution. The bed thickness data of each sedimentary log were used to calculate the average sandstone thickness and sandstone beds proportion per log (the ratio of sandstone thickness to the total thickness of the measured interval). Cross-plotting the average of sandstone layer thickness against sandstone beds proportion have shown four distinct trends (**Figure 4.12**).

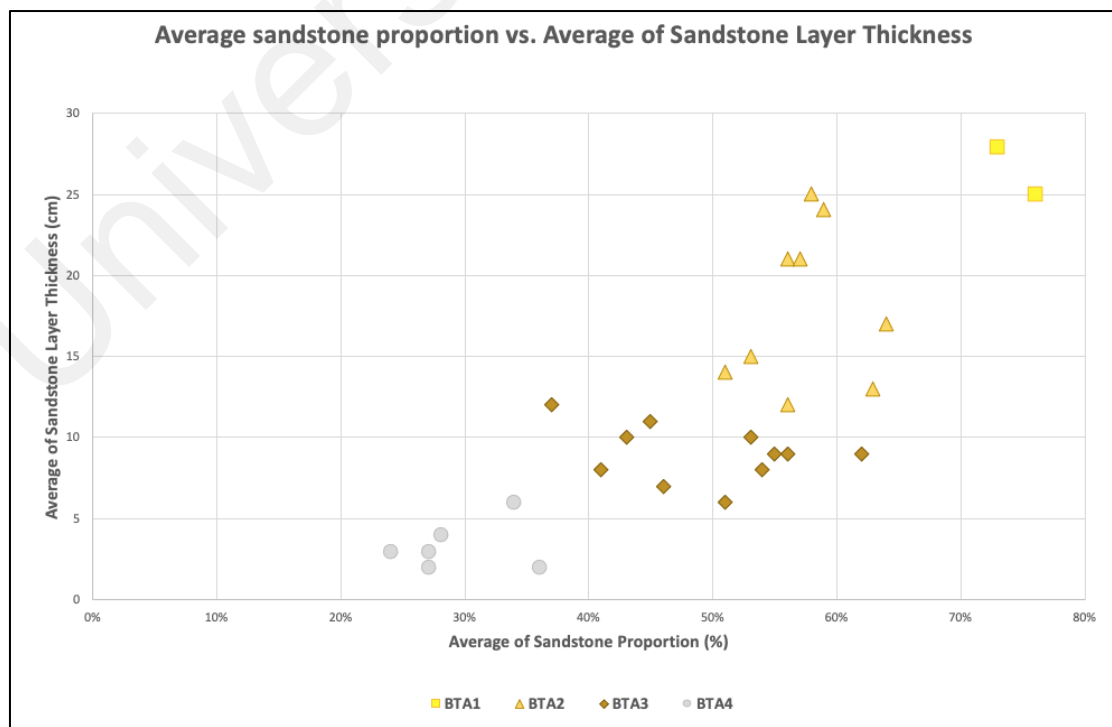
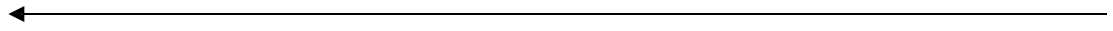


Figure 4.12 Cross-plots of average sandstone proportion vs. average sandstone layer thickness in which four distinct trends were observed. BTA 1 has the highest sandstone proportion and average sandstone layer thickness. BTA 2 has 51% to 64% of sandstone proportion, while BTA 3 has 37% to 56%. BTA 4 has lowest sandstone proportion which is less than 35% (refer Table 4.3).



The outcrop-based lobe hierarchy classification scheme (see Prelat et. al., 2009; Spychala et. al., 2017; Starek and Fuksi, 2017; Kuswandaru et. al., 2018; **Figure 3.10b**) were applied in this study, where the levels of genetically related composite elements, from bed to lobe element and lobe, were defined. Bed type in this study refers to a “bed”, which represents the deposits of a single depositional event. A stacking of bed types forms a “lobe element” which is separated vertically from another lobe element by a laterally persistent thick siltstone (BT4 with an average thickness of less than 0.3 m). Based on Prelat et. al. (2009), thickness of lobe elements in the Tanqua lobe deposits of the Karoo Basin, South Africa ranges from 1 to 3 m. Stacked lobe elements, capped by a thicker mud-dominated succession (average ~0.8 to 2 m), were grouped and assigned as a “lobe” (**Figure 4.13**). Each lobe identified was analysed and classified into several bed type associations, in which represents a different sub-environment in the lobe system comparable to lobe deposits in deep-water fan systems: lobe off-axis, lobe fringe and lobe distal fringe (Prelat et al., 2009; Prelat and Hodgson, 2013; Spychala et. al., 2017).

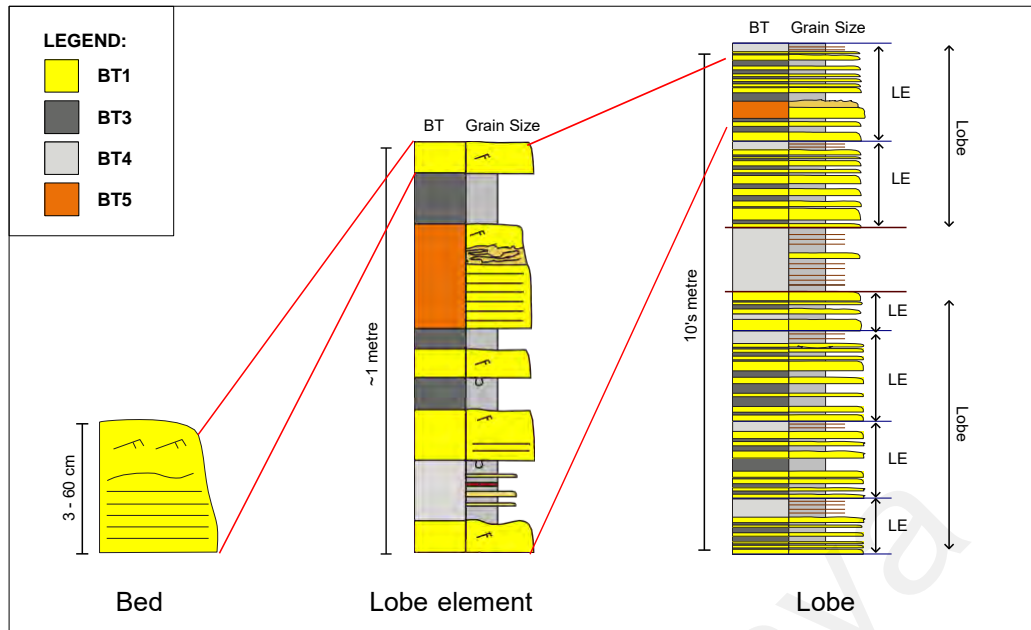


Figure 4.13 Architectural hierarchy of lobe deposits ranging from beds, lobe elements and lobes. A lobe is bounded above and below by fine-grained units (BT4) and consists of several lobe elements.

Five bed type associations were recognized; (i) BTA 1: lobe-off axis, (ii) BTA 2: frontal lobe fringe, (iii) BTA 3: lateral lobe fringe, (iv) BTA 4: lobe distal fringe/distal fan fringe, and (v) BTA 5: slump deposit. Statistical summary and bed type distribution of each bed type association is shown in **Figure 4.14** and **Table 4.3** as below.

Table 4.3 Summary of statistical data of bed type associations in the Early Miocene Temburong Formation, Kampung Bebuloh, Labuan.

BTA	Average of Sandstone Proportion (%)	Average Sandstone Thickness (cm)	Min. of Total BTA Thickness (m)	Max. of Total BTA Thickness (m)	Average of Total BTA Thickness (m)
BTA1: Lobe-off axis	75%	27.4	1.25	9.09	5.17
BTA2: Frontal lobe fringe	58%	15.2	1.35	7.66	3.31
BTA3: Lateral lobe fringe	48%	9.4	1.55	12.50	4.57
BTA4: Lobe distal fringe	29%	3.4	0.87	2.08	1.37

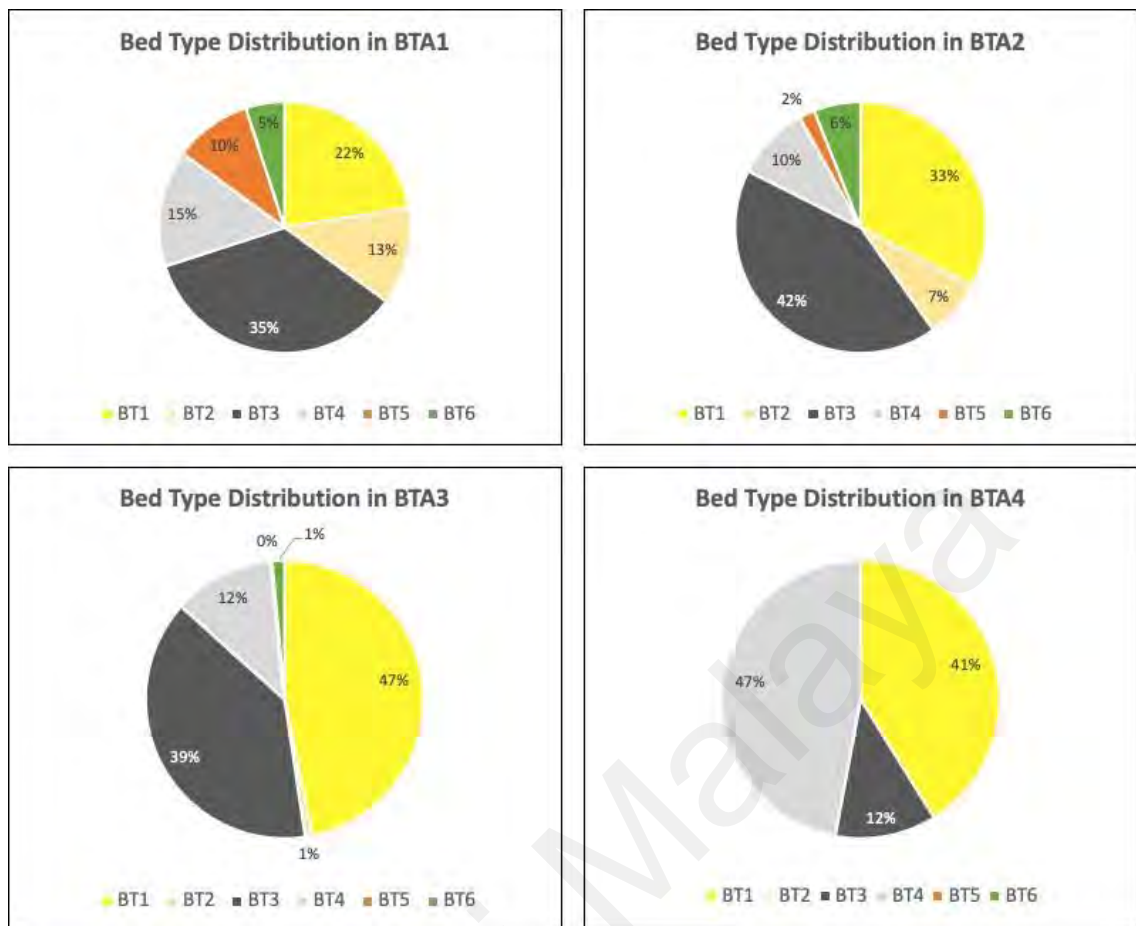


Figure 4.14 Distribution of bed types in each bed type association of the Early Miocene Temburong Formation at Kampung Bebuloh, Labuan

4.3.1 BTA 1: LOBE-OFF AXIS

DESCRIPTION

BTA 1 predominantly consists of medium-bedded sandstone (BT2), hybrid event beds (BT5), and thin-bedded sandstone (BT1), interbedded with mudstone (BT3) and heterolithics (BT4). Overall, BTA 1 is sand-rich, with average of 75% sandstone proportion while the average thickness of an individual sandstone is 27.4 cm. This bed type association can be up to 9 m thick and is known only from two examples in the study area (**Figure 4.15**).

BT2 often displays thicker intervals of parallel lamination (F2) and thin intervals of ripple cross-lamination (F3). Climbing ripple cross-lamination is rarely observed within this BTA. BT5 is common in BTA 1, comprising both bipartite and tripartite beds. Some beds are seen to be amalgamated to form units up to 0.9 m thick. The vertical succession of BTA 1 shows a generally blocky and thickening upward pattern. Beds are tabular in geometry. Long carbonaceous fragments (up to 20 cm) are observed within some BT2 and BT5 beds. Bioturbation is rare within BTA 1, with only *Nereites* and *Scolicia* trace fossils observed.

INTERPRETATION

BTA 1 is interpreted as **lobe-off axis** deposits based on the bed geometry and high sandstone proportion, as compared to the other bed type associations. The higher sandstone proportion and average sandstone layer thickness is attributed to the proximity of these areas to the axis of the lobe at the time of deposition. Even though BTA 1 was mainly deposited by low-density turbidity currents, the dominant presence of BT2 indicates that this BTA was deposited by high energy currents or located more proximally to the main distributary channels. Lower degree of sandstone amalgamation is also

characteristic of an off-axis lobe setting (Prelat et. al., 2009; Prelat and Hodgson, 2013; Kuswandaru et. al., 2018). The common presence of hybrid event beds (BT5) and long carbonaceous fragments further support that this BTA was deposited in a proximal location to the main distributary channel supplying sediment, as compared to other BTAs.

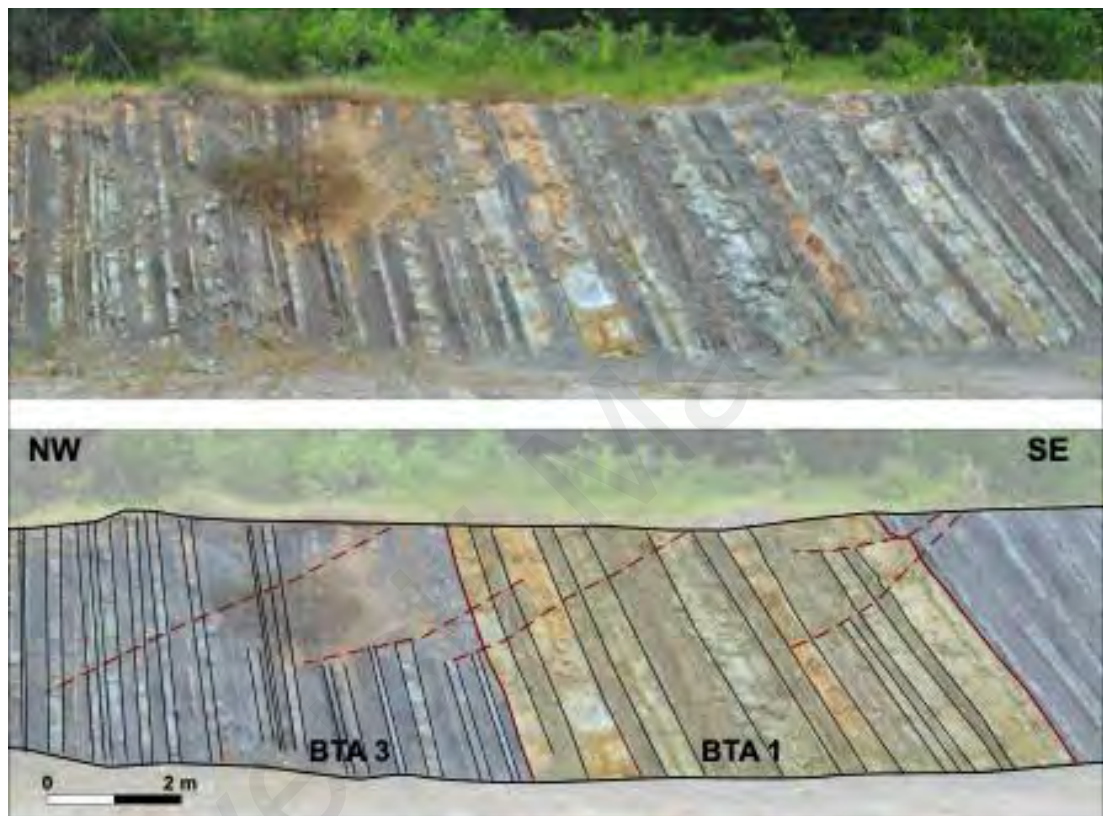


Figure 4.15 Example of BTA 1 from Outcrop B. Younging direction is towards SE direction.

4.3.2 BTA 2: FRONTAL LOBE FRINGE

DESCRIPTION

BTA 2 forms up to 7.66 m thick successions and consists of at least 1 to 3 stacks of lobe element packages. Each lobe element is capped by thin- to medium-bedded BT4 and the thickness of each lobe element ranges from 0.79 up to 3.26 m. Generally, BTA2 displays a tabular bed geometry, but a pinch out geometry was observed at Outcrop A, where the BTA 2 is abruptly overlain by BTA 5.

BTA 2 consists of all bed types described in this study. It is dominated by BT1 (33%), interbedded with BT3 (43%). Medium-bedded sandstone beds BT2 (7%) and ungraded sandstone BT6 (6%) are also observed, while hybrid event beds are rare (only 2%). Grain size in BTA 2 is fine to very fine. The base of the sandstones are slightly erosive with 17% of the beds having flute casts and localized erosional scours. However, not all base of beds are well exposed especially in outcrop B. Overall, BTA 2 is slightly erosional and sand-dominated as the sandstone proportion ranges from 51% to 64%, and average thickness of individual sandstones is around 15.2 cm.

Vertical successions of BTA 2 show both thinning and thickening upward trends. No amalgamation is observed in this BTA. Bioturbation is common; generally dominated by *Nereites*, *Tubutomaculum*, and *Ophiormorpha*. Rare presence of *Zoophycos* and possible *Halopoa* burrows can also be observed. Other graptolites such as *Megagraption*, *Desmagraption* and *Cosmorhapha* are also present within this BTA.

INTERPRETATION

BTA 2 is interpreted as **frontal lobe fringe** deposits based on the predominance of low- to medium-density turbidites with slightly erosional bases, bed thickness trends and bed geometry. Frontal lobe fringe deposits have relatively higher sand-content and more common higher density turbidites and hybrid event beds (Spychala et. al., 2017).

Hybrid event beds are common in lobe fringe environments, particularly in frontal areas (Haughton et. al., 2003; Talling et. al. 2004; Hodgson, 2009; Kane, and Ponten, 2012; Kane et. al., 2017; Fonnesu et. al., 2018; Spychala et. al., 2017). These hybrid event beds are often developed farther down-dip, in response to deceleration of flow due to radial flow expansion from the lobe apex (Kane et. al., 2017; Fonnesu et. al., 2018; Spychala et. al, 2017). This caused the reduction in bed shear stress and flow suspension capacity, in which flows can become transitional to laminar. The finer-grained and mud-prone nature of the Temburong Formation also promoted this flow transformation where the fine suspended load transformed to low yield-strength driven flows as it started losing suspension capacity, hence resulting in the development of a transitional or co-genetic flow (Kane et. al., 2017).

4.3.3 BTA3: LATERAL LOBE FRINGE

DESCRIPTION

BTA 3 forms up to 12.5 m thick successions, with at least 3 to 7 stacks of lobe element packages. Similar to BTA 2, BTA 3 predominantly consists of BT1 (47%) interbedded with BT3 (39%). Each lobe element is capped by medium- to thick-bedded BT4 (12%). Very rare occurrence of medium-bedded sandstone BT2 and ungraded sandstone BT6 can be observed, both only having 1% occurrence within this BTA with thicknesses of less than 30 cm. Bipartite/tripartite beds BT5 is absent. Overall, BTA3 display both thinning and thickening upward trends, and tabular bed geometries.

BTA 3 has lower sand-content as compared to BTA 2, with average of 50% sandstone proportion. The thickness of individual sandstones is not more than 20 cm with average of 9 cm. The base of the sandstone layers are less erosive with 12% of the beds having flute casts and localized erosional scours. Most of the sandstone layers display ripple and climbing ripple cross-lamination, overlain sharply or gradually by mudstone deposits of BT3 and BT4. Rare parallel lamination can be observed near the base of some sandstones. BT5 is rare.

Bioturbation within BTA3 is not common with the average of 20% beds being bioturbated. Overall, the diversity of trace fossil is similar to BTA 2 except BTA 3 has presence of cubichnia traces, i.e., ?*Bergularia* and *Protovirgularia*. The trace fossil assemblage predominantly consists of ichnogenera of the *Nereites* ichnofacies e.g. *Paleodictyon*, *Megagraption*, *Helminthopsis*, *Nereites* and *Cosmorharphe*. *Tubutomaculum* is more common here, as compared to BTA2. *Ophiomorpha* is also commonly observed within this bed type association.

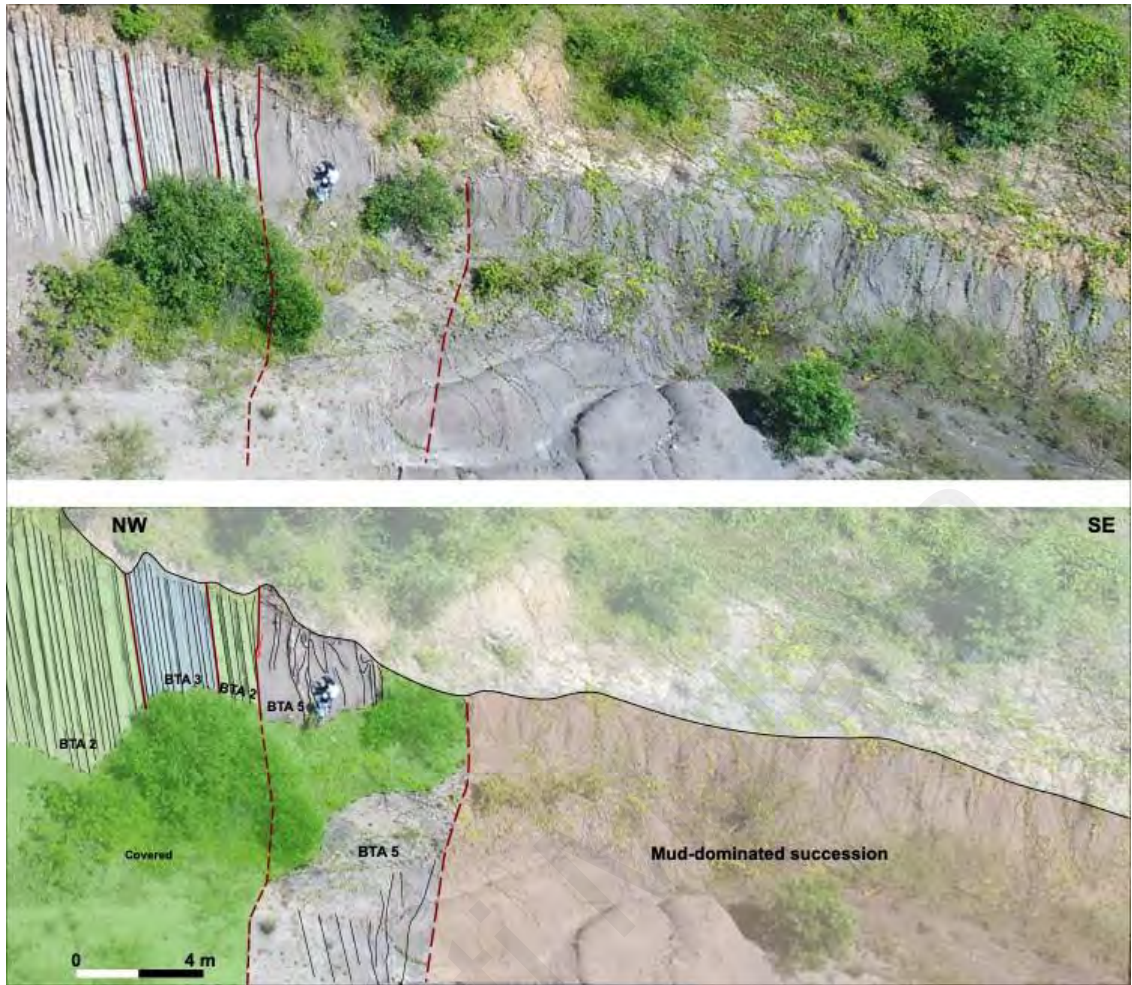


Figure 4.16 Example of BTA 2, BTA3 and BTA 5, from Outcrop A. Generally, BTA 2 has thicker sandstone beds, as compared to BTA 3. BTA 5 was identified based on its folded and heavily deformed strata. The thickness of BTA5 in outcrop A is about ~4 m and was gradually overlain by mud-dominated succession. The boundary between BTA 5 and mud-dominated succession is unclear. Younging direction towards SE direction.

INTERPRETATION

BTA 3 is interpreted as lateral lobe fringe deposits dominated by low density turbidites. The relatively thinner beds and lower sand content of BTA 3 compared to BTA 2 indicate a more lateral position (Spychala et. al., 2017). Lower current velocities would have caused a decrease in flow thickness as the flow moved laterally away from the central flow axis (Luthi, 1981). Lateral lobe fringes commonly show tabular geometries at the scale of outcrop observation (Spychala et. al., 2017). Common presence of *Tubutomaculum* suggests low rates of sedimentation, which further supports a relatively distal location for BTA 3.

4.3.4 BTA 4: LOBE DISTAL FRINGE

DESCRIPTION

BTA 4 is mud-rich and forms successions up to 2 m thick. BTA 4 predominantly consists of silty to muddy deposits of BT4 (47%), interbedded with BT1 (41%). BT3 (12%) can also be observed within this BTA. Average sandstone proportion for BTA 4 is 29%. Individual sandstone beds are less than 10 cm thick, with BT1 only displaying ripple cross-lamination (F3) and no basal erosional surfaces. Bed geometry is tabular and vertical successions usually fine upward. Bioturbation is rare, only in the form of *Tubutomaculum*.

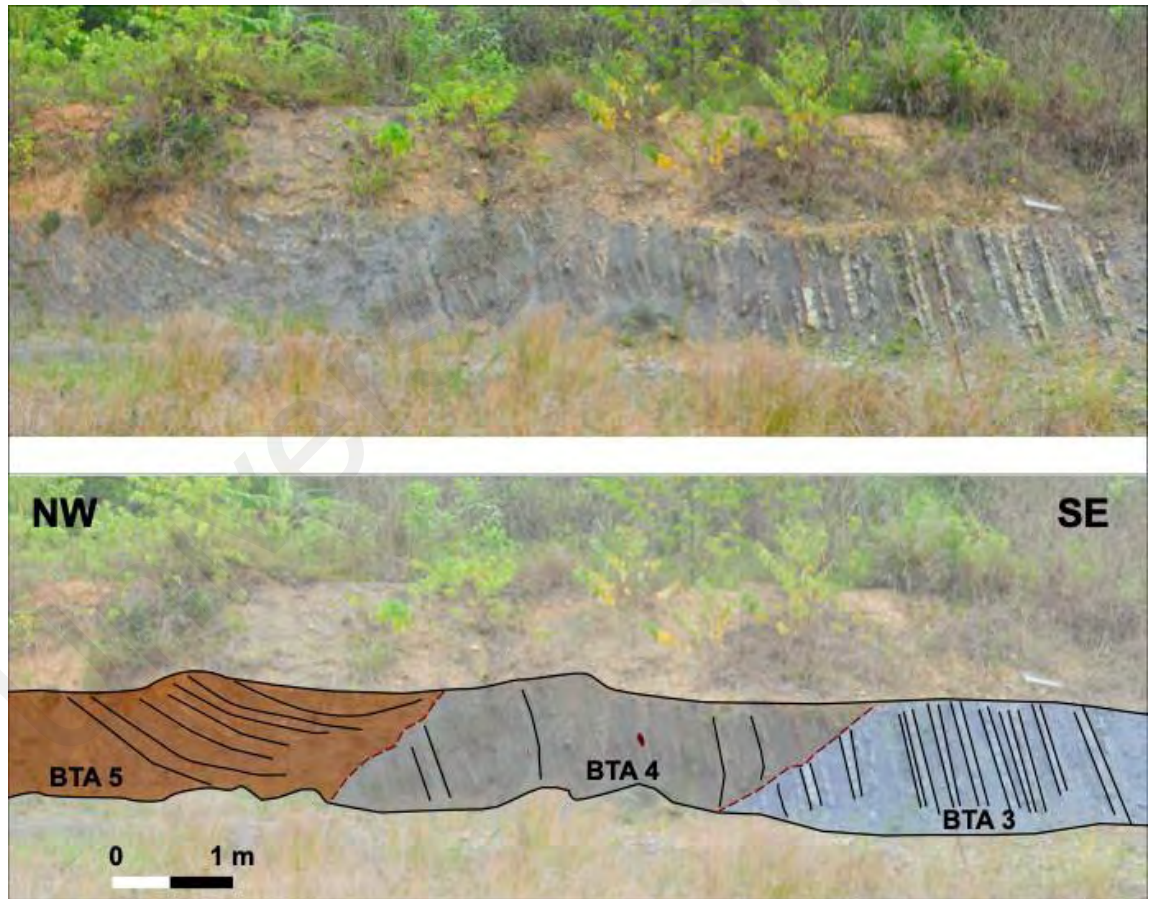


Figure 4.17 Example of BTA 3, BTA 4 and BTA 5 from Outcrop B. BTA 4 is generally mud-dominated, with average of 29% sand proportion. BTA 5 was identified based on its deformed strata. Younging direction is towards SE direction.

INTERPRETATION

Based on the bed thickness trend, absence of BT2 and BT5 and higher mud-content, BTA 4 is interpreted as **lobe distal fringe** deposits (Heard and Pickering, 2008; Prelat et. al., 2009; Spychala et. al., 2017; Kuswandaru et. al., 2018). The dominant presence of F3 also supports this interpretation because ripple-laminated sandstone are common in distal area due to the insufficient energy for grain to move and form parallel lamination (Kane et. al., 2007).

Universiti Malaysia

4.3.5 BTA 5: SLUMP DEPOSITS

DESCRIPTION

BTA 5 comprises mud-dominated chaotic beds. The chaotic beds predominantly consist of BT3, BT4, and BT1. Sandstone is moderate to poorly sorted, mostly display ripple cross-lamination, and some have undergone sideritization and have turned reddish-coloured. Individual siltstone and sandstone layers are roughly <6 cm thick. Note that the total thickness of BTA 5 cannot be measured due to the inaccessible area and poor exposure in the area. However, the maximum observed thickness is 30 m, with a minimum of 4.6 m.

The strata in BTA 5 are folded, heavily deformed and typically display a coarsening upwards succession, where the sandy layers are seen to get thicker upwards. This BTA is bounded by undisturbed beds of BTA 2 and BTA 3. Carbonaceous nodules, siderite layers and clasts were observed. The top and bottom boundaries of BT6 are sharp, with the internal strata having an angular relationship to the truncated underlying and overlying beds.



Figure 4.18 BTA 5 from Outcrop A. BTA 5 was identified based on its folded and heavily deformed strata. Younging direction towards SE direction.

INTERPRETATION

BTA5 is interpreted as **slump deposits**, which are characterized by significant internal distortion of bedding (Posamentier and Martinsen, 2011). This interpretation is made based on (i) presence of intraformational deformational structures such as folds and faults; and (ii) absence of matrix-supported texture with the largest clasts like in debrites.

Slumps probably formed due to the collapse of a sediment pile through slope instability caused by tectonic activity, seismicity or sediment over-steepening. It can be formed on slopes as low as 0.1° or less and can range in thickness from 0.5 m to several hundreds of meters on continental margin slopes (as seen in Posamentier and Martinsen, 2011). In Kampung Bebuloh, thickness of BTA5 can roughly reach 30 m, hence it is reasonable to interpret this BTA as slump deposits.

Jackson and Johnson (2009) observed debrites that range from 1.5 up to 60 m thick in the Temburong Formation at Tanjung Kiamas. Similarly, debrites in Tanjung Kiamas also comprise a matrix of structureless, poorly-sorted, dark grey silty mudstones which contain a variety of clasts. However, clasts are not observed in Kampung Bebuloh, hence this bed type association is shown to be more characteristic of slumps than debrites.

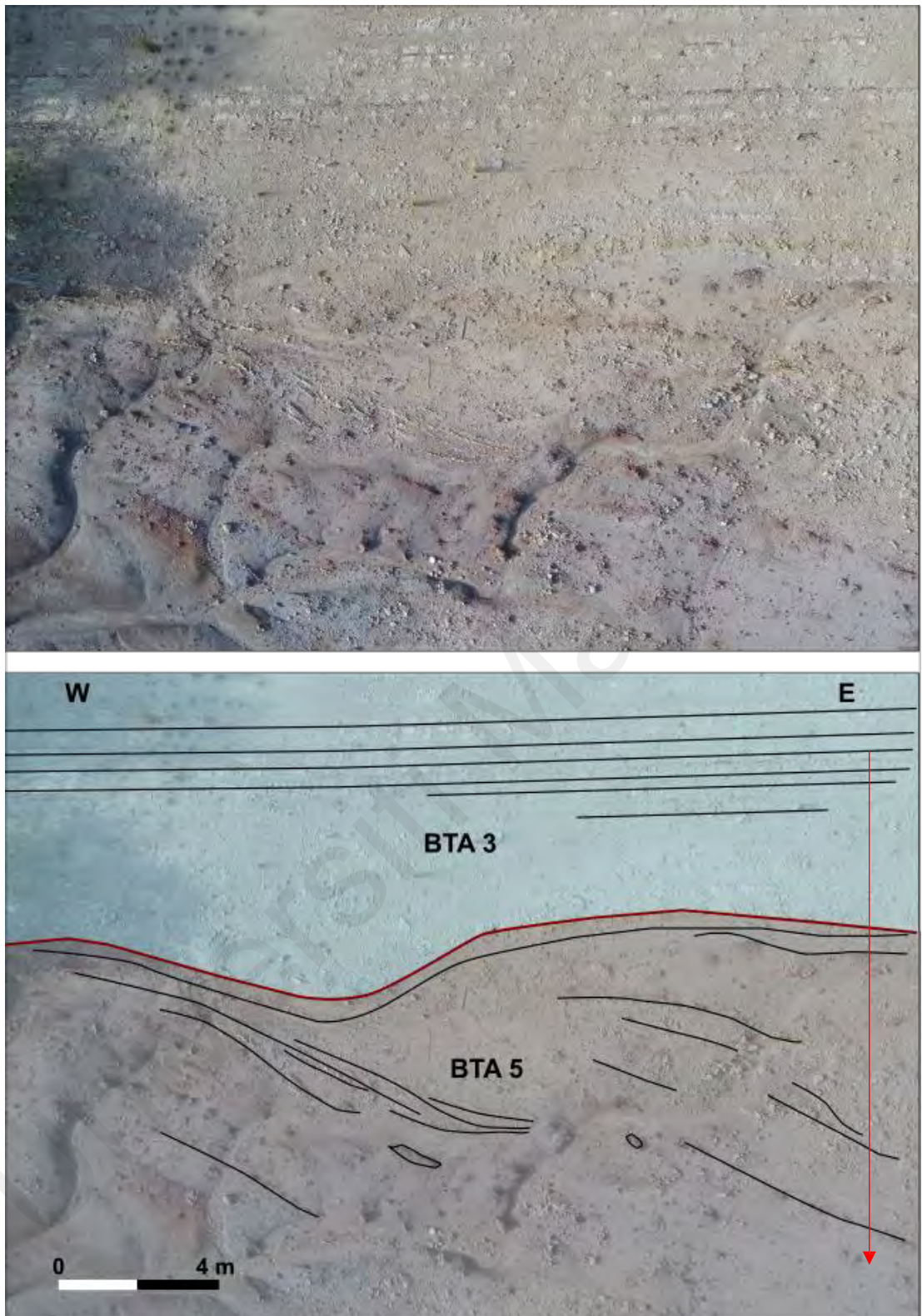


Figure 4.19 Example of BTA 5 from Outcrop A from plan view. The strata within BTA 5 is folded and there are deformed structures and siderite clasts. Red arrow is showing the younging direction.

4.3.6 MUD-DOMINATED SUCCESSION

Thick mud-dominated successions are commonly observed in this study area, where the thickness ranges from 8 to 40 m (**Figure 4.16 and 4.20**). This succession only comprises of dark-grey, mudstone (BT3). However, similar to BTA 5, the detailed observation of this succession could not be recorded due to inaccessibility.

Based on the vertical trend, the mud-dominated succession is interpreted as basin plain deposits. Thick-bedded mudstone facies suggests deposition predominantly from suspension in a quiet, low-energy environments, i.e., the abyssal plain in the deep water system where the hemipelagic/ pelagic sediments are laid down (Abu Bakar et. al., 2007).

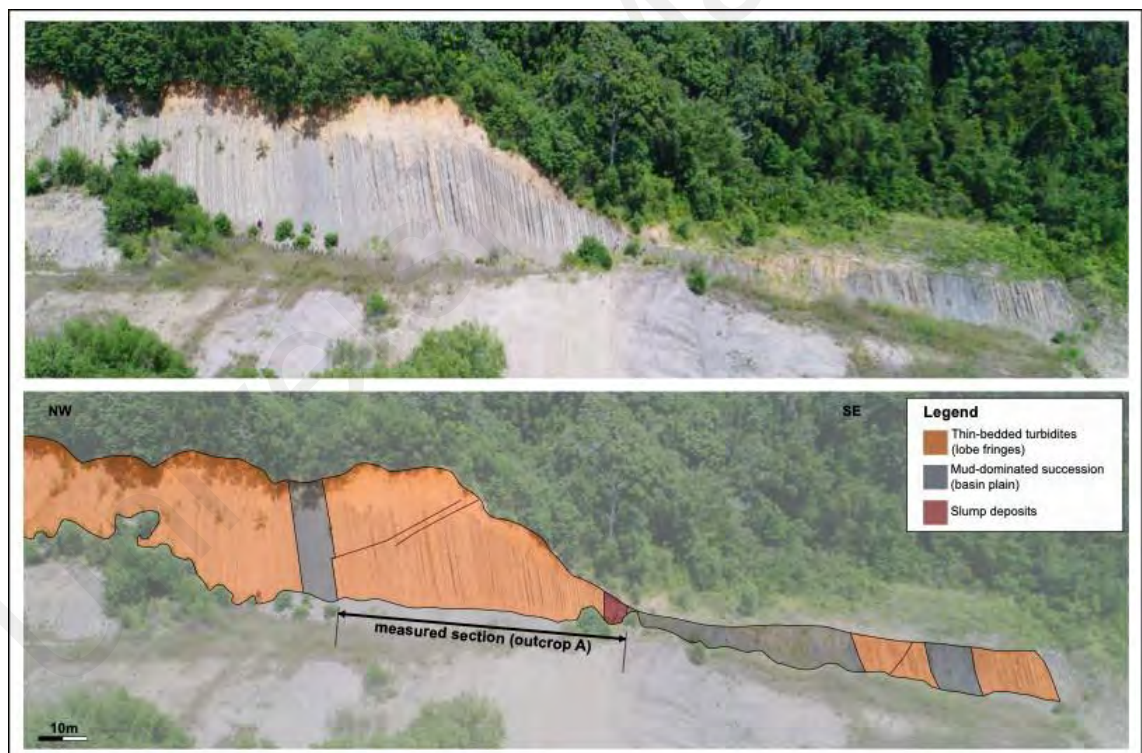


Figure 4.20 Example of mud-dominated succession from outcrop A, Early Miocene Temburong Formation, Kampung Bebuloh, Labuan. Note that red lines represent faults.

4.4 DETAILED SEDIMENTARY LOGS

Outcrop A | Kg. Bebuloh, Labuan | Nov 2018

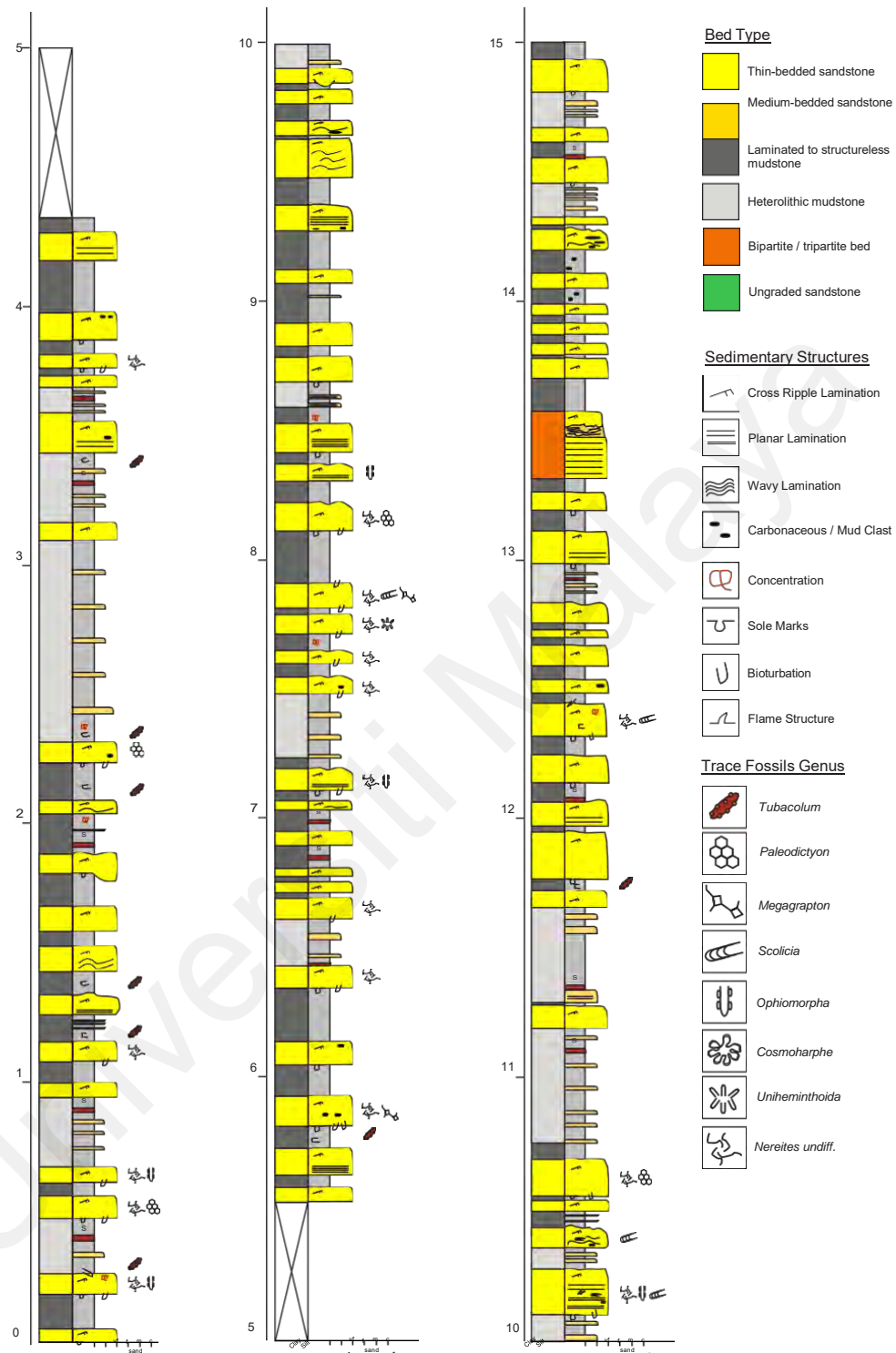


Figure 4.21 Detailed sedimentary logging for outcrop A. Total thickness logged is 47.21 m. Scale is in metre.

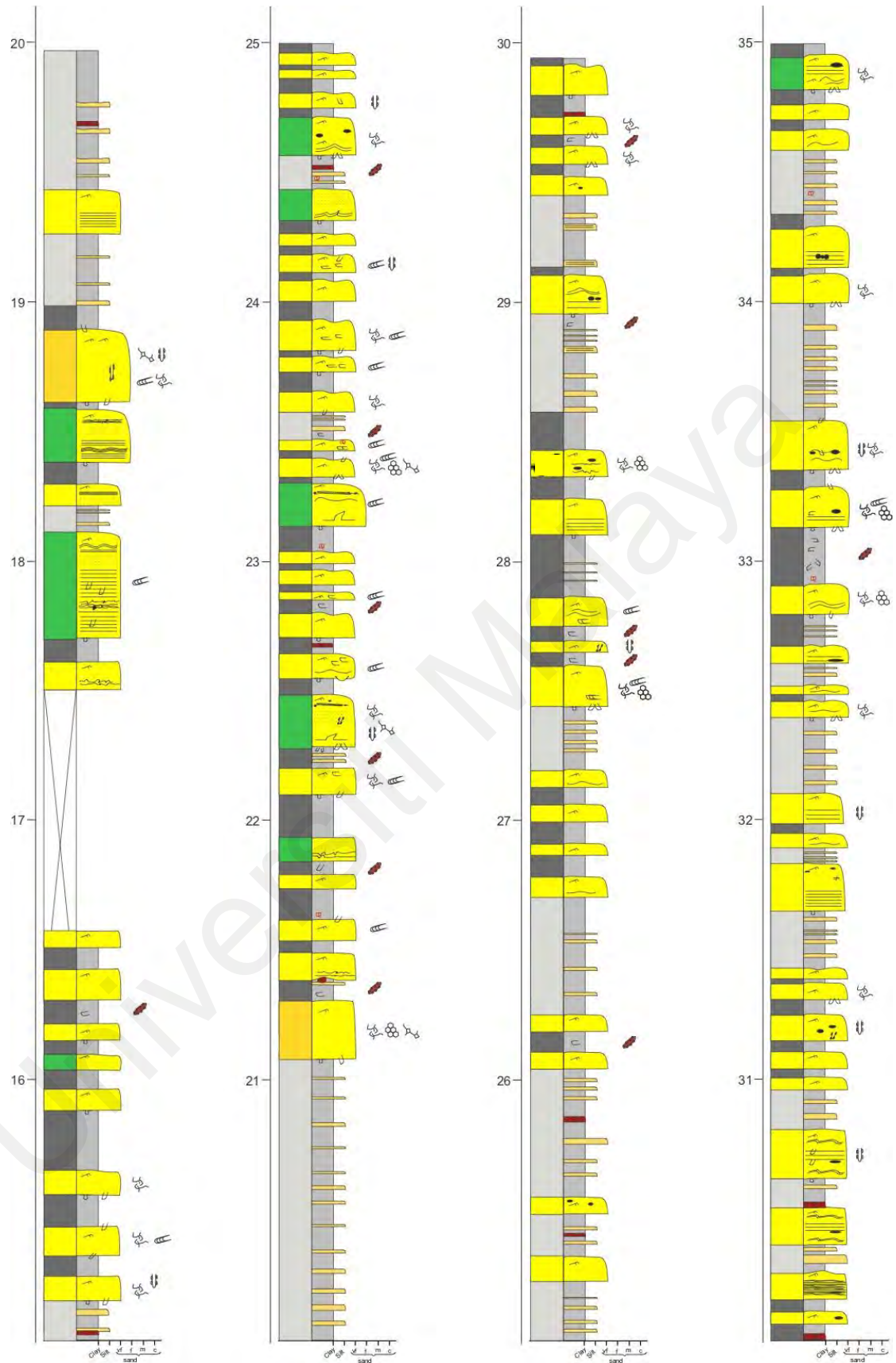


Figure 4.21, continued.

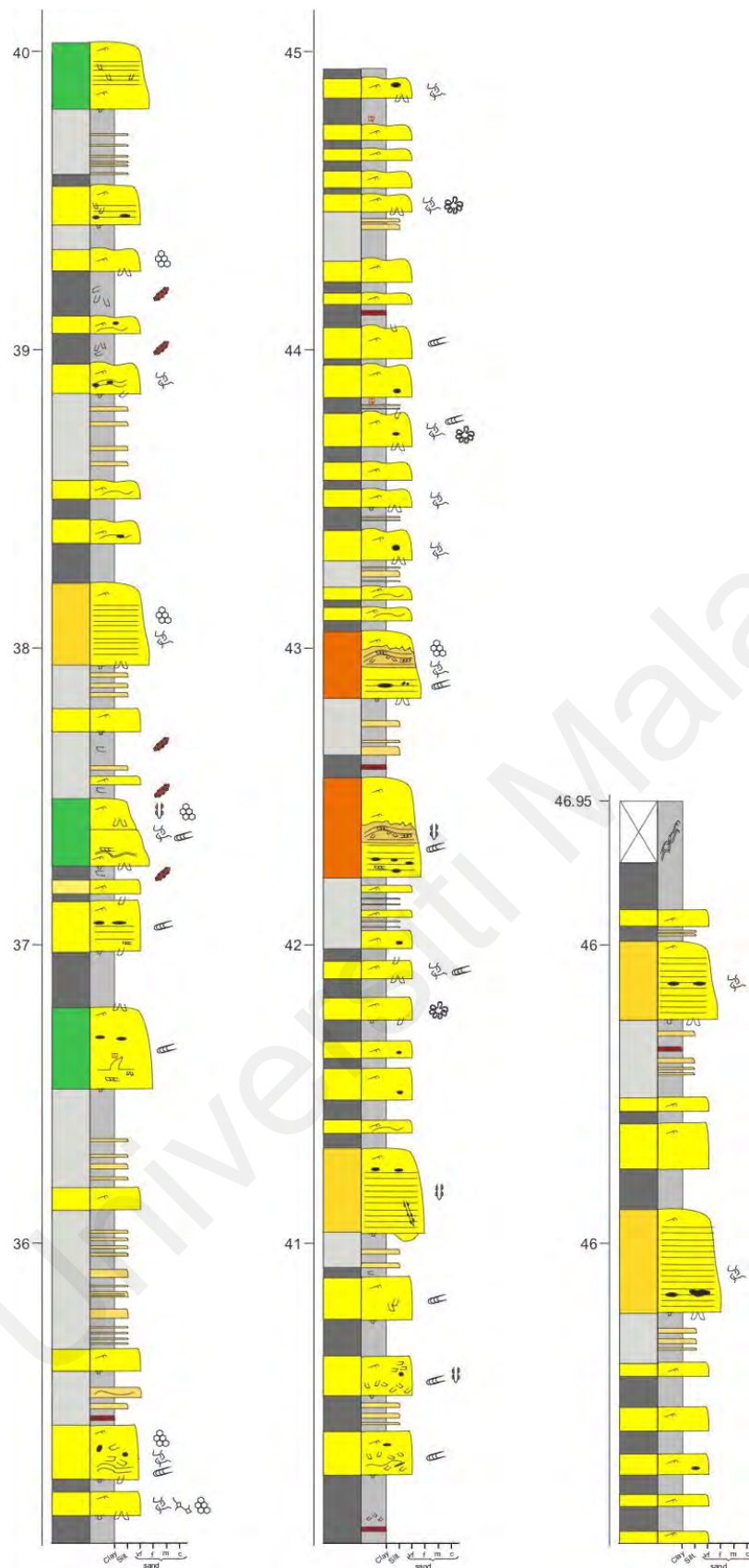


Figure 4.21, continued.

Outcrop B | Kg. Bebuloh, Labuan | Feb 2020

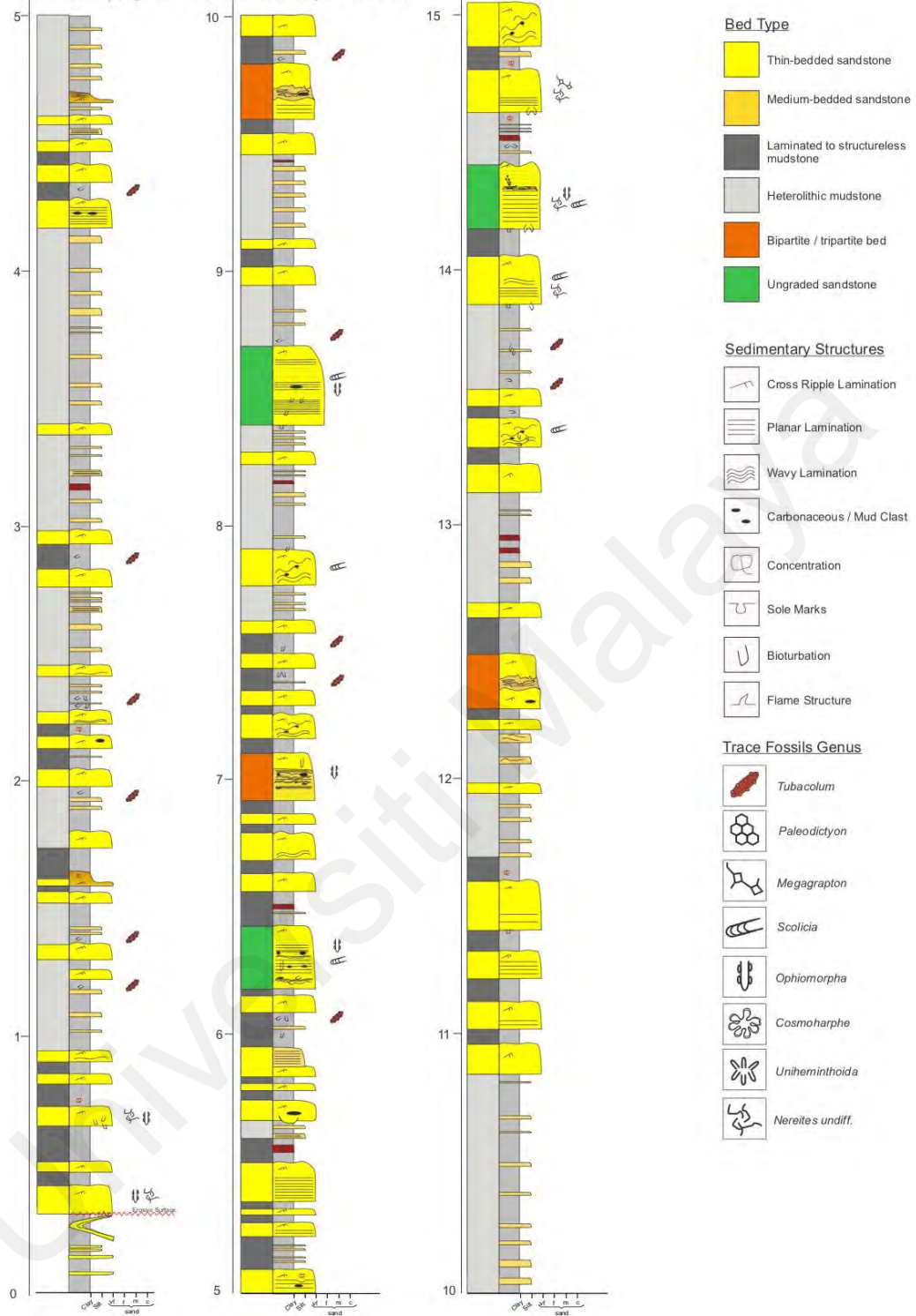


Figure 4.22 Detailed sedimentary logging for outcrop B. Total thickness logged is 54.22 m. Scale is in metre.

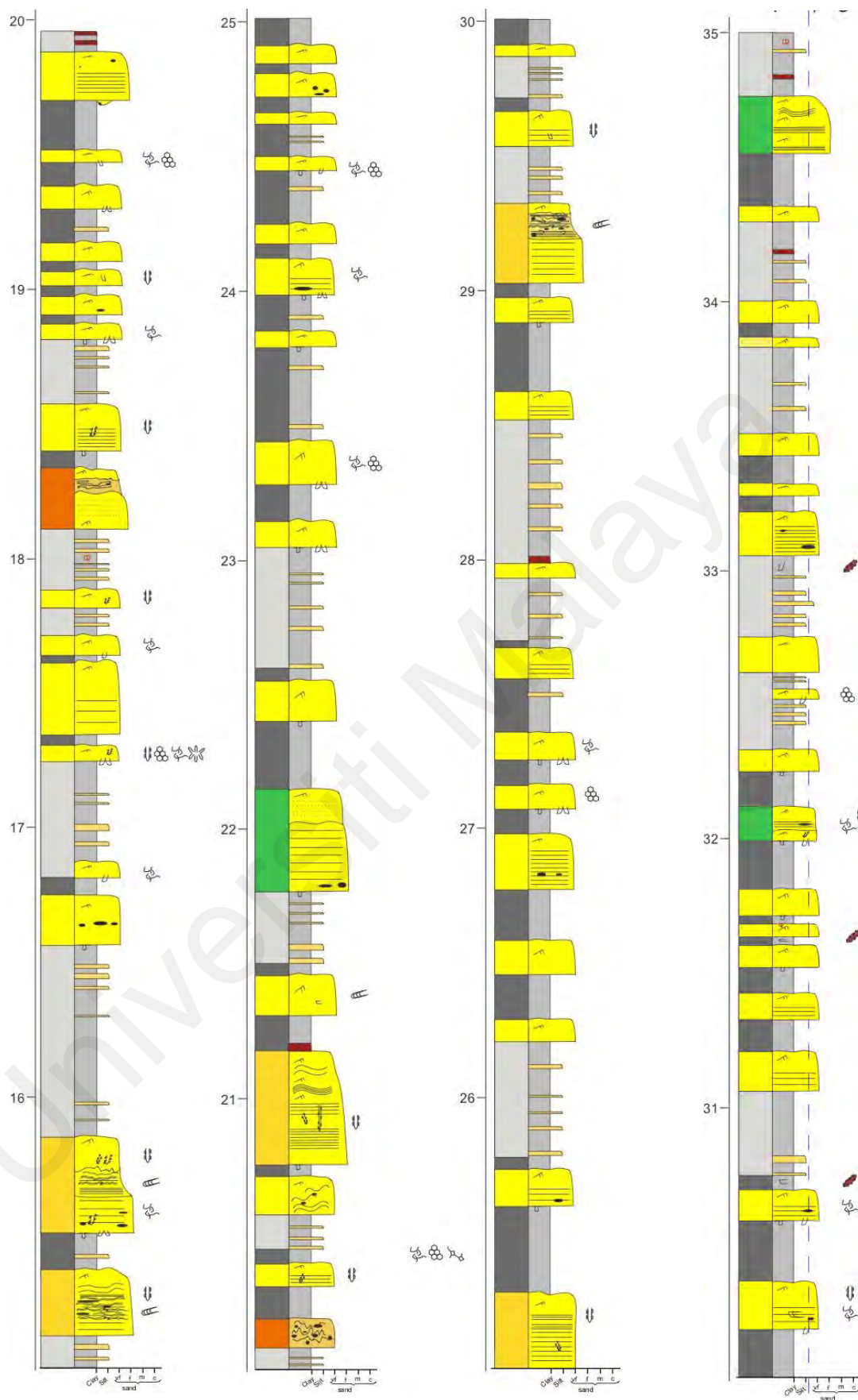


Figure 4.22, continued.



Figure 4.22, continued.

CHAPTER 5: ICHNOLOGY ANALYSIS OF THE EARLY MIOCENE TEMBURONG FORMATION

5.1 OVERVIEW

Trace fossil analysis, if properly done and integrated with sedimentology, palaeontology and stratigraphy of the succession, can be a powerful tool for high-resolution reconstruction of depositional environment (MacEachern et. al., 2007). Originally, the classification of trace fossil assemblages into ichnofacies was seen as a tool to interpret paleobathymetry (Seilacher, 1967). Now, it is widely recognized that the great diversity and disparity of deep sea benthos is also controlled by nutrient supply, and by the general stability through time of this low-productivity environment, rather than by bathymetry alone (Frey et. al., 1990; Seilacher, 2007). The type, morphology, and the diversity of the trace fossils can be a proxy to paleo-environmental parameters such as energy level, substrate stability, salinity variations, and oxygen levels (Frey et. al., 1990; Heard and Pickering, 2008; Cumming and Hodgson, 2011).

The integration of ichnological and sedimentological data in turbidite facies analysis could help to differentiate sub-environments within deep-water systems (e.g., Heard and Pickering, 2008; Monaco et. al., 2010; Cumming and Hodgson, 2011; and Callow et. al., 2012; Hansen et. al., 2017). This chapter aims to describe the distribution and diversity of trace fossils observed in the Early Miocene Temburong Formation at Kampung Bebuloh, Labuan Island. The trace fossil assemblages will then be compared with other published works in order to support the depositional model for Temburong Formation.

Table 5.1 List of ichnogenera and ichnospecies identified in the Early Miocene Temburong Formation, Kampung Bebuloh, Labuan. Ethology classification is mainly taken from previous work, especially from Uchman (1998). Rare occurrence is defined as <5 traces observed.

Toponomic Classification	Ichnogenera/Ichnospecies	Legend	Ethology classification	Occurrence
Epichnial Traces (Trace fossil observed on the top of the beds)	<i>Scolicia prisca</i>	<i>S.pr</i>	Pascichnia	Rare
	<i>Nereites irregularis</i>	<i>N.irr</i>	Pascichnia	Rare
Hypichnial traces (Trace fossils observed on the sole of the beds)	<i>?Bergaueria</i>	<i>Ber</i>	Cubichnia	Rare
	<i>Cosmorhapse lobata</i>	<i>C.lob</i>	Agrichnia	Rare
	<i>Cosmorhapse sinuaso</i>	<i>C.sin</i>	Agrichnia	Rare
	<i>Desmograption</i>	<i>D.alt</i>	Agrichnia	Rare
	<i>Helminthopsis abeli</i>	<i>H.abe</i>	Pasricha	Rare
	<i>Helminthopsis tenuis</i>	<i>H.ten</i>	Pascichnia	Rare
	<i>Megagraption irregulare</i>	<i>M.irr</i>	Agrichnia	Rare
	<i>Megagraption submontanum</i>	<i>M.subm</i>	Agrichnia	Rare
	<i>Ophiomorpha annulate</i>	<i>O.ann</i>	Domichnia	Rare
	<i>Palaeophycus isp.</i>	<i>Pp.tub</i>	Domichnia	Common
	<i>Paleodictyon latum</i>	<i>P.lat</i>	Agrichnia	Common
	<i>Paleodictyon majus</i>	<i>P.maj</i>	Agrichnia	Common
	<i>Paleodictyon miocenicum</i>	<i>P.mio</i>	Agrichnia	Common
	<i>Protovirgularia rugosa</i>	<i>Pr.rug</i>	Cubichnia	Rare
	<i>Spirophycus</i>	<i>Sp</i>	Agrichnia	Rare
	<i>Tubotomaculum mediterraneensis</i>	<i>Tu</i>	Fodinichnia	Common
Endichnial traces (5 Trace fossils observed on the cross section)	<i>Scolicia</i>	<i>S</i>	Pascichnia	Common
	<i>Ophiomorpha</i>	<i>Op</i>	Domichnia	Common
	<i>Nereites</i>	<i>N</i>	Pascichnia	Common
	<i>?Phycosiphon</i>	<i>Ph</i>	Fodinichnia	Common
	<i>?Halopoa</i>	<i>Ha</i>	Pascichnia	Rare
	<i>?Zoophycus</i>	<i>Z</i>	Fodinichnia	Rare

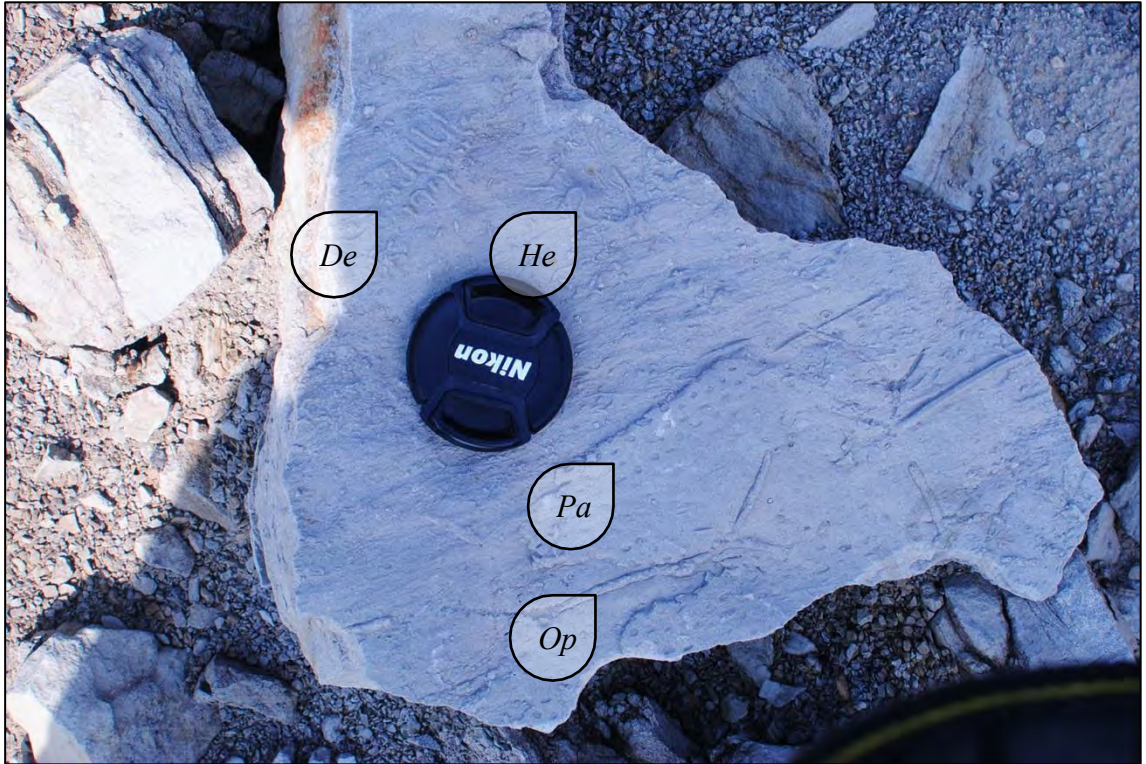


Figure 5.1 Bioturbation observed on the sole of BT1. *De* = *Desmagrpton*, *He* = *Helminthopsis*, *Pa* = *Paleodictyon*, *Op* = *Ophiomorpha*

5.2 DESCRIPTION OF TRACE FOSSILS

5.2.1 COSMORHAPHE

Cosmorhapse is observed on the soles of BT1. It is an unbranched, graphoglyptid trace fossil that can be easily recognised by its hypichnial, two-order meanders (Seilacher, 1977; Uchman, 1998; Fan et. al., 2018).

Two ichnospecies were observed in Temburong Formation. First is *C. lobata*, which has fairly dense first order meanders, and containing 8 to 16 turns of regular second order meanders. The second ichnospecies *C. sinuosa* is smaller, displaying widely spaced, complex and random meandering patterns. *C. sinuosa* is more commonly observed in this study, as compared to *C. lobata*.

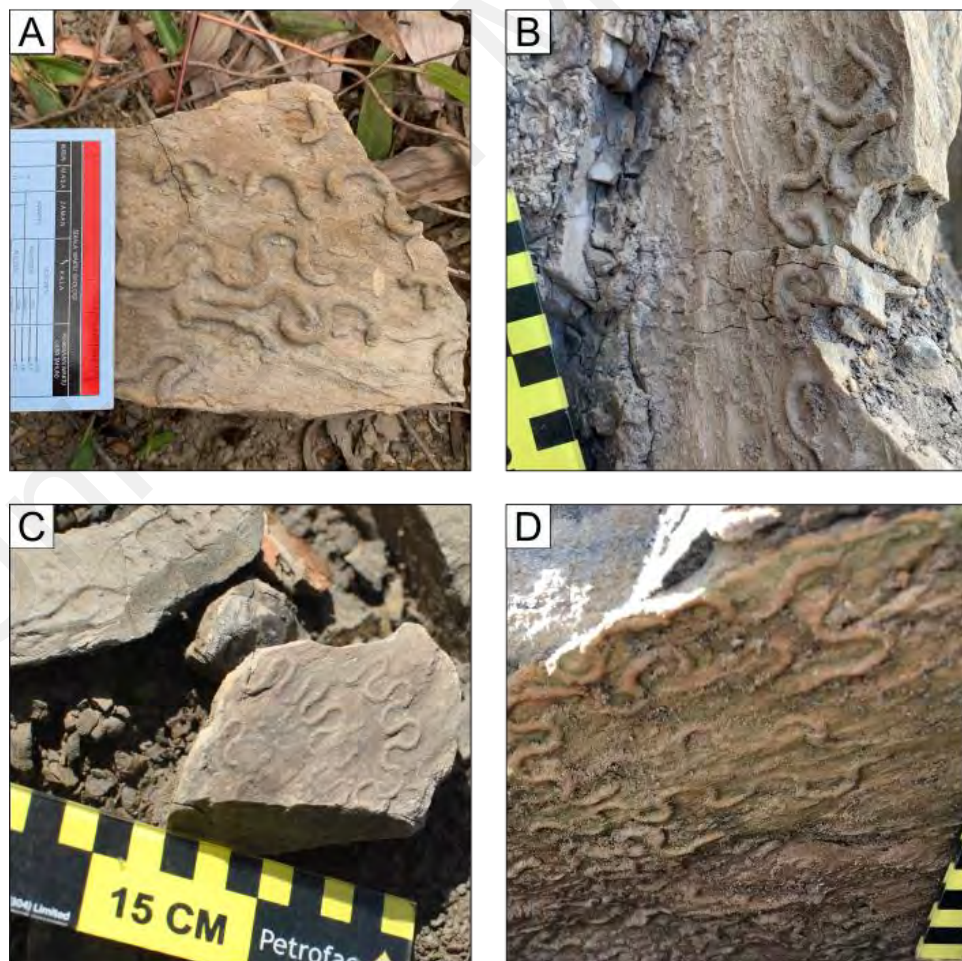


Figure 5.2 Examples of *Cosmorhapse*. (A-B) *C. sinuosa* displaying a random, complex meandering pattern. (C-D) *C. lobata* displaying 2-order meanders.

5.2.2 DESMOGRAPTON

Desmograption is present as hypichnial traces, often on the sole of BT1, in the form of long semi-parallel tubes and U-shaped connecting tunnels (Uchman, 1995; Fan et. al., 2018). It is one of the most common graphoglyptid trace fossils observed in the study area and usually co-occurs with *Paleodictyon*.

This trace fossil can be easily confused with *Urohelminthoida*, but *Desmograption* usually has two connected component series, semiparallel tube series and alternate connecting-tunnel series, while *Urohelminthoida* only has one straight or gently undulated connecting component (**Figure 5.3**, Fan et. al., 2018).

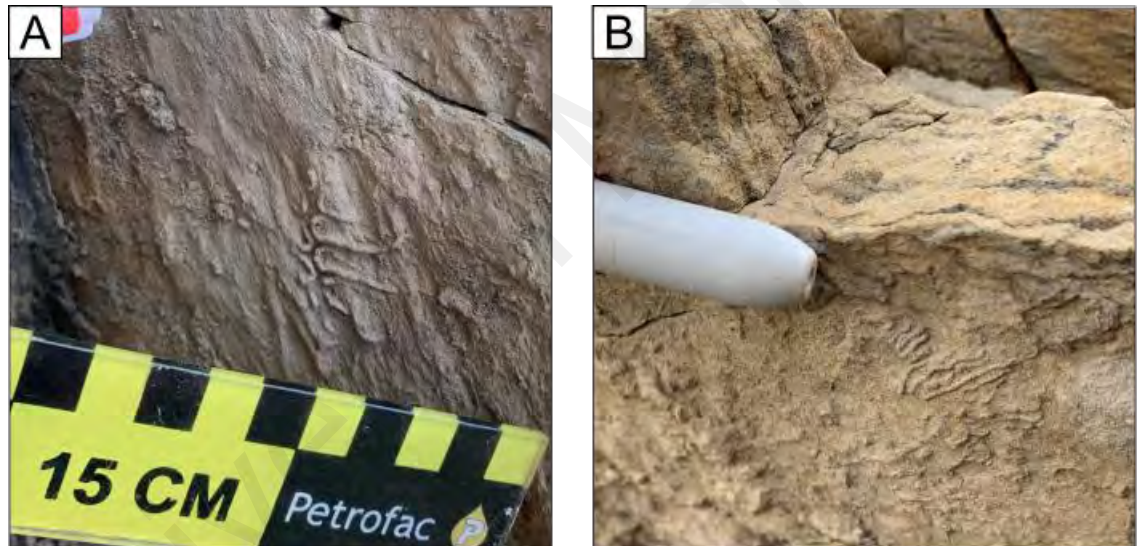


Figure 5.3 Examples of *Desmograption* in study area.

5.2.3 HELMINTHOPSIS

Helminthopsis is present on the sole of BT1 and BT2. The ichnogenus is observed as hypichnial, unbranched, loosely winding or meandering traces, with no straight segments or loops (Uchman, 1998).

Two ichnospecies have been identified, based on the shape of the meanders. *H. abeli* often displays bell-shaped segments, while *H. tenuis* displays repeated, wide, shallow meanders and deeper narrow but obtuse meanders (**Figure 5.4**).

Ksiazkiewicz (1977) interpreted *Helminthopsis* as a grazing trail (pascichnia), which may have been produced by deposit-feeding organisms.

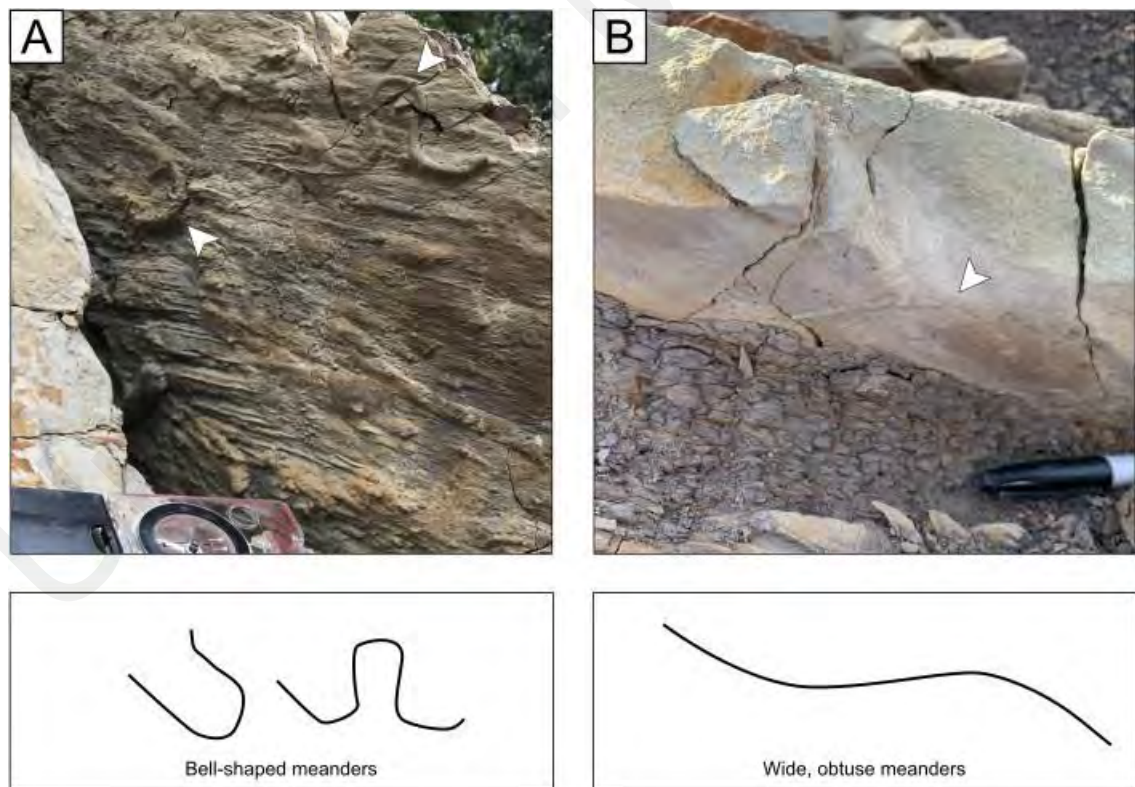


Figure 5.4 Examples of *Helminthopsis* in the study area. Note the difference in the meandering shapes. (A) *H. abeli*. (B) *H. tenuis*.

5.2.4 MEGAGRAPTON

Megagraption is a graphoglyptid trace fossil found on the sole of BT1. It can be easily recognized by its irregular network, and preserved as hypichnial, branching. In this study area, it consists of meshes bounded by smooth to slightly winding strings with a diameter of up to 55 mm.

Megagraption in the studied sections most probably belong to *M. irregulare* which has a single connected network and the branching observed is often at approximately right angles (Uchman, 1998; Fan et. al., 2018).

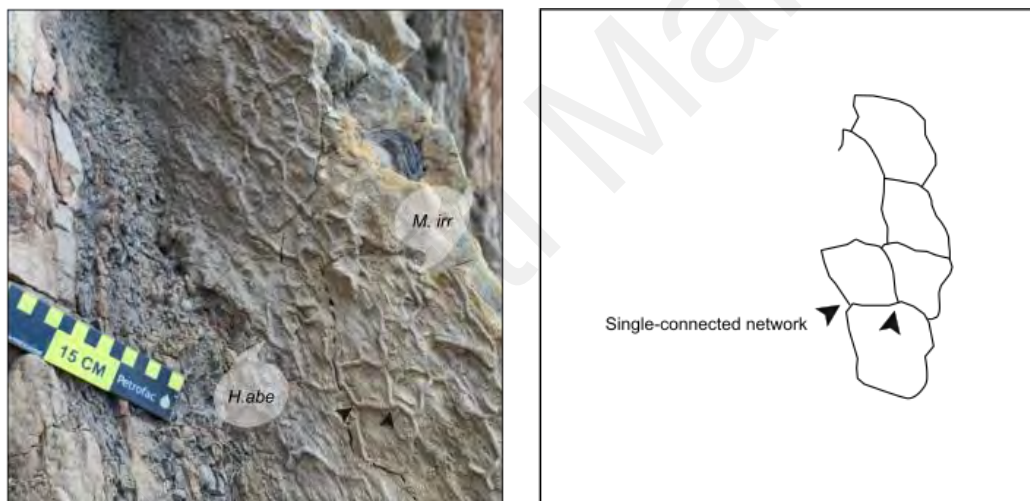


Figure 5.5 Example of *Megagraption* in the study area. The arrow is showing single-connected network. The angle of branching is approximately at right angle.

M. irr = *Megagraption irregulare*, *H.abe* = *Helminthopsis abeli*

5.2.5 NEREITES AND ASSOCIATED BIOTURBATED FABRIC

Nereites is commonly observed in the study area as endichnial traces within BT1, BT2 and BT6, which can produce moderate to intensely bioturbated fabrics. In moderately bioturbated beds, *Nereites* occurs as dark, mud-rich, ellipsoidal burrows with a lighter concentric halo within siltstone or very fine-grained sandstone (**Figure 5.6A**). This burrow can sometimes be mistakenly identified as clasts, but the burrows are flat in cross-section.

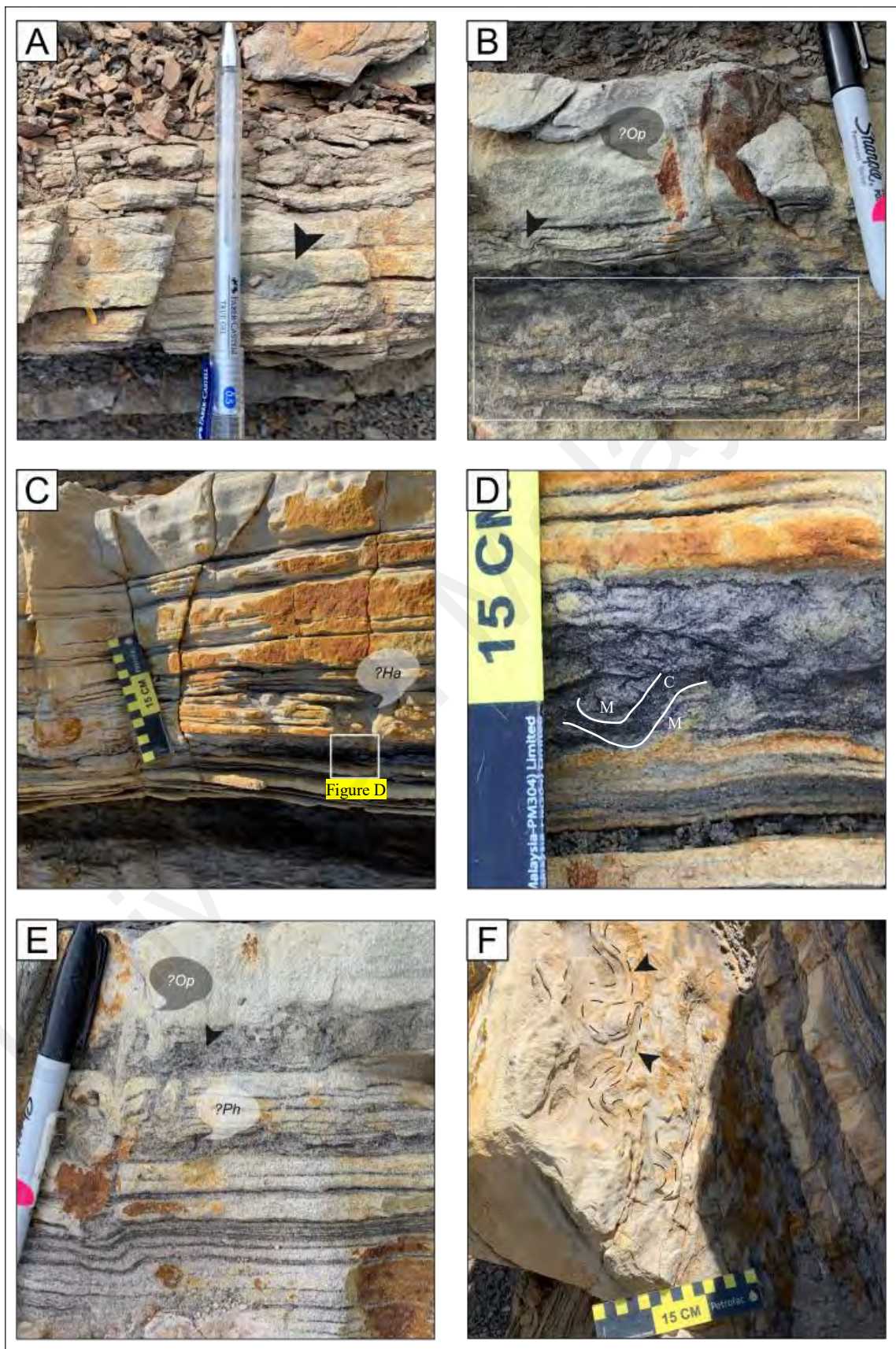
One epichnial *Nereites irregularis* was identified at the top of a BT6 (**Figure 5.6F**). This trace fossil was recognized based on its unbranched, meandering to winding furrow, consisting of an actively filled central core and a thick lobed mantle (Uchman, 1995). It is about 6 mm wide and displays an irregular meandering pattern. *Nereites* is classified as pascichnia trace based on its locomotion and feeding activity (Uchman, 1998).

Nereites can occur together with *Phycosiphoniform* (*sensu* Bednarz and McIlroy, 2009) and both ichnogenera have similar morphological characteristics (i.e., dark core surrounded by a lighter halo) (Callow et. al., 2012; Knaust, 2017). However, *Phycosiphoniform* has a smaller burrow (less than 1 mm), and often displays a ‘frog-spawn’ texture (Bednarz and McIlroy, 2009). The oblique burrow observed in the study area is considered large, with a diameter of up to 10 mm, which is consistent with the description for *Nereites* (Uchman, 1995; Callow et. al., 2012; Knaust, 2017). There was also no ‘frog-spawn’ texture observed within this bioturbated fabric.

However, within some intensely bioturbated beds, it was difficult to distinguish between these two trace fossils and to identify other possible traces that are often associated with *Nereites* (i.e., *Planolites*, *Chondrites*, *Palaeophycus*, *Taenidium*). Additionally, there is also lack of outcrop examples of *Nereites* in vertical cross-section recorded from published works, hence limiting our comparisons. Nevertheless, this trace fossil resembles *Nereites* in sectioned core, as shown in Knaust (2017, their figure 5.79). It must be noted that there are many possible ichnotaxa which could have produced the bioturbated fabric observed in Kampung Bebuloh, but more work is required before many taxa can be convincingly recognized in vertical cross section. Having thin sections or clean and fresh slabs of the bioturbated fabric would help for future work, but for the time being I interpret this bioturbated fabric as being mainly comprising *Nereites*.

Figure 5.6 Examples of *Nereites* in the study area. (A) Endichnial trace of *Nereites*. Presence of lighter halo around the dark coloured burrow. No ‘bulging’ appearance indicates that this is not a mud/carbonaceous clast. (B) Intensely bioturbated fabric (white box) due to the *Nereites*. Arrow is showing possible ?*Halopoa* burrow. (C) The bottom part of the bed has moderate bioturbated fabric due to *Nereites*. Co-occurred together with dwelling traces, which could be ?*Halopoa*. (D) is showing a close-up photo of the bioturbated fabric, where a complex muddy core (C) surrounded by sandy mantle (M) can be observed. (E) Bioturbated fabric within BT2 due to the colonization of *Nereites* and ?*Phycosiphoniform*. Co-occurred together with the ?*Ophiomorpha* burrow. (F) Epichnial trace of *N. Irregularis*, displaying irregular meandering pattern.

?Op = ?*Ophiomorpha*, ?Ha = ?*Halopoa*, ?Ph = *Phycosiphoniform*



5.2.6 OPHIOMORPHA

Ophiomorpha is one of the most common trace fossils observed in the studied sections, which is often observed within BT1 and BT2. This trace fossil is mostly preserved as endichnial, straight to slightly curved burrows with meniscate filling. The diameter of the burrow is less than 15 mm and the length is up to 200 mm. It also can be observed as hypichnial, with smooth walls and typical Y-shaped branching.

Due to its smaller size and smooth surface, this trace fossil is identified as *O. annulata* (Uchman, 1998). *O. annulata* is often observed with swellings (up to 7 mm in diameter) at the sharp-angle branching points, and a few traces display very short branches with dead ends. *Ophiomorpha* is commonly interpreted as dwelling structures, representing the domichnia group.

Hypichnial, long traces (no preservation of branching) of *O. annulata* can be distinguished from *Halopoa* because *H. imbricata* is often unbranched and covered with longitudinal irregular ridges or wrinkles, which are composed of several imperfectly overlapping cylindrical probes. Meanwhile, *O. annulata* in the Temburong Formation forms smooth, branching traces. Branched *Halopoa*, *H. annulata* is not considered as it only ranges until the Lower Oligocene (Uchman, 1998).

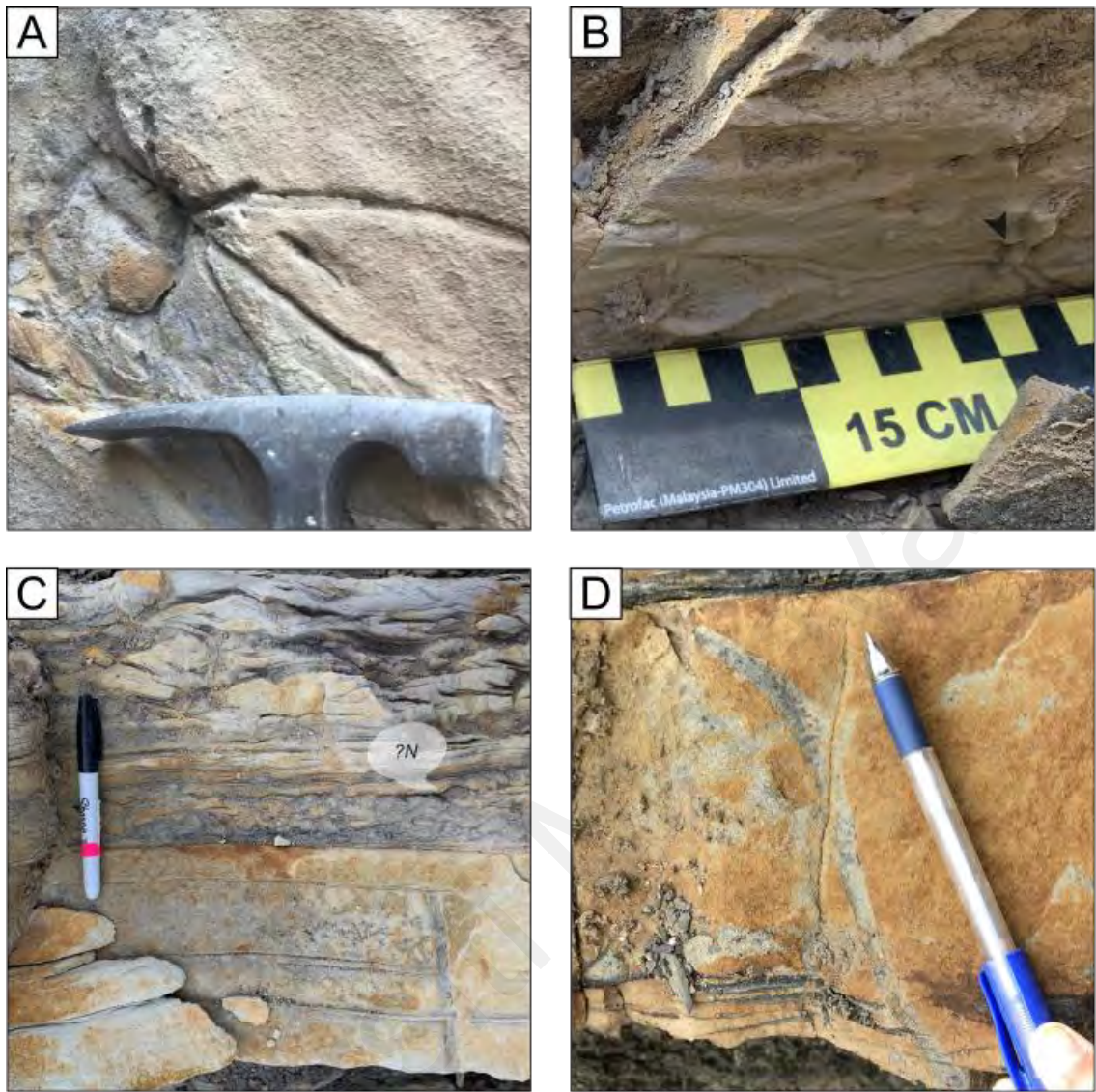


Figure 5.7 Examples of *Ophiomorpha* in the study area. (A – B) *O. annulata*, preserved as hypichnial furrow on the soles of BT1. Arrow in (B) is showing swelling at the sharp branching. (C – D) *Ophiomorpha* preserved as endichnial burrows.

?N = ?*Nereites*

5.2.7 PALAEOPHYCUS

Palaeophycus is found on the sole of BT1, and is often characterized by hypichnial, winding, rarely branched tubular burrows. The observed fossils are simple, straight or gently curved and have diameters ranging from 4 to 10 mm.

Palaeophycus in Temburong Formation resembles the specimens described by Madon (2021) in the West Crocker Formation. The observed trace fossils are unlined and only observed as hypichnial semirelief. Uchman et. al. (2004) has described similar specimens and classified it as cf. *Planolites* due to the absence of lining. However, this trace fossil has smooth exteriors, which may indicate the presence of a lining (Madon, 2021), and the sediment infilling is also typically of the same lithology and texture as the host bed (Pemberton and Frey, 1982; Uchman, 1998; Hammersburg et. al., 2018)

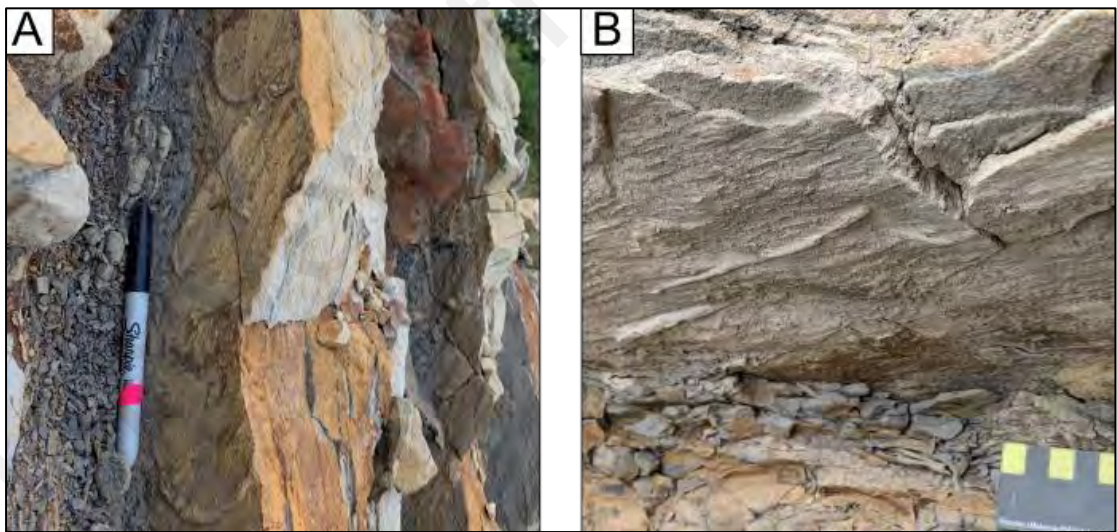


Figure 5.8 Examples of *Palaeophycus* traces in the study area. (A) *Palaeophycus* displaying slightly curved burrows. (B) Simple, straight, unbranched *Palaeophycus* burrows.

5.2.8 PALEODICTYON

Paleodictyon is often observed at the base of BT1 and can be easily recognized due to its regular hexagonal meshes bordered by semi-cylindrical ridges (between 1 and 2 mm thick), forming hypichnial honeycomb-like imprints. The mesh size observed is commonly between 2 – 8 mm. At least three ichnospecies of *Paleodictyon* were observed in the study area; *P. majus*, *P. latum*, and *P. miocenicum*.

Ichnospecies of *Paleodictyon* were assigned based on the mesh-size and the type of network connection. *P. majus* is medium-sized with a mesh-size of 6 to 14 mm, while *P. latum* is considered as small-sized with a mesh-size of up to 2 mm. *P. miocenicum* is considered as a single connected network, with a mesh-size of between 2 to 6 mm (Uchman, 1998; Fan et. al., 2018).

Paleodictyon is one of the graphoglyptid trace fossil, and is interpreted to represent agrichnia traces (Cumming and Hodgson, 2011).

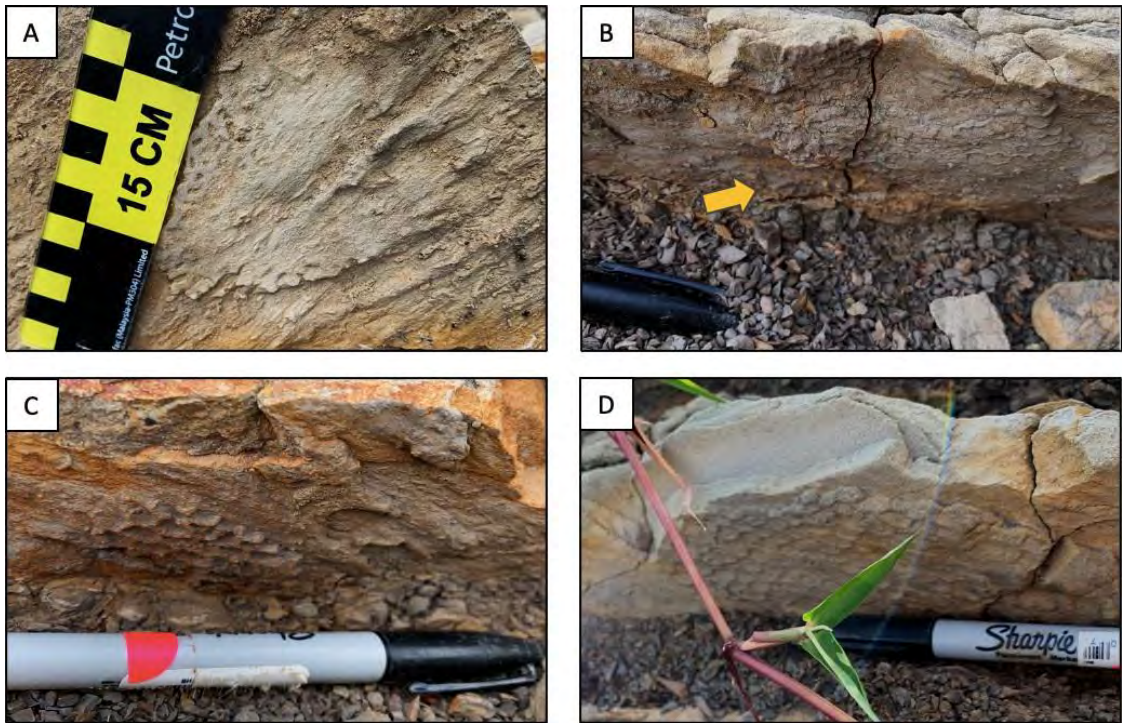


Figure 5.9 *Paleodictyon* ichnospecies observed at the base of BT1: (A) *P. latum* with mesh-size around 1 to 2 mm; (B) *P. miocenicum* with mesh-size around 4 mm; (C, D) *P. majus* with a mesh-size of 6 to 8 mm.

5.2.9 SCOLICIA

Scolicia traces in the Temburong Formation are commonly observed within BT1 as epichnial furrows. Its morphology is winding and meandering, with bilobate oblique slopes showing inclined ribs (Uchman, 1998), with the furrow's diameter reaching up to 30 mm. The ichnospecies is identified as *S. prisca*, and it is often preserved at the junction between fine-grained (F3) sandstone and the overlying fine-grained siltstone (F4) or mudstone (F5).

Scolicia is also observed as endichnial traces, displaying horizontal to sub-horizontal burrows filled with dense meniscate laminae, with the diameter around 10 to 20 mm. It often occupies the top tier of the sandstone, within the silty or carbonaceous laminae (Knaust, 2017).

Scolicia is interpreted as a grazing trace (pascichnia) produced by irregular echinoids (Uchman, 1995).

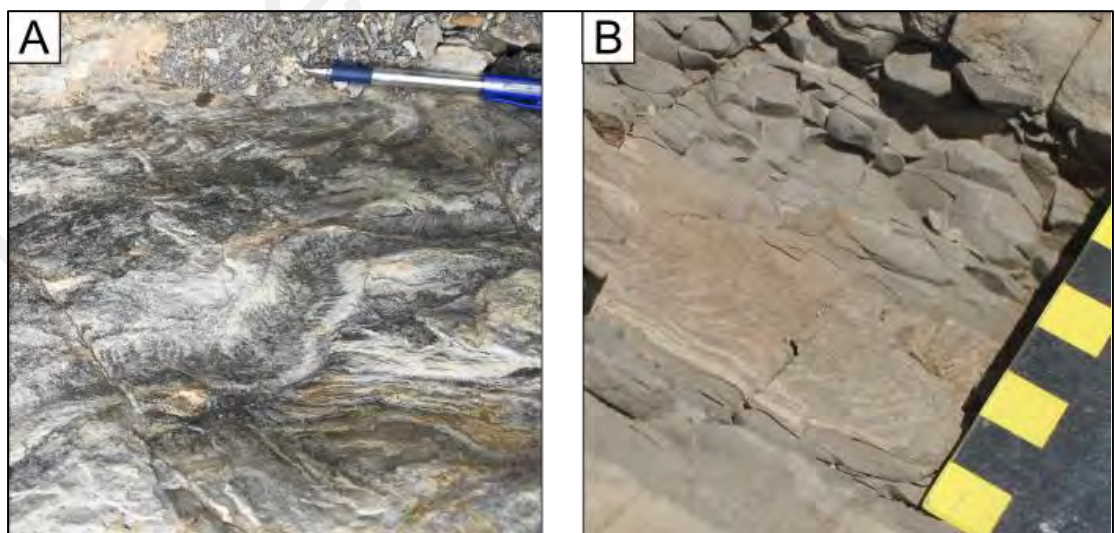


Figure 5.10 (A) *Scolicia prisca* observed on the top of BT1. (B) *Scolicia* preserved as endichnial traces on the vertical cross-section. Often observed at the top interval, within F3 or F4.

F3 = Cross ripple laminated sandstone, F4 = Planar laminated siltstone

5.2.10 *PROTOVIRGULARIA*

Protovirgularia traces in the Temburong Formation was observed on the soles of BT1 and can only be observed within BTA 3. It occurs as bilobate, horizontal to subhorizontal, cylindrical burrows with a straight to slightly curving median ridge and chevron-shaped markings, with a diameter of 3 to 9 mm. The examples shown in **Figure 5.11** are similar to the specimens described by Uchman (1998), Buatois and Mangano (2011) and Madon (2021).

Protovirgularia traces observed here is identified as *P. rugosa* as it resembles specimens described by Uchman (1998, their figure 67C). The occurrence of *P. rugosa* is consistent with the age of Temburong Formation as it is known to range from the Devonian to the Miocene (Uchman and Gazdziki, 2006), while *P. pennatus* ranges only until the Oligocene (Uchman, 1998).

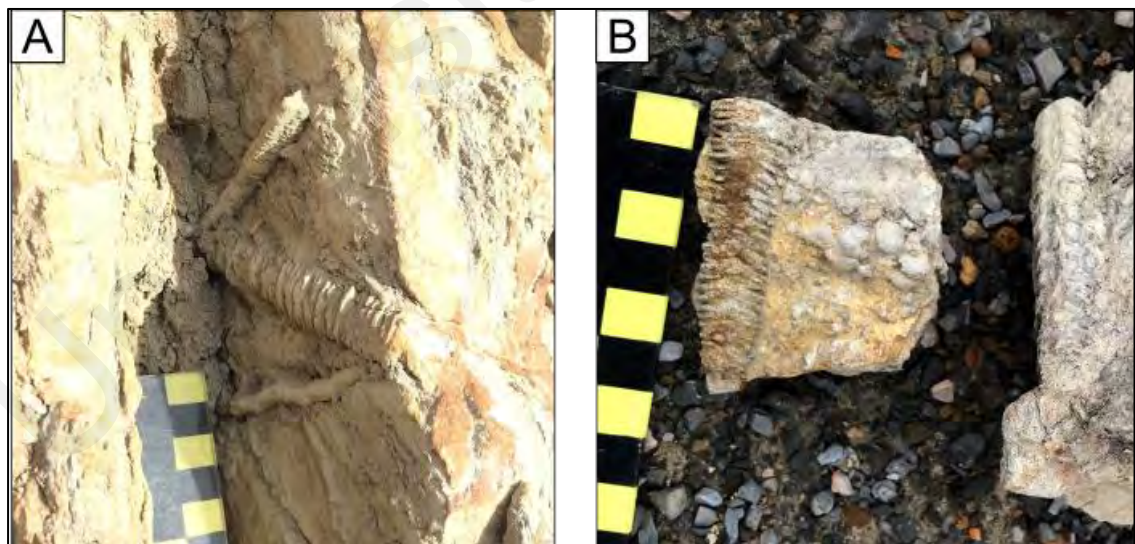


Figure 5.11 Examples of *Protovirgularia* in the Early Miocene Temburong Formation, Kg, Bebuloh, Labuan.

5.2.11 TUBUTOMACULUM

Tubutomaculum is observed within mudstone beds of both BT 3 and BT 4, commonly oriented horizontally to the bedding plane and preserved as full relief. It is recognized by its typical reddish-coloured, sideritized, spindle-shaped burrows, filled with ellipsoidal pellets. In this study area, the diameter of *Tubutomaculum* traces are about 10 – 40 mm and up to 15 cm in length (Figure 5.12).

This ichnogenus is interpreted as fodinichnia traces, based on the *Teichichnus*-like spreiten and pellet infill (Garcia-Ramos et. al., 2014).

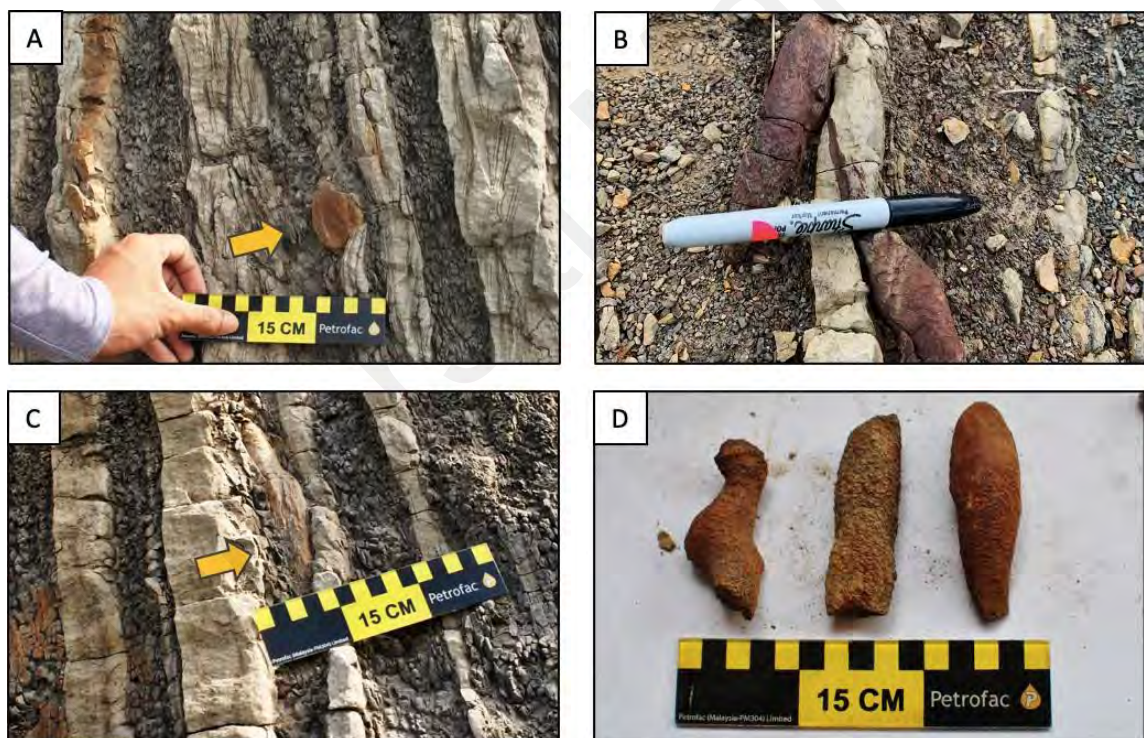


Figure 5.12 Examples of *Tubutomaculum* trace fossil.

5.2.12 OTHER TRACE FOSSILS OF RARE OCCURRENCE

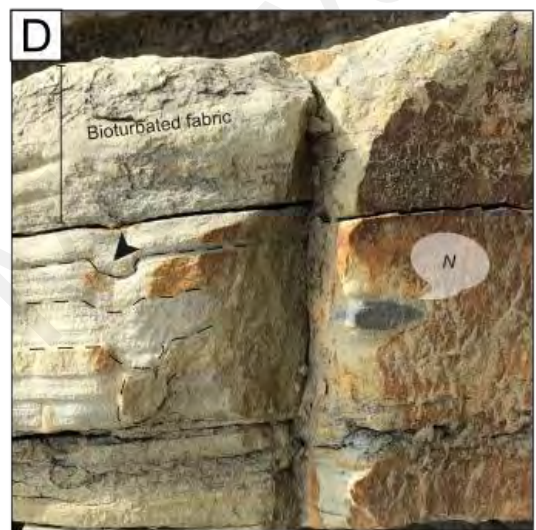
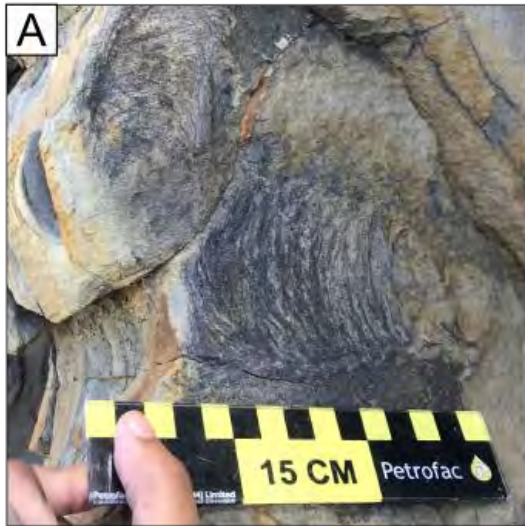
Endichnial tentatively identified as ?*Halopoa* were observed in cross-sections of BT6. The trace fossil displays several overlapping probes, often stacked in a vertical plane, and form a *Teichichnus*-like structure, but is much less vertically and regularly developed. This trace fossil resembles the specimen in Uchman (1998, their Figure 8B-C) and matches with its description. It is often observed along organic-rich laminae, causing the laminae to be disrupted and producing a moderately bioturbated fabric. *Halopoa* commonly exploits rarely occupied tiers in the sandstone part of turbiditic beds (Uchman, 1998).

A few trace fossils observed in the Temburong Formation also resemble *Zoophycos* (Figure 5.13 A-B). They display spreite structures with U-shaped protrusive burrows. These trace fossils are not *Scolicia* and *Nereites* based on the absence of lobate structures.

The rare presence of ?*Bergaueria* and *Spirophycus* are also recorded, but their limited occurrence in the study area does not allow for their detailed description and ichnospecies identification.

Figure 5.13 (A-B) Possible ?*Zoophycos*, based on its spreite structures with U-shaped protrusive burrows. Both traces were observed on the top of BT1. (C) Unknown, full-relief, sideritized burrow found within BT3. (D) Possible endichnial ?*Halopoa* burrows, often associated with *Nereites* and bioturbated fabric. (E) ?*Bergaueria* on the sole of BT1 (F) *Spirophycus* found on the sole of thin-bedded sandstone.

N = *Nereites*



5.3 SIGNIFICANCE OF THE TRACE FOSSIL DISTRIBUTION TO DEPOSITIONAL ENVIRONMENT INTERPRETATION

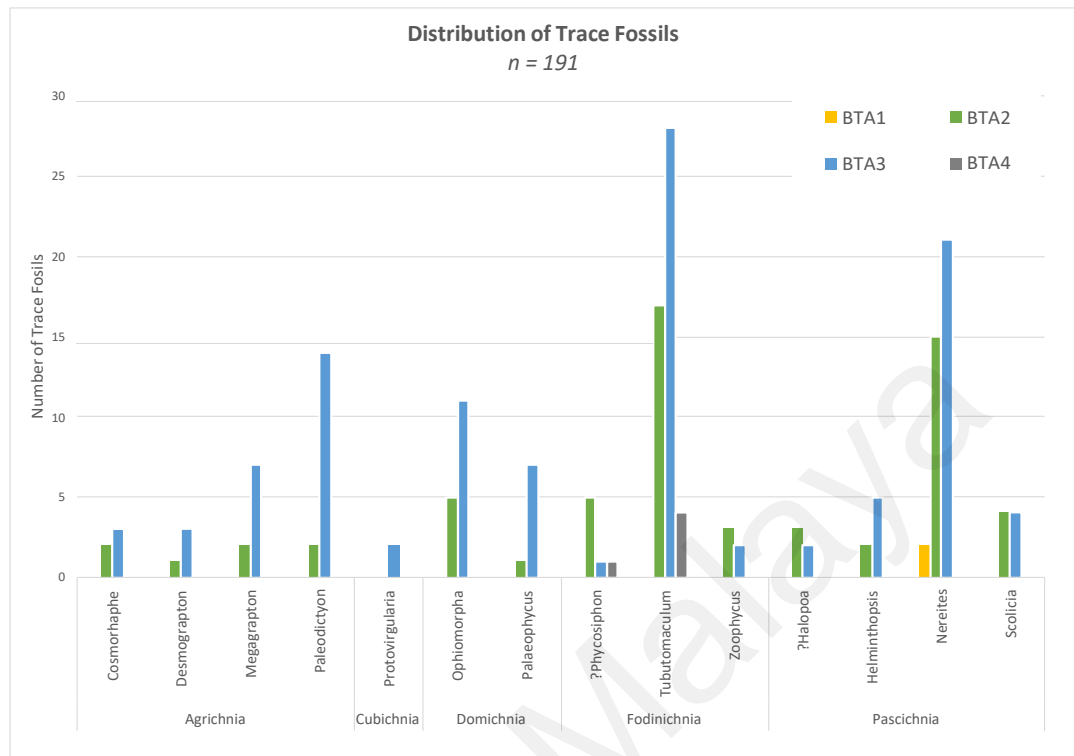


Figure 5.14 Trace fossils distribution across all bed type associations in the Early Miocene Temburong Formation, Labuan.

The trace fossil assemblages documented in the study area display a moderate diversity with a total of 15 identified ichnogenera. 78 epichnial and hypichnial traces and 113 endichnial traces were observed. However, there might a bias in sampling attributed to low or poor preservation, as not all sandstone beds have well-exposed bedding planes. The potential diversity of burrow mottling in mudstone facies (BT3 and BT4) were not fully captured too as it was difficult to discern due to the weathering effect.

Overall, trace fossils observed in Kampung Bebuloh are typical ichnogenera of the *Nereites* Ichnofacies (**Table 5.1**). The most common trace fossil is *Tubutomaculum* as it has good, full-relief preservation and can be easily recognized within the mudstone facies (BT3 and BT4). *Nereites* is also quite commonly observed as endichnial traces and it often produces a bioturbated texture in cross-section.

The abundance of representatives of the *Nereites* Ichnofacies is typical of a deep marine background community (e.g., Seilacher, 2007; Uchman, 2001; Kane et. al., 2007). Uchman (2001) proposed the subdivision of the *Nereites* ichnofacies into 3 sub-ichnofacies (**Table 5.2**), which can indirectly help to provide information in terms of general position (i.e., proximal–medial–distal) within a submarine fan system (Cumming and Hodgson, 2011).

Table 5.2 Characteristics of sub-ichnofacies of *Nereites* ichnofacies based on Heard and Pickering (2008) and Cumming and Hogdson (2011)

Sub-ichnofacies	Trace fossils assemblages	Possible depositional environment
<i>Ophiomorpha rudis</i>	<i>Ophiomorpha rudis</i> , <i>Ophiomorpha annulata</i> , and <i>Scolicia strozzii</i>	Proximal axial environments and channel-lobe transition
<i>Paleodictyon</i>	Abundance of open tunnels preserved on the soles of turbidites (e.g. <i>Paleodictyon</i>)	Lobe, lobe fringe to fan fringe
<i>Nereites</i>	Dominated by post-depositional back-filled burrow systems made by sediment feeders (e.g. <i>Nereites</i> , <i>Phycosiphon</i> , <i>Zoophycos</i>)	Fan fringe to basin floor

The Early Miocene Temburong Formation at Kampung Bebuloh is dominated by the *Paleodictyon* sub-ichnofacies and *Nereites* sub-ichnofacies, which align with the sedimentological interpretation discussed in the previous chapter. In general, the ichnofacies assemblages in the Temburong Formation, Kampung Bebuloh are similar to a number of examples from distal turbidite systems i.e., Eocene Hecho Group in the Ainsa–Jaca Basin, Spanish (Uchman, 2001, Heard and Pickering, 2008); Central Pondites, Turkey (Uchman et al., 2004), and nearby Oligocene – Miocene West Crocker, Sabah (Madon, 2021). Findings from this study are also similar with the previous ichnology analysis done by Jasin and Firdaus (2019) and Burley et. al. (2020), where they observed the dominant presence of *Paleodictyon* subichnofacies, characterized by the occurrence of ichnofossils including *Megagraption*, *Paleodictyon*, *Zoophycos*, and *Cosmoraphe*. However, *Nereites* and bioturbated fabric were not mentioned in both studies.

5.3.1 ETHOLOGY DISTRIBUTION

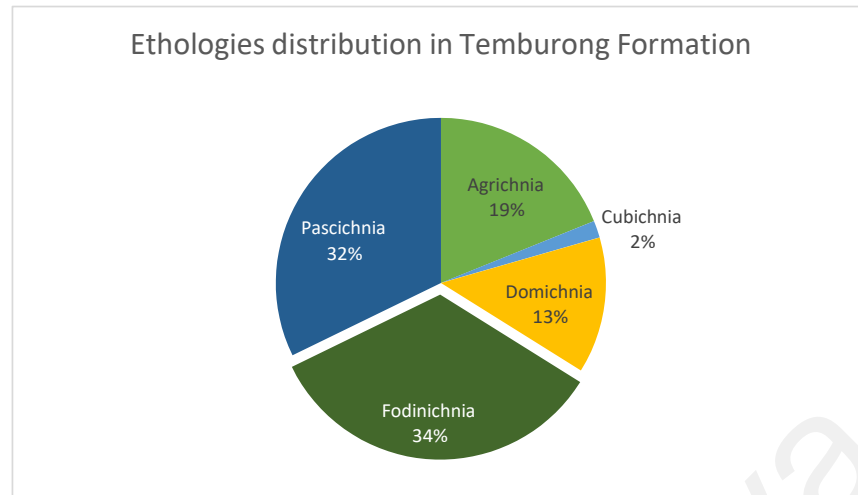


Figure 5.15 Distribution of ethological classification from the measured sections in the Early Miocene Temburong Formation, Kampung Bebuloh, Labuan

In terms of trace fossil behaviour, Temburong Formation preserved 34% fodinichnia, 32% pascichnia, followed by 19% agrichnia, 13% domichnia, and 2% cubichnia. Fodinichnia is the dominant ethology in this study, due to the common occurrence of well-preserved *Tubutomaculum*, followed by pascichnia traces with *Nereites* being the dominant ichnogenera. Meanwhile, graphoglyptid trace fossils identified include typical *Paleodictyon*, *Megagraption*, *Cosmorhapse* and *Desmograption*, are interpreted to represent agrichnia traces (Cumming and Hodgson, 2011). However, this observation could be biased because dominant ichnogenera from fodinichnia and pascichnia have better endichnial preservation. Agrichnia are often preserved as hypichnial traces on the soles of beds, and unfortunately turbidite soles are poorly exposed in the study area.

5.3.2 INTERPRETATION

Moderate diversity of trace fossils observed in this study suggests a quiescent palaeoenvironment and lower hydrodynamic energy conditions, which allowed preservation of a more diverse assemblage (Phillips et. al., 2011).

Common occurrence of graphoglyptid traces such as *Nereites*, *Paleodictyon*, *Helminthopsis*, *Desmograption* and *Megagraption* are indicative of reduced food supply and appropriate bottom energy conditions, allowing their preservation (Buatois and Mangano, 2011). In this study, the graphoglyptids occur in abundance within a few beds, suggesting a narrow preference for certain environmental conditions and/or favourable preservation potential. This type of environment is most likely in the most distal parts of the turbidite fan system which are less susceptible to frequent disruptions by sediment-gravity flows (Madon, 2021). *Nereites* is also commonly associated with muddy and distal environments such as fan fringe, distal overbank, and the transition of lobe fringes to basin plain, but is absent from the axial regions of channel systems (Buatois and Mangano, 2011; Callow et. al., 2012).

Small *Paleodictyon* species such as *P. majus* and *P. latum* often can be found in the stable areas of basin plain sub-environments. The three *Paleodictyon* species observed in the Temburong Formation are known to be associated with ancient lobe deposits (Heard and Pickering, 2008; Cummings and Hodgson, 2011). Meanwhile, *Cosmorhappe* can be found in both levee and lobe environment, and its presence shows no strong environmental control (Cumming and Hodgson, 2011).

The presence of *Tubutomaculum* indicates a deep-marine setting with a low rate of sedimentation (Gracia-Ramos et. al., 2014). This ichnotaxon was previously recorded to

occur within a slope setting environment based on its association with *Rotundusichnium zumayensis*, *Zoophycos* and *Chondrites*. *Tubutomaculum* may also represent an adaptation to fluctuating food content in deep-water settings (Gracia-Ramos et. al., 2014). However, this trace fossil is considered a relatively newly identified genus, perhaps its presence in other sub-environments (i.e., lobe fringes) is not yet documented.

In this study, *Palaeophycus* is commonly associated with thin sandstone beds (Tb, Tc divisions). They are post-depositional traces formed during quiescent periods when the seabed was probably soft-ground in order for the organisms to tunnel through to produce the delicate burrows (Uchman and Wetzel, 2012). Meanwhile, *Scolicia* traces are commonly present in both overbank deposits (especially in depositional terrace settings) as well as lobe fringe environments (Knaust, 2009; Cumming and Hodgson, 2011; Callow et. al., 2012; Hansen et. al., 2017). It is often present in sand-rich environments (Wetzel and Uchman, 2001), though *Scolicia prisca* observed in the Temburong Formation is known to mostly occur in lobe and lobe fringe environments (see Heard and Pickering, 2008; Cumming and Hodgson, 2011).

Meanwhile, *Protovirgularia* is typically associated with shallow marine settings, but can also be present in deep marine turbidites (Uchman, 1998; Buatois and Mángano, 2011; Callow et. al., 2012; Madon, 2021). It is often described as a product of bivalves moving on muddy substrate, which produces a transverse, often “chevronate”, ribbed pattern due to the “push-and-pull” locomotion mechanism or, in the case of soft-bodied organisms, peristalsis of the animal (Madon, 2021). A few authors have identified *Protovirgularia* within channel-levee systems. Callow et. al. (2012) identified *Protovirgularia pennatus* in the Late Cretaceous Rosario Formation, Baja California, Mexico within a confined levee setting while Madon (2021) recognized *Protovirgularia*

in the West Crocker Formation, Sabah, Malaysia within channel-levee complex deposits. Meanwhile, Buatois and Mangano (2012) described this ichnogenus as being often found in thin-bedded sandy turbidites, mostly present in outer fan (frontal splays) and also hyperpycnal-outer levee deposits. *P. rugosa* is interpreted as an escape trace due to its common occurrence under sandy tempestites (Uchman, 1998). This suggests that the organisms were trying to escape in response to storm sand sedimentation (Seilacher and Seilacher, 1994), or turbidite sedimentation (Uchman, 1998). Occurrence of *P. rugosa* in my study area is considered rare and it may indicate that there were times of high sedimentation.

Based on the ichnospecies assemblages, the common occurrence of graphoglyptid traces and moderate diversity of the total trace fossils assemblages, it is likely that the Early Miocene Temburong Formation in Kampung Bebuloh represents a lobe fringe environment.

CHAPTER 6: DISCUSSION

6.1 OVERVIEW

The Early Miocene Temburong Formation in Kampung Bebuloh, Labuan, consists predominantly of thin-bedded turbidites, which represent the deposits of low-density turbidity currents. Published ichnology and biostratigraphic analysis already support a deep-marine setting, probably within external levee or outer fan lobe fringe sub-environments (e.g., Bakar et. al., 2017; Jasin and Firdaus, 2019; Burley et. al., 2020).

Both levee and outer fan lobe fringe deposits are dominated by low density turbidites, hence they share many characteristics in terms of bed thickness, sandstone proportions, grain size and internal sedimentary structures. However, several sedimentary characteristics can be used to differentiate between these two deposits. These include: (i) association with other thick-bedded sandstone deposits; (ii) presence of hybrid beds; (iii) lateral bed geometry and vertical bed thickness trend, and; (iv) ichnofacies assemblages (see Mutti, 1977; Talling et. al., 2004; 2007; Amy and Talling, 2006, Hodgson, 2009; Fonnesu et. al., 2018; Spychala et. al., 2017; Heard and Pickering, 2008; Monaco et. Al., 2010; Callow et. Al., 2012). These criteria will be used in the discussion below to construct a depositional model for the Early Miocene Temburong Formation on Labuan.

6.2 CHARACTERISTICS SHARED BY LEVEE AND LOBE FRINGE DEPOSITS

Overall, the Temburong Formation succession at Kampung Bebuloh have an average sandstone proportion of 49%, dominated by very fine-grained sandstone with sandstone thickness ranging from 3 to 90 cm (average = 11 cm). Sedimentary structures include ripple cross-lamination (BT1), overlain by mudstone beds (BT3 and BT4), which indicate that these beds were deposited by dilute, waning, low-density turbidity currents.

These bed types are shared by both levee and lobe fringe deposits. External levee deposits often have sandstone proportions of 15 to 50%, depending on the distance from the channel belt (Kane and Hogdson, 2011). Hansen et. al. (2017) also recorded 49% sandstone proportion in depositional terrace deposits. Similarly in lobe fringe deposits, recorded sandstone proportions range from 12% to 62% (Mutti, 1977), with individual sandstone thickness ranging from 5 to 20 cm. However, Sychala et. al. (2017) noted that frontal lobe fringes would display highly variable sandstone thicknesses, from 10 to 150 cm.

Both levee and lobe fringe deposits are mainly deposited by low density turbidity current, hence they commonly consist of Bouma's T_{C-E} sequences. Climbing ripples and parallel lamination are also observed in the T_C division of both deposits. These sedimentary features are common in Temburong Formation. Therefore, based on the average sandstone proportion, sandstone thickness, grain size and internal sedimentary features, the Temburong Formation can represent either levee or lobe fringe deposits.

6.3 CRITERIA DIFFERENTIATING LEVEE AND LOBE FRINGE DEPOSITS

Other criteria to distinguish between levee and lobe fringe deposits will be discussed below, except for ichnology criteria as it has been discussed in previous chapter.

6.3.1 ASSOCIATION WITH OTHER THICK-BEDDED DEPOSITS

Levee and depositional terrace deposits are often associated with thick-bedded channel fill deposits. Channel-fill deposits are commonly massive, display tabular to lenticular geometries, and dominated by amalgamated high-density turbidites. The base of the beds often contains conglomerate clasts attributed to erosion by the heads of high-velocity turbidity currents, indicating the incision of channels (Jackson et. al., 2009; Zakaria et. al., 2013). In the channelized inner fan, distributary channels could be identified based on stacks of fining-upward, amalgamated sandstone bodies. However, levees are often poorly develop within the channelized inner fan due to the presence of multiple channels (Zakaria et. al., 2013). Nevertheless, levee deposits could extend over 2 km away from the channel-belt (Hickson and Lowe, 2002; Kane and Hodgson, 2011), hence they would be difficult to identify if the study area has limited lateral exposure as the channel-filled deposits may be missing and cannot be observed nearby.

Meanwhile, lobe fringe deposits are associated with thicker sandstone deposits of the lobe axis and lobe off-axis. Prelat et. al. (2009) described lobe axis deposits as being thick-bedded, consisting of structureless to planar-laminated sandstone. These sandstones can form amalgamated packages of up to 5 m thick where there is scouring at the base of the lobe. Similarly, the lobe off-axis is also dominated by medium-bedded, planar-laminated sandstone, and often amalgamated. Both deposits display thickening upward patterns and tabular geometries in the outcrop scale.

6.3.2 PRESENCE OF HYBRID EVENT BEDS (HEB)

HEBs are recognized as a bed type in unconfined distal and lateral fringes of distributive lobe systems and basin plain sheet systems (Haughton et al., 2003; Hodgson, 2009; Kane and Ponten, 2012; Kane et al., 2017; Spsychala et. al., 2017; Fonnesu et. al., 2018). This is because HEBs are formed when there is a transition or switch from non-cohesive to cohesive flow behaviour during deposition, followed by a variably developed, but generally volumetrically minor dilute turbulent wake (Haughton et. al., 2009). This downstream transition is often associated with the expansion and deceleration of flow due to the radial spreading from the lobe apex (Kane et. al., 2017), in which commonly happened in the lobe system. The occurrence of an HEB may also record the progressive deceleration of clay-enriched flows in which the turbulence was suppressed as flow energy dissipated on flatter and more distal fan sectors (Fonnesu et. al., 2018).

6.3.3 LATERAL BED GEOMETRY AND VERTICAL BED THICKNESS

TRENDS

According on Mutti (1977), one of the criteria to differentiate the sub-environment for thin-bedded turbidite succession is by observing the lateral bed geometries and trends. External and internal levee deposits have a wedge-shaped geometry that thins perpendicularly away from a channel-belt (Kane and Hodgson, 2011; Hansen et. al., 2017), while lobe fringe deposits display a tabular geometry at outcrop scale (Mutti, 1977; Prelat et. al., 2009; Spychala et. al., 2017).

For vertical bed thickness trends, previous researchers have used thickening-upward trends as a criterion for identifying lobe deposits but recent studies conducted on ancient deepwater systems show that vertical bed thickness trends are not a diagnostic criterion (see Kane et. al., 2007; Prelat and Hodgson, 2013). Vertical bed thickness trends in levee deposits often suggest both allocyclic controls (increasing magnitude and perhaps frequency of flows) and autocyclic controls (channel-axis aggradation maintaining levee relief) (Kane et. al., 2007). Meanwhile in lobe deposits, vertical bed thickness trends are often influenced by the stacking pattern of smaller-scale components (lobe elements and single beds) and proximity to feeder channels (Prelat and Hodgson, 2013). This is because sediment gravity flows tend to fill topographical lows and create low-amplitude relief, therefore subtle shifts in the location of the depocentre exist at all scales of a depositional element hierarchy.

Nevertheless, vertical bed thickness trends can support interpretation of a position within a lobe or levee, and also provide insights on the migration history of the levee crest, but should not be a diagnostic recognition criterion (Kane et. al., 2007; Prelat and Hodgson, 2013).

6.4 CONCLUSIONS BASED ON INTEGRATED SEDIMENTARY AND ICHNOLOGICAL CHARACTERISTICS

Based on the characteristics of the thin-bedded turbidites in Temburong Formation as discussed above, a simple decision tree can be constructed in order to determine whether they are levee or lobe fringe deposits (**Figure 6.1**).

Overall, the Temburong Formation in Kampung Bebuloh has the following characteristics: (i) tabular bed geometries; (ii) presence of hybrid event beds; (iii) absence of thick-bedded channel-fill sandstones, and (iv) ichnofacies assemblages that are representative of a lobe-fringe environment. Hence, the thin-bedded turbidites characteristics observed in Kampung Bebuloh are more likely consistent with a lobe fringe interpretation, rather than levee deposits.

The approximately 40 m thick succession of the studied Early Miocene Temburong Formation Kampung Bebuloh is too thick to represent the deposits of a single lobe fringe. A single lobe fringe often has a thickness ranging from 0.1 to 2 m (Spychala et. al., 2017). However, thicknesses for BTA 2 and BTA 3 in this study range from 3 to 12 m. For this reason, the relatively monotonous, thick succession (~40 m) of the Temburong Formation at Kampung Bebuloh may represent the **fringes to lobe complexes** (Prelat and Hodgson, 2013; Young et. al., 2013; Spsychala et. al., 2017).

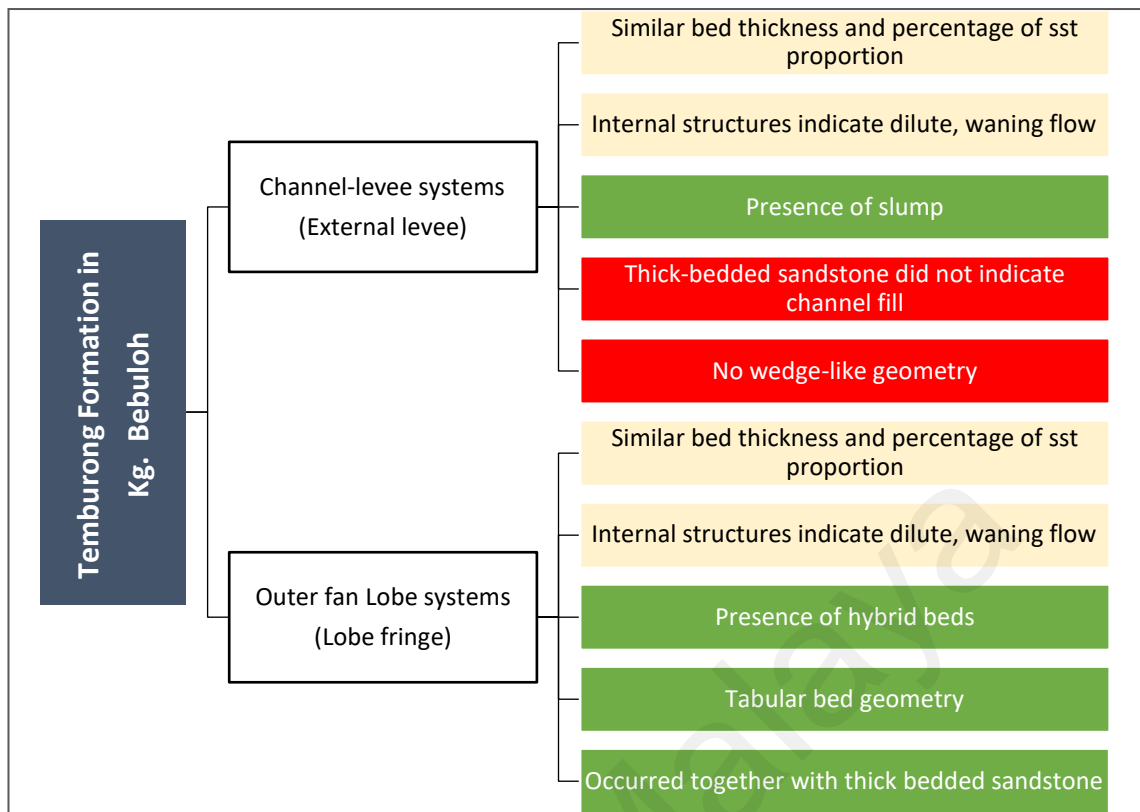


Figure 6.1 Decision tree diagram showing the criteria of levee deposits vs. lobe fringe deposits observed in the study area. Yellow box indicate the similarities between these two sub-environments, green box indicate characteristics that were observed in this study, while red box indicate characteristic that were not observed in this study.

Additionally, strata observed in Temburong Formation have a flat, slightly erosive base, and display a sheet-like geometry, which are more characteristic of lobe fringe deposits (Young et. al., 2013). However, it should be noted that the lateral exposure of the Kampung Bebuloh turbidites is limited (from 2 up to ~50 m), hence pinch-out or wedge geometry may not be visible at this scale. To determine the possible depositional environment of thin-bedded turbidites without good extensive lateral exposure is quite difficult. The absence of a distinct vertical stacking pattern observed in the study area may be result from random position of the incoming flow to the lobe depocenter (Prelat and Hodgson, 2013).

The medium-bedded sandstones observed in this study are interpreted as lobe-off axis deposits (BTA1). This is based on the tabular geometry, upward thickening trend, sandstone proportion, low degree of amalgamation and the absence of erosional basal conglomeratic/pebble lags.

The presence of HEBs further supports a lobe fringe interpretation for the Temburong Formation. Sporadic occurrence of HEB in Temburong Formation suggests shorter episodes of disequilibrium, which may be due to; (i) an initial phase of slope re-adjustment, or (ii) intermittent tectonically or gravity-driven surface deformation, or (iii) supply variations (Haughton et al., 2009). Jackson and Johnson (2009) interpreted the debrites observed in Tanjung Kiamas as controlling the topography of the Early Miocene submarine slope and influencing the pathway of the turbidity currents. This debrite-related relief would have led to a flow transition down dip, resulting in the deposition of hybrid beds deposited in the present-day Kampung Bebuloh area. At the time of deposition of the Temburong Formation (Early Miocene), the shelf margin was prograding across the active Labuan Anticline (Jackson and Johnson, 2009). Hence, the shorter episodes of disequilibrium which resulted in debrites and HEB deposition may have been related to tectonically-driven tilting and seismicity associated with the development of this structure.

No hybrid beds were recorded in the Tanjung Kiamas exposure because based on the stratigraphic position, Tanjung Kiamas is considered a proximal part of the Temburong Formation as compared to Kampung Bebuloh. The absence of hybrid beds in proximal stratigraphic successions can be attributed to a combination of bypass of proximal areas by hybrid flows and down-dip flow transformation of the cohesive component (Hogdson, 2009). The presence of slumps in the studied Temburong

Formation succession is consistent with a lobe interpretation. Slumps can form on slopes as low as 0.1° or less (Posamentier and Martinsen, 2010). Slumps can be generated in lobe basin floor settings due to the sudden high sedimentation influxes or tectonic activity (Posamentier and Kolla, 2003; Claussman et. al., 2021).

Lastly, the trace fossil assemblages representing *Paleodictyon* sub-ichnofacies and *Nereites* sub-ichnofacies of the *Nereites* ichnofacies further support the interpretation of the Temburong Formation at Kampung Bebuloh as the fringes of lobe complexes.

6.5 DEPOSITIONAL MODEL FOR THE EARLY MIOCENE TEMBURONG FORMATION AT KAMPUNG BEBULOH, LABUAN

A depositional model for the Early Miocene Temburong Formation exposed at Kampung Bebuloh is constructed, based on detailed facies and ichnological work presented in this thesis, integrated with biostratigraphic, ichnologic and sedimentologic data from published literature (**Figure 6.2**).

Accurate interpretation of thin-bedded and fine-grained packages within lobe deposits will have significant implications in subsurface investigations as it can provide useful information in terms of understanding of connectivity/continuity between lobe axes and the geological modelling of lobes (Prelat et. al., 2009; Prelat and Hodgson, 2013). It can also help in identifying the controls (whether autogenic or allogenic or both) on the distribution, dimensions and development of lobes (see Prelat et. al., 2009). Vertical bed thickness trends can provide a better understanding of the evolution of sediment deposition through time and space as they can indicate the location of the successive depocentres at bed and lobe element scale (Prelat and Hodgson, 2013). However, in order to fully understand the lobe stacking patterns and the vertical bed thickness trends of lobes within lobe complexes in Temburong Formation, more data (i.e., detailed mapping from several localities, shallow subsurface reflection seismic data, numerical modelling techniques) is required (Prelat and Hodgson, 2013).

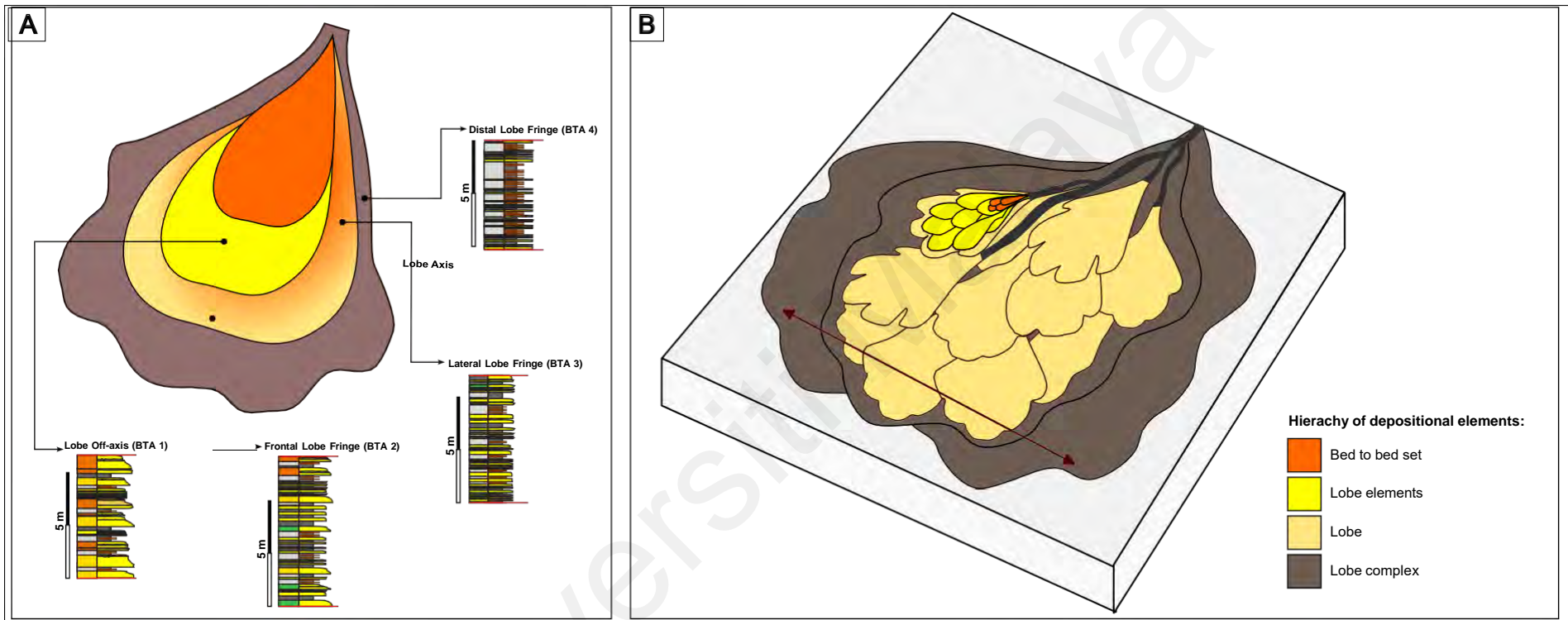


Figure 6.2 (A) Simplified plan view of a lobe, showing the distribution of lobe sub-environments and example logs for each sub-environment. (B) Turbidite lobe depositional model for the Early Miocene Temburong Formation at Kampung Bebuloh. The Temburong Formation at Kampung Bebuloh is interpreted as turbidite deposition at the fringes of lobe complexes (area marked by the red line). Both diagrams were modified from Spsychala et. al. (2017).

6.6 THE KAMPUNG BEBULOH EXPOSURE IN RELATION TO OTHER EXPOSURES OF THE TEMBURONG FORMATION ON LABUAN ISLAND

Previous sedimentological work on the Temburong Formation has focused on exposures located further SW of the Bebuloh outcrop. Burley et. al. (2020) described thick-bedded, amalgamated, fine- to medium-grained sandstone packages up to 35 m thick and associated Mass Transport Deposits (MTDs) on the islands of Rusukan Kecil and Rusukan Besar, about 10 km SW of the Bebuloh outcrop, and interpreted the succession as representing a mid to lower slope channel-levee system.

Meanwhile, Jackson and Johnson (2009) studied the Temburong Formation at Tanjung Kiamsam, which is located about 3 km SW of Bebuloh. Here, they observed medium-grained turbidites up to 2 m thick, which contain structureless (T_A) intervals alternating with planar-parallel (T_B) and current-ripple (T_C) laminated intervals. Laterally discontinuous, cobble-mantled scours are also locally developed within turbidite beds. They described and proposed that it was deposited within a lower-slope to proximal basin-floor environment. Based on the geological map in Burley et al. (2020) the Kiamsam and Rusukan island successions are roughly laterally equivalent, but with Kiamsam being located on the NW limb of the Labuan anticline, while the Rusukan and Bebuloh successions being on the opposite SE limb. However, exact correlation of the successions is not possible.

Stratigraphically, these two previous studies support the interpretation of the Temburong Formation in Kampung Bebuloh as the fringes of lobe complexes. The Temburong Formation in the Rusukan islands may represent a slope channel-levee system, with the Tanjung Kiamsam succession representing a channel lobe transition zone (CLTZ) or lobe axis deposits. Another possibility is that levee deposits are absent from the Temburong

Formation on Labuan and all the successions represent lobe deposits. Jackson and Johnson (2009) and Burley et al. (2020) do not actually describe any levee geometries and did not discuss a comparison between levee and lobe criteria for their deposits.

6.7 PALEO GEOGRAPHIC RECONSTRUCTION OF EARLY MIOCENE NORTHWEST BORNEO

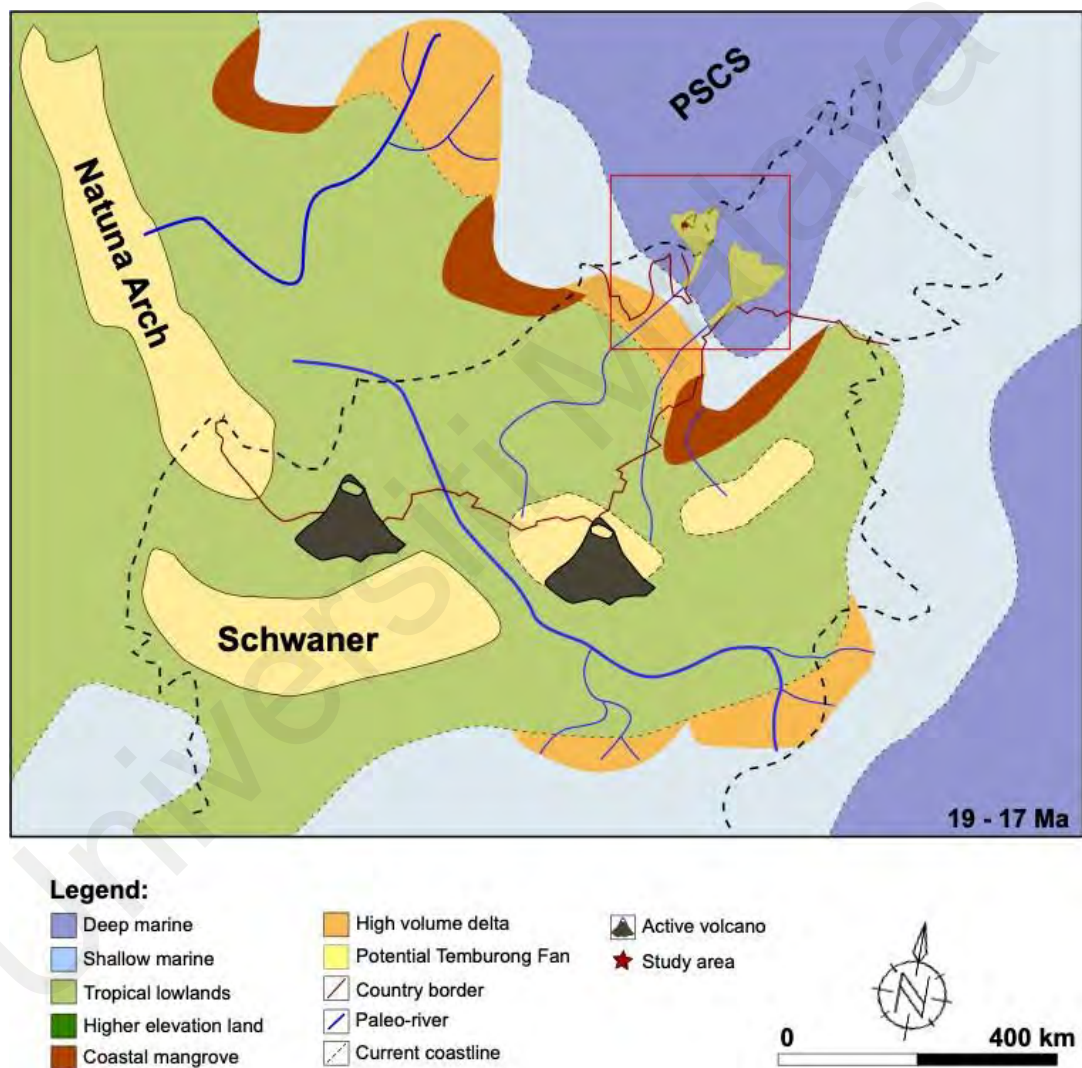


Figure 6.3 Regional paleogeographic reconstruction for Early Miocene (~20 – 17 Ma, Burdigalian) proposed by Burley et. al. (2020) based on the on the tuff U-Pb dating results and previous literature reviews. The map is showing few palaeo-drainages from central Borneo supplying sediments for the Temburong Formation. Map is modified from Burley

The sediment provenance or source for Temburong Formation probably originated from a SE direction (see Morley et. al., 2016; Hennig-Brietfield et. al., 2019; Burley et. al., 2020). Paleocurrent data from Crevello et. al. (2005) further support that the sediment source of Temburong Formation is from south to southeast (**Figure 6.3**).

Thin-bedded successions in the Temburong Formation are generally monotonous with no significant stratigraphic discontinuities or sudden changes in bed geometry at the outcrop scale. The stratigraphy and deposition were most likely influenced by autogenic/topographic control in the form of lobe switching, and the study area may represent the distal part of an entire lobe system. This study agrees with Burley et. al. (2020) where they concluded that the Temburong Formation was mainly deposited by distal turbidites rather than suspension fall-out as a result from a high sedimentation rate (62 km per 100 kyr), supplied by a major delta system.

The question is, which major system sourced the sediments to Temburong Formation? The sedimentation rate proposed is considered very high, even higher than the modern Mahakam Delta, however Morley et. al. (2016) did not map any major delta in Northwest Sabah area during 20 – 17 Ma (see their Map 2, Figure 5). One of the known Early Miocene delta systems in Northwest Sabah is the Meligan Formation, which was exposed in Sipitang in Sabah, Lawas in Sarawak and southern part of Temburong district, Brunei (e.g., Liechti et. al., 1960; Tate, 1994; Sandal, 1996; Hutchison et. al., 2005; Balaguru and Lukie, 2012; Cullen, 2010; Burley et. al., 2020; Lunt, 2022). Unfortunately, no modern detailed facies analysis of the Meligan Formation has ever been conducted, due to the limited and poor exposures. Meligan Formation consists largely of fine, well-sorted sandstone and was interpreted as a regressive deltaic succession capping the Temburong Formation (Sandal, 1996). Biostratigraphic analysis of the Meligan Formation indicates

a T_c age, equivalent to Temburong Formation in Labuan (Hutchison, 2005). Cullen (2010) reported that outcrop exposures of Meligan Formation typically show a sharp basal contact with the Temburong Formation and display modest structural discordance. This contact was interpreted as a tectonically induced unconformity (the Base Miocene Unconformity), reflecting collision of the Dangerous Grounds around 20 Ma (Balaguru and Hall, 2008; Cullen, 2010).

The Meligan Formation is interpreted as a major Early Miocene fluvio-deltaic system which prograded northeastwards into the Baram Delta area, however its origin remains poorly known because of its general inaccessibility (Hutchison, 2005). One possible origin may be coming from the emergence of Central Borneo during Early Miocene times. Throughout this period, Central Borneo began to uplift in stages, starting with the intrusion of the Sintang Volcanics (Morley et. al., 2016; Burley et. al., 2020). Erosion of the highland areas established during the Palaeogene may have resulted in the development of new river systems and establishment of deltas around the Sunda region (Morley et. al., 2016).

Detrital Pb-U zircons analysis showed differences between Oligocene Crocker Formation and Early Miocene Temburong Formation. Van Hattum et. al. (2013) reported that Oligocene Crocker Formation is dominated by Permo-Triassic zircons, which could be derived mainly from East Malaya or Indochina via a 'Sunda River' with only minor input from central and southern Borneo, passing through the western Borneo (van Hattum et. al., 2013; Hennig-Brietfield et. al., 2019). Meanwhile, Burley et. al., (2020) reported Temburong Formation in Labuan predominantly contains Cretaceous zircons, which is similar to the Eocene and older succession (i.e., Eocene Crocker, Sapulut, Trusmadi) reported by van Hattum et. al. (2013), and younger Belait Formation reported by Hennig-Brietfield et. al. (2019) (refer Burley et. al., 2020, their Figure 15), and interpreted this

formation to be sourced from the reworking of uplifted Rajang Group, Sapulut or Trusmadi formations. This also reflects the first phase of uplift in the Early Miocene before the onshore depositional system changed to the shallow marine-fluvial systems.

Nonetheless, source of the Temburong Formation turbidites do not necessary need to be directly from a deltaic conduit, but can come from a sediment-rich shelf, perhaps within the tidal embayment of the South China Sea (Burley et. al., 2020). Having said this, the presence of a major sediment source supplying sediments to Temburong Formation can explain the origin of the sustained turbidity currents mentioned by Jackson and Johnson (2009). This type of flow is also described in my study as producing the ungraded sandstone bed type (BT6). Generation of sustained turbidity currents may be sourced from this sediment-rich shelf, due to multiple retrogressive collapse events. These collapse events may be triggered from seismic activity related to growth of the Labuan Anticline, or may be related to rapid sediment loading and slope oversteepening related to river flood events (Jackson and Johnson, 2009).

An interpretation of the Meligan delta system being the source of the Early Miocene Temburong Formation is consistent with work by Balaguru and Lukie (2012) where they described the sequence of deep water turbidites, slope channels, turbidite fans and mass-transport deposits exposed at the northern tip of the Klias Peninsula and southwestern part of Labuan Island as the distal equivalent of the Meligan Delta System. However, most of the previous literature established that Meligan Formation is younger than Temburong Formation (see Hutchison, 2005; Cullen, 2010), and was interpreted as the regressive deltaic succession capping the Temburong Formation (Sandal, 1996). However, it is likely that what is referred to as the Temburong Formation exposed in Labuan may not be genetically related to the Temburong Formation proper in the type

location exposed in Northwest Sabah (i.e., Tenom and Padas Valley) and Brunei (i.e., lithostratigraphy vs. chronostratigraphy). A recent stratigraphic review by Lunt (2022) has put the age of Base Miocene Unconformity (BMU) as close to the Te₄ to Te₅ Letter Stage boundary, close to the Oligo-Miocene epoch boundary, which reflect the end of deformation and onset of a new phase of sedimentation. The sediments below the BMU, deposited during a time of compression and deformation are characterised, over a wide area of north Borneo, by downslope transport of calciturbidites, olistoliths, lithic fragments and stratigraphically reworked microfossils, while the sediments deposited after the BMU, which are still mostly deep marine facies, lack these features. Hence, Temburong Formation in Labuan may have been deposited after the BMU, which supports the interpretation from Balaguru and Lukie (2012). To test this hypothesis, a comparison analysis in petrographic, geochemistry and biostratigraphic analysis needs to be conducted between the Temburong Formation in Labuan, Sabah and Sarawak-Brunei border. Heavy mineral analysis, focusing on the garnet geochemistry, can also be considered as it can provide a better understanding on the provenance (see Thrane and Keulen, 2012).

In conclusion, the Early Miocene, thin-bedded turbidite succession of the Temburong Formation exposed at Kampung Bebuloh, Labuan is interpreted as the fringes of lobe complexes. This interpretation supports the sedimentation rate proposed by Burley et. al. (2020) and suggests that the poorly studied Meligan Formation could be the potential source of sediments supplying the Temburong Formation. However, further biostratigraphic, sedimentological and mineralogical work is required to understand the relationship between the Temburong Formation in Labuan and supposed equivalents on mainland Borneo.

CHAPTER 7: SUMMARY

7.1 CONCLUSIONS

A detailed facies, bed type and ichnological analysis was conducted on a 97 m thick sedimentary succession of the Early Miocene Temburong Formation at Kampung Bebuloh, Labuan. Based on facies assemblages, bed thickness and sedimentary structures, six bed types were identified in the study area: (i) BT1: thin-bedded sandstone, deposited by dilute low-density turbidity current, (ii) BT2: medium-bedded sandstone, deposited by surge-like, high- to low-density turbidity currents (iii) BT3: structureless to finely laminated mudstone, representing suspension or dense mud (iv) BT4: heterolithic mudstone, deposited by waning, dilute low-density turbidity currents with pulses in sedimentation (iv) BT5: bipartite or tripartite beds, identified as hybrid event beds recording flow transformations, and lastly (vi) BT6: ungraded sandstone indicative of sustained turbidity flows.

The six bed types are observed to form larger-scale, repeatable assemblages of bed types, which are grouped and assigned to five bed type associations; (i) BTA 1: lobe-off axis, (ii) BTA 2: frontal lobe fringe, (iii) BTA 3: lateral lobe fringe, (iv) BTA 4: lobe distal fringe/distal fan fringe, (v) BTA 5: slump deposit.

Ichnology analysis showed that the study area is dominated by *Paleodictyon* sub-ichnofacies and *Nereites* sub-ichnofacies, which are commonly observed in lobe fringe deposits. In terms of ethological classification, the Kampung Bebuloh succession is dominated by fodinichnia (i.e. *Tubutomaculum*) and pascichnia (i.e. *Nereites*) traces. Cubichnia traces (?*Bergularia* and *P. rugosa*) are also present in study area, which are absent from levee settings.

The depositional environment of the Temburong Formation in Kampung Bebuloh is interpreted as fringes of lobe complexes based on: (i) thick accumulation of lobe fringe bed type associations (up to ~40m); (ii) sheet-like/tabular bed geometries; (iii) no distinct observable vertical trend; (iv) presence of medium-bedded turbidites representing lobe off-axis deposits; (v) presence of hybrid event beds, and; (vi) trace fossil assemblages representing *Paleodictyon* sub-ichnofacies and *Nereites* sub-ichnofacies of *Nereites* ichnofacies. Source of sediment for Temburong Formation is said to be from SW to NE direction, which could be sourced from the Meligan Formation. Overall, this study is align with two previous studies done by Jackson and Johnson (2009) and Burley et. al. (2020).

7.2 RECOMMENDATIONS FOR FUTURE WORK

To have a better understanding on the development and evolution of the lobe system in the Early Miocene Temburong Formation, bed thickness and stacking pattern analysis should be done for all exposed outcrops in Labuan and Klias Peninsula. Having new outcrop exposures can help us better understand the lateral extent and geometry of beds within this formation. Other than that, improving the stratigraphic framework of Meligan Formation, Temburong Formation and Base Miocene Unconformity could also be an important stratigraphic problem that warrants further field study (Cullen, 2010). Conducting a comparison analysis on petrographic and biostratigraphic data across all exposed Temburong Formation deposits, together with heavy mineral analysis focusing on the garnet geochemistry, might be a good effort to solve the current stratigraphic problem, with the aim to transition from a traditional lithostratigraphic to integrated chronostratigraphic nomenclature for the Temburong Formation.

REFERENCES

- Abu Bakar, Z. A., Madon, M., & Muhamad, A. J. (2007). Deep-marine sedimentary facies in the Belaga Formation (Cretaceous-Eocene), Sarawak: Observations from new outcrops in the Sibuan and Tatau areas. *Bulletin of the Geological Society of Malaysia*, 53, 35–45. <https://doi.org/10.7186/bgsm53200707>
- Albaghdady, A., Abdullah, W. H., & Lee, C. P. (2003). An organic geochemical study of the Miocene sedimentary sequence of Labuan Island, offshore western Sabah, East Malaysia. *Bulletin of the Geological Society of Malaysia*, 46, 455–460. <https://doi.org/10.7186/bgsm46200374>
- Amy, L. A., & Talling, P. J. (2006). Anatomy of turbidites and linked debrites based on long distance (120 x 30 km) bed correlation, Marnoso Arenacea Formation, Northern Apennines, Italy. *Sedimentology*, 53(1), 161–212. <https://doi.org/10.1111/j.1365-3091.2005.00756.x>
- Asis, J., Abdul Rahman, M. N. L., Jasin, B., & Tahir, S. (2015). Late Oligocene and Early Miocene planktic foraminifera from the Temburong Formation, Tenom, Sabah. *Bulletin of the Geological Society of Malaysia*, 61, 43–47. <https://doi.org/10.7186/bgsm61201505>
- Asis, J., Tahir, S., Musta, B., & Jasin, B. (2018). Lower Miocene planktic foraminifera from the Temburong Formation in Menumbok, Klias Peninsula, Sabah. *Bulletin of the Geological Society of Malaysia*, 65(1), 59–62. <https://doi.org/10.7186/bgsm65201806>
- Baas, J. H., Best, J. L., & Peakall, J. (2011). Depositional processes, bedform development and hybrid bed formation in rapidly decelerated cohesive (mud-sand) sediment flows. *Sedimentology*, 58(7), 1953–1987. <https://doi.org/10.1111/j.1365-3091.2011.01247.x>
- Babonneau, N., Savoye, B., Cremer, M., & Bez, M. (2010). Sedimentary Architecture in Meanders of a Submarine Channel: Detailed Study of the Present Congo Turbidite Channel (Zaiango Project). *Journal of Sedimentary Research*, 80(10), 852–866. <https://doi.org/10.2110/jsr.2010.078>
- Bakar, B., Hj. Tahir, S., & Asis, J. (2017). Deep marine benthic foraminiferal from temburong formation in labuan island. *Earth Science Malaysia*, 1(2), 17–22. <https://doi.org/10.26480/esmy.02.2017.17.22>
- Balaguru, A., & Lukie, T. (2012). Tectono-Stratigraphy and Development of the Miocene Delta Systems on an Active Margin of Northwest Borneo, Malaysia. *PGCE 2012*. <https://doi.org/10.3997/2214-4609-pdb.297.b8>

- Bednarz, M., & McIlroy, D. (2009). Three-Dimensional Reconstruction Of “Phycosiphoniform” Burrows: Implications For Identification Of Trace Fossils In Core. *Palaeontologia Electronica*, 12(3).
- Bergen, A. L., Cunningham, C. M., Terlaky, V., & Arnott, R. W. C. (2022). Influence of channelized-flow density structure on the stratal architecture of deep-marine levee deposits. *Journal of Sedimentary Research*, 92(4), 381–403. <https://doi.org/10.2110/jsr.2020.183>
- Berkner, L. V., & Marshall, L. C. (1965). On the Origin and Rise of Oxygen Concentration in the Earth’s Atmosphere. *Journal of the Atmospheric Sciences*, 22(3), 225–261. [https://doi.org/10.1175/1520-0469\(1965\)022](https://doi.org/10.1175/1520-0469(1965)022)
- Bol, A., & Van Hoorn, B. (1980). Structural Styles in Western Sabah Offshore. *Bulletin of the Geological Society of Malaysia*, 12, 1–16. <https://doi.org/10.7186/bgsm12198001>
- Bouma, A. H. (1962). Sedimentology of some Flysch deposits : a graphic approach to facies interpretation. *Amsterdam : Elsevier eBooks*. <http://ci.nii.ac.jp/ncid/BA02319007/>
- Brondijk, J. F. (1962a). Reclassification of part of the Setap Shale Formation as Temburong Formation. In *Brit. Borneo Geol. Surv. Ann. Rpt.*
- Brondijk, J. F. (1962b). Sedimentological investigations in North Borneo and northern Sarawak. In *Brit. Borneo Geol. Surv. Ann. Rpt.*
- Buatois, L. A., & Mángano, M. G. (2011). Ichnology of deep-marine clastic environments. *Ichnology*, 181–196. <https://doi.org/10.1017/cbo9780511975622.010>
- Burley, S. D., Breitfeld, H. T., Stanbrook, D. S., Morley, R. J., Kassan, J., Sukarno, M., & Wantoro, D. W. (2021). A tuffaceous volcanoclastic turbidite bed of Early Miocene age in the Temburong Formation of Labuan, North-West Borneo and its implications for the Proto-South China Sea subduction in the Burdigalian. *The Depositional Record*, 7(1), 111–146. <https://doi.org/10.1002/dep2.132>
- Callow, R. H., McIlroy, D., Kneller, B., & Dykstra, M. (2012). Integrated ichnological and sedimentological analysis of a Late Cretaceous submarine channel-levee system: The Rosario Formation, Baja California, Mexico. *Marine and Petroleum Geology*, 41, 277–294. <https://doi.org/10.1016/j.marpetgeo.2012.02.001>
- Callow, R. H. T., & McIlroy, D. (2011). Ichnofabrics and ichnofabric-forming trace fossils in Phanerozoic turbidites. *Bulletin of Canadian Petroleum Geology*, 59(2), 103–111. <https://doi.org/10.2113/gscpgbull.59.2.103>

- Claussmann, B., Bailleul, J., Chanier, F., Mahieux, G., Caron, V., McArthur, A. D., Chaptal, C., Morgans, H. E. G., & Vendeville, B. C. (2021). Shelf-derived mass-transport deposits: origin and significance in the stratigraphic development of trench-slope basins. *New Zealand Journal of Geology and Geophysics*, 65(1), 17–52. <https://doi.org/10.1080/00288306.2021.1918729>
- Crevello, P. D., Johnson, H., Clayburn, J., & Rahman, R. A. (2005). *Deltaic and turbidite reservoir systems of SE Asia: high resolution exploration and development models and applications, from outcrop to subsurface*. AAPG Field Seminar Guide Book.
- Cullen, A. B. (2010). Transverse segmentation of the Baram-Balabac Basin, NW Borneo: refining the model of Borneo's tectonic evolution. *Petroleum Geoscience*, 16(1), 3–29. <https://doi.org/10.1144/1354-079309-828>
- Cummings, J. P., & Hodgson, D. M. (2011). Assessing controls on the distribution of ichnotaxa in submarine fan environments, the Basque Basin, Northern Spain. *Sedimentary Geology*, 239(3–4), 162–187. <https://doi.org/10.1016/j.sedgeo.2011.06.009>
- Cunningham, C. M., & Arnott, R. W. C. (2021). Systematic organization of thin-bedded turbidites in ancient deep-marine levees: Possible evidence of rhythmic pulsing in turbidity currents. *Journal of Sedimentary Research*, 91(11), 1257–1274. <https://doi.org/10.2110/jsr.2021.003>
- Deptuck, M. E., Piper, D. J. W., Savoye, B., & Gervais, A. (2008). Dimensions and architecture of late Pleistocene submarine lobes off the northern margin of East Corsica. *Sedimentology*, 55(4), 869–898. <https://doi.org/10.1111/j.1365-3091.2007.00926.x>
- Deptuck, M. E., Steffens, G. S., Barton, M., & Pirmez, C. (2003). Architecture and evolution of upper fan channel-belts on the Niger Delta slope and in the Arabian Sea. *Marine and Petroleum Geology*, 20(6–8), 649–676. <https://doi.org/10.1016/j.marpetgeo.2003.01.004>
- Fan, R. Y., Gong, Y. M., & Uchman, A. (2018). Topological analysis of graphoglyptid trace fossils, a study of macrobenthic solitary and collective animal behaviors in the deep-sea environment. *Paleobiology*, 44(2), 306–325. <https://doi.org/10.1017/pab.2018.1>
- Fonnesu, M., Felletti, F., Haughton, P. D. W., Patacci, M., & McCaffrey, W. D. (2018). Hybrid event bed character and distribution linked to turbidite system sub-environments: The North Apennine Gottero Sandstone (north-west Italy). *Sedimentology*, 65(1), 151–190. <https://doi.org/10.1111/sed.12376>

- Fonnesu, M., Haughton, P., Felletti, F., & McCaffrey, W. (2015). Short length-scale variability of hybrid event beds and its applied significance. *Marine and Petroleum Geology*, 67, 583–603. <https://doi.org/10.1016/j.marpetgeo.2015.03.028>
- Frey, R. W., Pemberton, S. G., & Saunders, T. D. A. (1990). Ichnofacies and bathymetry: a passive relationship. *Journal of Paleontology*, 64(1), 155–158. <https://doi.org/10.1017/s0022336000042372>
- García-Ramos, J. C., Mángano, M. G., Piñuela, L., Buatois, L. A., & Rodríguez-Tovar, F. J. (2014). The ichnogenus *Tubotomaculum*: an enigmatic pellet-filled structure from Upper Cretaceous to Miocene deep-marine deposits of southern Spain. *Journal of Paleontology*, 88(6), 1189–1198. <https://doi.org/10.1666/13-123>
- Hall, R. (2013). Contraction and extension in northern Borneo driven by subduction rollback. *Journal of Asian Earth Sciences*, 76, 399–411. <https://doi.org/10.1016/j.jseaes.2013.04.010>
- Hammersburg, S. R., Hasiotis, S. T., & Robison, R. A. (2018). Ichnotaxonomy of the Cambrian Spence Shale Member of the Langston formation, Wellsville Mountains, Northern Utah, USA. *Paleontological Contributions*. <https://doi.org/10.17161/1808.26428>
- Hansen, L. A., Callow, R. H., Kane, I. A., Gamberi, F., Rovere, M., Cronin, B. T., & Kneller, B. C. (2015). Genesis and character of thin-bedded turbidites associated with submarine channels. *Marine and Petroleum Geology*, 67, 852–879. <https://doi.org/10.1016/j.marpetgeo.2015.06.007>
- Hansen, L., Janocko, M., Kane, I., & Kneller, B. (2017). Submarine channel evolution, terrace development, and preservation of intra-channel thin-bedded turbidites: Mahin and Avon channels, offshore Nigeria. *Marine Geology*, 383, 146–167. <https://doi.org/10.1016/j.margeo.2016.11.011>
- Haughton, P. D. W., Barker, S. P., & McCaffrey, W. D. (2003). ‘Linked’ debrites in sand-rich turbidite systems - origin and significance. *Sedimentology*, 50(3), 459–482. <https://doi.org/10.1046/j.1365-3091.2003.00560.x>
- Haughton, P., Davis, C., McCaffrey, W., & Barker, S. (2009). Hybrid sediment gravity flow deposits – Classification, origin and significance. *Marine and Petroleum Geology*, 26(10), 1900–1918. <https://doi.org/10.1016/j.marpetgeo.2009.02.012>
- Hazebroek, H. P., & Tan, D. N. (1993). Tertiary tectonic evolution of the NW Sabah Continental Margin. *Bulletin of the Geological Society of Malaysia*, 33, 195–210. <https://doi.org/10.7186/bgsm33199315>
- Heard, T. G., & Pickering, K. T. (2008). Trace fossils as diagnostic indicators of deep-marine environments, Middle Eocene Ainsa-Jaca basin, Spanish Pyrenees.

Sedimentology, 55(4), 809–844. <https://doi.org/10.1111/j.1365-3091.2007.00922.x>

- Hennig-Breitfeld, J., Breitfeld, H. T., Hall, R., BouDagher-Fadel, M., & Thirlwall, M. (2019). A new upper Paleogene to Neogene stratigraphy for Sarawak and Labuan in northwestern Borneo: Paleogeography of the eastern Sundaland margin. *Earth-Science Reviews*, 190, 1–32. <https://doi.org/10.1016/j.earscirev.2018.12.006>
- Hickson, T. A., & Lowe, D. R. (2002). Facies architecture of a submarine fan channel-levee complex: the Juniper Ridge Conglomerate, Coalinga, California. *Sedimentology*, 49(2), 335–362. <https://doi.org/10.1046/j.1365-3091.2002.00447.x>
- Hiscott, R. N., & Middleton, G. V. (1980). Fabric of Coarse Deep-water Sandstones Tourelle Formation, Quebec, Canada. *SEPM Journal of Sedimentary Research*, Vol. 50. <https://doi.org/10.1306/212f7ac7-2b24-11d7-8648000102c1865d>
- Hodgson, D. M. (2009). Distribution and origin of hybrid beds in sand-rich submarine fans of the Tanqua depocentre, Karoo Basin, South Africa. *Marine and Petroleum Geology*, 26(10), 1940–1956. <https://doi.org/10.1016/j.marpetgeo.2009.02.011>
- Hutchinson, C. S. (1996). *Geological evolution of South-East Asia* (New edition). Geological Society of Malaysia.
- Hutchison, C. S. (2005). *Geology of North-West Borneo: Sarawak, Brunei and Sabah*. Elsevier.
- Hutchison, C. S., Bergman, S. C., Swauger, D. A., & Graves, J. E. (2000). A Miocene collisional belt in north Borneo: uplift mechanism and isostatic adjustments quantified by thermochronology. *J. Geol. Soc. London*, 157, 783–793.
- Jackson, C. a. L., & Johnson, H. D. (2009). Sustained turbidity currents and their interaction with debrite-related topography; Labuan Island, offshore NW Borneo, Malaysia. *Sedimentary Geology*, 219(1–4), 77–96. <https://doi.org/10.1016/j.sedgeo.2009.04.008>
- Jackson, C. a. L., Zakaria, A. A., Johnson, H. D., Tongkul, F., & Crevello, P. D. (2009). Sedimentology, stratigraphic occurrence and origin of linked debrites in the West Crocker Formation (Oligo-Miocene), Sabah, NW Borneo. *Marine and Petroleum Geology*, 26(10), 1957–1973. <https://doi.org/10.1016/j.marpetgeo.2009.02.019>
- Jamil, M., Abd Rahman, A. H., Siddiqui, N. A., Ibrahim, N. A., & Ahmed, N. (2020). A contemporary review of sedimentological and stratigraphic framework of the Late Paleogene deep marine sedimentary successions of West Sabah, North-West Borneo. *Bulletin of the Geological Society of Malaysia*, 69, 53–65. <https://doi.org/10.7186/bgsm69202005>

- Jasin, B., & Firdaus, M. S. (2019). Some deep-marine ichnofossils from Labuan and Klias Peninsula, west of Sabah. *Bulletin of the Geological Society of Malaysia*, 67, 47–51. <https://doi.org/10.7186/bgsm67201906>
- Jobe, Z. R., Lowe, D. R., & Morris, W. R. (2011). Climbing-ripple successions in turbidite systems: depositional environments, sedimentation rates and accumulation times. *Sedimentology*, 59(3), 867–898. <https://doi.org/10.1111/j.1365-3091.2011.01283.x>
- Kane, I. A., Dykstra, M. L., Kneller, B. C., Tremblay, S., & McCaffrey, W. D. (2009). Architecture of a coarse grained channel-levee system: the Rosario Formation, Baja California, Mexico. *Sedimentology*, 56(7), 2207–2234. <https://doi.org/10.1111/j.1365-3091.2009.01077.x>
- Kane, I. A., & Hodgson, D. M. (2011). Sedimentological criteria to differentiate submarine channel levee subenvironments: Exhumed examples from the Rosario Fm. (Upper Cretaceous) of Baja California, Mexico, and the Fort Brown Fm. (Permian), Karoo Basin, S. Africa. *Marine and Petroleum Geology*, 28(3), 807–823. <https://doi.org/10.1016/j.marpetgeo.2010.05.009>
- Kane, I. A., Kneller, B. C., Dykstra, M., Kassem, A., & McCaffrey, W. D. (2007). Anatomy of a submarine channel–levee: An example from Upper Cretaceous slope sediments, Rosario Formation, Baja California, Mexico. *Marine and Petroleum Geology*, 24(6–9), 540–563. <https://doi.org/10.1016/j.marpetgeo.2007.01.003>
- Kane, I. A., & Pontén, A. S. (2012). Submarine transitional flow deposits in the Paleogene Gulf of Mexico. *Geology*, 40(12), 1119–1122. <https://doi.org/10.1130/g33410.1>
- Kane, I. A., Pontén, A. S. M., Vangdal, B., Eggenhuisen, J. T., Hodgson, D. M., & Spychala, Y. T. (2017). The stratigraphic record and processes of turbidity current transformation across deep-marine lobes. *Sedimentology*, 64(5), 1236–1273. <https://doi.org/10.1111/sed.12346>
- Khan, Z. A., Arnott, B., & Pugin, A. J. M. (2011). An alternative model of producing topography in the crest region of deep-water levees. *AAPG Bulletin*, 95(12), 2085–2106. <https://doi.org/10.1306/03281110024>
- Khan, Z. A., & Arnott, R. (2011a). Stratal attributes and evolution of asymmetric inner- and outer-bend levee deposits associated with an ancient deep-water channel-levee complex within the Isaac Formation, southern Canada. *Marine and Petroleum Geology*, 28(3), 824–842. <https://doi.org/10.1016/j.marpetgeo.2010.07.009>
- Khan, Z. A., & Arnott, R. W. C. (2011b). Stratal attributes and evolution of asymmetric inner- and outer-bend levee deposits associated with an ancient deep-water channel-levee complex within the Isaac Formation, southern Canada. *Marine and*

- Knaust, D. (2009). Characterisation of a Campanian deep-sea fan system in the Norwegian Sea by means of ichnofabrics. *Marine and Petroleum Geology*, 26(7), 1199–1211. <https://doi.org/10.1016/j.marpetgeo.2008.09.009>
- Knaust, D. (2017). *Atlas of Trace Fossils in Well Core: Appearance, Taxonomy and Interpretation*. Springer Publishing.
- Kneller, B. C., & Branney, M. J. (1995). Sustained high-density turbidity currents and the deposition of thick massive sands. *Sedimentology*, 42(4), 607–616. <https://doi.org/10.1111/j.1365-3091.1995.tb00395.x>
- Książkiewicz, M. (1977). *Trace fossils in the flysch of the Polish Carpathians*. Państwowe Wydawn.
- Kuswandaru, G. Y., Amir Hassan, M. H., Matenco, L. C., Taib, N. I., & Mustapha, K. A. (2018). Turbidite, debrite, and hybrid event beds in submarine lobe deposits of the Palaeocene to middle Eocene Kapit and Pelagus members, Belaga Formation, Sarawak, Malaysia. *Geological Journal*, 54(6), 3421–3437. <https://doi.org/10.1002/gj.3347>
- Lambiase, J. J., Damit, A. R., Simmons, M. S., Abdoerrias, R., & Hussin, A. (2003). A Depositional Model And The Stratigraphic Development Of Modern And Ancient Tide-Dominated Deltas In NW Borneo. In *SEPM (Society for Sedimentary Geology) eBooks* (pp. 109–123). <https://doi.org/10.2110/pec.03.76.0109>
- Lee, C. P. (1977). *The geology of Labuan Island, Sabah, East Malaysia* [BSc. Hons Thesis]. University of Malaya.
- Levell, B. (1987). The nature and significance of regional unconformities in the hydrocarbon-bearing Neogene sequence offshore West Sabah. *Bulletin of the Geological Society of Malaysia*, 21, 55–90. <https://doi.org/10.7186/bgsm21198704>
- Liechti, P., Roe, F. W., & Haile, N. S. (1960). The geology of Sarawak, Brunei and western part of North Borneo. *Geological Survey Department British Territories*.
- Lowe, D. R. (1982). Sediment Gravity Flows: II Depositional Models with Special Reference to the Deposits of High-Density Turbidity Currents. *SEPM Journal of Sedimentary Research*, Vol. 52. <https://doi.org/10.1306/212f7f31-2b24-11d7-8648000102c1865d>
- Lunt, P. (2022). Re-examination of the Base Miocene Unconformity in west Sabah, Malaysia, and stratigraphic evidence against a slab-pull subduction model. *Journal of Asian Earth Sciences*, 230, 105193. <https://doi.org/10.1016/j.jseaes.2022.105193>

- Luthi, S. A. (1981). Experiments on non-channelized turbidity currents and their deposits. *Marine Geology*, 40(3–4), M59–M68. [https://doi.org/10.1016/0025-3227\(81\)90139-0](https://doi.org/10.1016/0025-3227(81)90139-0)
- MacEachern, J. A., Bann, K. L., Pemberton, S. G., & Gingras, M. K. (2007). The Ichnofacies Paradigm_{title}High-Resolution Paleoenvironmental Interpretation of the Rock Record_{title} *Applied Ichnology*. <https://doi.org/10.2110/pec.07.52.0027>
- MacEachern, J. A., Pemberton, S. G., Gingras, M. K., & Bann, K. L. (2007). The Ichnofacies Paradigm: A Fifty-Year Retrospective. *Trace Fossils*, 52–77. <https://doi.org/10.1016/b978-044452949-7/50130-3>
- Madon, M. (1994). The stratigraphy of northern Labuan, NW Sabah Basin, East Malaysia. *Geological Society of Malaysia Bulletin*, 36, 19–30.
- Madon, M. (1997). Sedimentological aspects of the Temburong and Belait Formations, Labuan (offshore west Sabah, Malaysia). *Bulletin of the Geological Society of Malaysia*, 41, 61–84. <https://doi.org/10.7186/bgsm41199707>
- Madon, M. (1999a). *Plate tectonic elements and evolution of South East Asia*. Petronas.
- Madon, M. (1999b). *Sabah Basin*. Petronas.
- Madon, M. (2021). Deep-Sea Trace Fossils In The West Crocker Formation, Sabah (Malaysia), And Their Palaeoenvironmental Significance. *Bulletin of the Geological Society of Malaysia*, 71, 23–46. <https://doi.org/10.7186/bgsm71202103>
- Mansor, H. E., & Amir Hassan, M. H. (2021). Facies and bed type characteristics of channel-lobe transition deposits from the Oligocene-Miocene Tajau Sandstone Member, Kudat Formation, Sabah, Malaysia. *Geological Journal*, 56(11), 5642–5672. <https://doi.org/10.1002/gj.4263>
- Martinsen, O. (1994). Mass movements. *The Geological Deformation of Sediments*, 127–165. https://doi.org/10.1007/978-94-011-0731-0_5
- Martinsen, O. J. (1989). Styles of soft-sediment deformation on a Namurian (Carboniferous) delta slope, Western Irish Namurian Basin, Ireland. *Geological Society, London, Special Publications*, 41(1), 167–177. <https://doi.org/10.1144/gsl.sp.1989.041.01.13>
- Martinsen, O. J., & Bakken, B. (1990). Extensional and compressional zones in slumps and slides in the Namurian of County Clare, Ireland. *Journal of the Geological Society*, 147(1), 153–164. <https://doi.org/10.1144/gsjgs.147.1.0153>
- Martinsson, A. (1970). *Toponymy of trace fossils* (Vol. 3, pp. 323–330). Geological Journal Special Issue.

- McIlroy, D. (2004). Some ichnological concepts, methodologies, applications and frontiers. *Geological Society, London, Special Publications*, 228(1), 3–27. <https://doi.org/10.1144/gsl.sp.2004.228.01.02>
- Middleton, G. V. (1978). Flame structure. In *Encyclopedia of Sediments and Sedimentary Rocks* (pp. 281–282). Springer. https://doi.org/10.1007/978-1-4020-3609-5_85
- Middleton, G. V., & Hampton, M. A. (1973). Sediment gravity flows: mechanisms of flow and deposition. In *Turbidites and Deep-Water Sedimentation*. SEPM Pacific Section, Short course lecture note.
- Monaco, P. (2008). Taphonomic Features of Paleodictyon and Other Graphoglyptid Trace Fossils in Oligo-Miocene Thin-Bedded Turbidites, Northern Apennines, Italy. *PALAIOS*, 23(10), 667–682. <https://doi.org/10.2110/palo.2007.p07-016r>
- Monaco, P., Milighetti, M., & Checconi, A. (2010). Ichnocoenoses in the Oligocene to Miocene foredeep basins (Northern Apennines, central Italy) and their relation to turbidite deposition. *Acta Geologica Polonica*, 60(1), 53–70. <https://geojournals.pgi.gov.pl/agp/article/download/9820/8354>
- Morley, C. K., Tingay, M., Hillis, R., & King, R. (2008). Relationship between structural style, overpressures, and modern stress, Baram Delta Province, northwest Borneo. *Journal of Geophysical Research*, 113(B9). <https://doi.org/10.1029/2007jb005324>
- Morley, R. J., Morley, H. P., & Swiecicki, T. (2016). Mio-Pliocene Palaeogeography, Uplands And River Systems of the Sunda Region Based on Mapping Within a Framework of Vm Depositional Cycles. *Proc. Indonesian Petrol. Assoc., 40th Ann. Conv.* <https://doi.org/10.29118/ipa.0.16.506.g>
- Morris, E. A., Hodgson, D. M., Brunt, R. L., & Flint, S. S. (2014). Origin, evolution and anatomy of silt-prone submarine external levées. *Sedimentology*, 61(6), 1734–1763. <https://doi.org/10.1111/sed.12114>
- Mueller, P., Patacci, M., & Di Giulio, A. (2017). Hybrid event beds in the proximal to distal extensive lobe domain of the coarse-grained and sand-rich Bordighera turbidite system (NW Italy). *Marine and Petroleum Geology*, 86, 908–931. <https://doi.org/10.1016/j.marpetgeo.2017.06.047>
- Mulder, T., & Alexander, J. (2001). The physical character of subaqueous sedimentary density flows and their deposits. *Sedimentology*, 48(2), 269–299. <https://doi.org/10.1046/j.1365-3091.2001.00360.x>
- Mutti, E. (1977). Distinctive thin-bedded turbidite facies and related depositional environments in the Eocene Hecho Group (South-central Pyrenees, Spain). *Sedimentology*, 24(1), 107–131. <https://doi.org/10.1111/j.1365-3091.1977.tb00122.x>

- Mutti, E. (1992). *Turbidite Sandstones*. Agip, Istituto di geologia, Università di Parma.
- Mutti, E., Bernoulli, D., Lucchi, F. R., & Tinterri, R. (2009). Turbidites and turbidity currents from Alpine 'flysch' to the exploration of continental margins. *Sedimentology*, 56(1), 267–318. <https://doi.org/10.1111/j.1365-3091.2008.01019.x>
- Mutti, E., & Nielson, T. (1981). Significance of intraformational rip-up clasts in deep-sea fan deposits. *Int. Assoc. Sedimentol. 2nd Eur. Regional Mtg. Abstr.*, 117–119.
- Mutti, E., Tinterri, R., Benevelli, G., Biase, D. D., & Cavanna, G. (2003). Deltaic, mixed and turbidite sedimentation of ancient foreland basins. *Marine and Petroleum Geology*, 20(6–8), 733–755. <https://doi.org/10.1016/j.marpetgeo.2003.09.001>
- Owen, G. (2003). Load structures: gravity-driven sediment mobilization in the shallow subsurface. *Geological Society, London, Special Publications*, 216(1), 21–34. <https://doi.org/10.1144/gsl.sp.2003.216.01.03>
- Peakall, J., Best, J., Baas, J. H., Hodgson, D. M., Clare, M. A., Talling, P. J., Dorrell, R. M., & Lee, D. R. (2020). An integrated process-based model of flutes and tool marks in deep-water environments: Implications for palaeohydraulics, the Bouma sequence and hybrid event beds. *Sedimentology*, 67(4), 1601–1666. <https://doi.org/10.1111/sed.12727>
- Phillips, C., McIlroy, D., & Elliott, T. (2011). Ichnological characterization of Eocene/Oligocene turbidites from the Grès d'Annot Basin, French Alps, SE France. *Palaeogeography, Palaeoclimatology, Palaeoecology*, 300(1–4), 67–83. <https://doi.org/10.1016/j.palaeo.2010.12.011>
- Pickering, K. T., Hiscott, R. N., & Hein, F. J. (1989). Deep Marine Environments: Clastic sedimentation and tectonics. *Unwin Hyman, London*.
- Piper, D. J. W. (1976). Turbidite muds and silts on deepsea fans and abyssal plains. In *Sedimentation in Submarine Canyons, Fans and Trenches* (pp. 163–176). Dowden, Hutchinson & Ross.
- Posamentier, H. W., & Kolla, V. (2003). Seismic Geomorphology and Stratigraphy of Depositional Elements in Deep-Water Settings. *Journal of Sedimentary Research*, 73(3), 367–388. <https://doi.org/10.1306/111302730367>
- Posamentier, H. W., & Martinsen, O. J. (2011). The Character and Genesis of Submarine Mass-Transport Deposits: Insights from Outcrop and 3D Seismic Data. *Mass-Transport Deposits in Deepwater Settings*, 7–38. <https://doi.org/10.2110/sepmsp.096.007>
- Posamentier, H. W., & Walker, R. G. (2006). Deep-Water Turbidites and Submarine Fans. *Facies Models Revisited*, 399–520. <https://doi.org/10.2110/pec.06.84.0399>

- Prélat, A., Covault, J., Hodgson, D., Fildani, A., & Flint, S. (2010). Intrinsic controls on the range of volumes, morphologies, and dimensions of submarine lobes. *Sedimentary Geology*, 232(1–2), 66–76. <https://doi.org/10.1016/j.sedgeo.2010.09.010>
- Prélat, A., & Hodgson, D. M. (2013). The full range of turbidite bed thickness patterns in submarine lobes: controls and implications. *Journal of the Geological Society*, 170(1), 209–214. <https://doi.org/10.1144/jgs2012-056>
- Prélat, A., Hodgson, D. M., & Flint, S. S. (2009). Evolution, architecture and hierarchy of distributary deep-water deposits: a high-resolution outcrop investigation from the Permian Karoo Basin, South Africa. *Sedimentology*, 56(7), 2132–2154. <https://doi.org/10.1111/j.1365-3091.2009.01073.x>
- Sandal, S. T. (1996). *The Geology and Hydrocarbon Resources of Negara Brunei Darussalam*. Brunei Shell Petroleum Company.
- Seilacher, A. (1967). Bathymetry of trace fossils. *Marine Geology*, 5(5–6), 413–428. [https://doi.org/10.1016/0025-3227\(67\)90051-5](https://doi.org/10.1016/0025-3227(67)90051-5)
- Seilacher, A. (1977). Chapter 11 Evolution of Trace Fossil Communities. *Developments in Palaeontology and Stratigraphy*, 359–376. [https://doi.org/10.1016/s0920-5446\(08\)70331-5](https://doi.org/10.1016/s0920-5446(08)70331-5)
- Seilacher, A. (2007). *Trace Fossil Analysis* (1st ed.). Springer.
- Seilacher, A., & Seilacher, E. (1994). *Bivalvian trace fossils a lesson from actuopaleontology*. Courier Forschungsinstitut Senckenberg.
- Shan, X., Yu, X. H., Jin, L., Li, Y. L., Tan, C. P., Li, S. L., & Wang, J. H. (2020). Bed type and flow mechanism of deep water sub-lacustrine fan fringe facies: an example from the Middle Permian Lucaogou Formation in Southern Junggar Basin of NW China. *Petroleum Science*, 18(2), 339–361. <https://doi.org/10.1007/s12182-020-00534-x>
- Shanmugam, G. (1997). The Bouma Sequence and the turbidite mind set. *Earth-Science Reviews*, 42(4), 201–229. [https://doi.org/10.1016/s0012-8252\(97\)81858-2](https://doi.org/10.1016/s0012-8252(97)81858-2)
- So, Y. S., Rhee, C. W., Choi, P. Y., Kee, W. S., Seo, J. Y., & Lee, E. J. (2013). Distal turbidite fan/lobe succession of The Late Paleozoic Taean Formation, Western Korea. *Geosciences Journal*, 17(1), 9–25. <https://doi.org/10.1007/s12303-013-0016-0>
- Som, M. R. M., Kadir, M. F. A., Ali, S. S. M., Jirin, S., Sulaiman, W. M. K. a. B. W., Mohsin, N., & Shah, S. S. M. (2011). Labuan Outcrop Revisited: New Findings on Belait formation Facies Evolution. *PGCE 2011*. <https://doi.org/10.3997/2214-4609-pdb.251.21>

- Spychala, Y. T., Hodgson, D. M., Pr  lat, A., Kane, I. A., Flint, S. S., & Mountney, N. P. (2017). Frontal and Lateral Submarine Lobe Fringes: Comparing Sedimentary Facies, Architecture and Flow Processes. *Journal of Sedimentary Research*, 87(1), 75–96. <https://doi.org/10.2110/jsr.2017.2>
- Starek, D., & Fuksi, T. (2017). Distal turbidite fan/lobe succession of the Late Oligocene Zuberec Fm. – architecture and hierarchy (Central Western Carpathians, Orava–Podhale basin). *Open Geosciences*, 9(1). <https://doi.org/10.1515/geo-2017-0030>
- Stow, D. a. V., & Bowen, A. J. (1978). Origin of lamination in deep sea, fine-grained sediments. *Nature*, 274(5669), 324–328. <https://doi.org/10.1038/274324a0>
- Stow, D. a. V., & Bowen, A. J. (1980). A physical model for the transport and sorting of fine-grained sediment by turbidity currents. *Sedimentology*, 27(1), 31–46. <https://doi.org/10.1111/j.1365-3091.1980.tb01156.x>
- Sylvester, Z., Pirmez, C., & Cantelli, A. (2011). A model of submarine channel-levee evolution based on channel trajectories: Implications for stratigraphic architecture. *Marine and Petroleum Geology*, 28(3), 716–727. <https://doi.org/10.1016/j.marpetgeo.2010.05.012>
- Talling, P. J. (2013). Hybrid submarine flows comprising turbidity current and cohesive debris flow: Deposits, theoretical and experimental analyses, and generalized models. *Geosphere*, 9(3), 460–488. <https://doi.org/10.1130/ges00793.1>
- Talling, P. J., Amy, L. A., & Wynn, R. B. (2007). New insight into the evolution of large-volume turbidity currents: comparison of turbidite shape and previous modelling results. *Sedimentology*, 54(4), 737–769. <https://doi.org/10.1111/j.1365-3091.2007.00858.x>
- Talling, P. J., Amy, L. A., Wynn, R. B., Peakall, J., & Robinson, M. (2004). Beds comprising debrite sandwiched within co-genetic turbidite: origin and widespread occurrence in distal depositional environments. *Sedimentology*, 51(1), 163–194. <https://doi.org/10.1111/j.1365-3091.2004.00617.x>
- Talling, P. J., Masson, D. G., Sumner, E. J., & Malgesini, G. (2012). Subaqueous sediment density flows: Depositional processes and deposit types. *Sedimentology*, 59(7), 1937–2003. <https://doi.org/10.1111/j.1365-3091.2012.01353.x>
- Tate, R. B. (1994). The sedimentology and tectonics of the Temburong Formation - deformation of early Cenozoic deltaic sequences in NW Borneo. *Bulletin of the Geological Society of Malaysia*, 35, 97–112. <https://doi.org/10.7186/bgsm35199410>
- Taylor, B., & Hayes, D. E. (1980). The tectonic evolution of the South China Basin. *The Tectonic and Geologic Evolution of Southeast Asian Seas and Islands*, 89–104. <https://doi.org/10.1029/gm023p0089>

- Thrane, K., & Keulen, N. T. (2012). *Provenance of sediments in the Faroe-Shetland Basin: Characterisation of possible source components in Southeast Greenland* (SINDRI C46-50-01). GEUS.
- Tinterri, R., Drago, M., Consonni, A., Davoli, G., & Mutti, E. (2003). Modelling subaqueous bipartite sediment gravity flows on the basis of outcrop constraints: first results. *Marine and Petroleum Geology*, 20(6–8), 911–933. <https://doi.org/10.1016/j.marpetgeo.2003.03.003>
- Tinterri, R., Muzzi Magalhaes, P., Tagliaferri, A., & Cunha, R. (2016). Convolute laminations and load structures in turbidites as indicators of flow reflections and decelerations against bounding slopes. Examples from the Marnoso-arenacea Formation (northern Italy) and Annot Sandstones (south eastern France). *Sedimentary Geology*, 344, 382–407. <https://doi.org/10.1016/j.sedgeo.2016.01.023>
- Tongkul, F. (1991). Tectonic evolution of Sabah, Malaysia. *Journal of Southeast Asian Earth Sciences*, 6(3–4), 395–405. [https://doi.org/10.1016/0743-9547\(91\)90084-b](https://doi.org/10.1016/0743-9547(91)90084-b)
- Tongkul, F. (2001). Sumber Geologi Intrinsik Pulau Labuan. In *Geological Heritage of Malaysia – Geosite Mapping and Geoheritage Characterisation* (pp. 377–387). LESTARI UKM.
- Uchman, A. (1995). *Taxonomy and Palaeoecology of Flysch Trace Fossils: The Marnoso-arenacea Formation and Associated Facies (Miocene, Northern Apennines, Italy)* (Vol. 15). Freunde der Würzburger Geowiss.
- Uchman, A. (1998). Taxonomy And Ethology Of Flysch Trace Fossils: Revision Of The Marian Książkiewicz Collection And Studies Of Complementary Material. *Annales Societatis Geologorum Poloniae*, 68, 105–218.
- Uchman, A. (2001). *Eocene flysch trace fossils from the Hecho Group of the Pyrenees, northern Spain*. Freunde der Würzburger Geowissenschaften.
- Uchman, A. (2004). Phanerozoic history of deep-sea trace fossils. *Geological Society, London, Special Publications*, 228(1), 125–139. <https://doi.org/10.1144/gsl.sp.2004.228.01.07>
- Uchman, A., & Gazdzicki, A. (2006). New trace fossils from the La Meseta Formation (Eocene) of Seymour Island, Antarctica. *Polish Polar Research*, 27(2), 153–170. <http://yadda.icm.edu.pl/yadda/element/bwmeta1.element.agro-article-698a6738-8207-40b9-adee-48f5608e08d4>
- Uchman, A., Janbu, N. E., & Nemec, W. (2004). Trace fossils in the Cretaceous-Eocene flysch of the Sinop-Boyabat Basin, Central Pontides, Turkey. *Annales Societatis Geologorum Poloniae*, 74(2), 197–235. <https://geojournals.pgi.gov.pl/asgp/article/download/12425/10899>

- Uchman, A., & Wetzel, A. (2012). Deep-Sea Fans. *Developments in Sedimentology*, 643–671. <https://doi.org/10.1016/b978-0-444-53813-0.00021-6>
- Van Hattum, M., Hall, R., Pickard, A., & Nichols, G. (2013). Provenance and geochronology of Cenozoic sandstones of northern Borneo. *Journal of Asian Earth Sciences*, 76, 266–282. <https://doi.org/10.1016/j.jseaes.2013.02.033>
- Van Hattum, M. W., Hall, R., Pickard, A. L., & Nichols, G. J. (2006). Southeast Asian sediments not from Asia: Provenance and geochronology of north Borneo sandstones. *Geology*, 34(7), 589. <https://doi.org/10.1130/g21939.1>
- Wan Hasiah, A., Lee, C. P., Gou, P., Shuib, M. K., Ng, T. F., Albaghdady, A. A., Mislan, M. F., & Mustapha, K. A. (2013). Coal-bearing strata of Labuan: Mode of occurrences, organic petrographic characteristics and stratigraphic associations. *Journal of Asian Earth Sciences*, 76, 334–345. <https://doi.org/10.1016/j.jseaes.2013.05.017>
- Wetzel, A., & Uchman, A. (2001). Sequential colonization of muddy turbidites in the Eocene Beloveža Formation, Carpathians, Poland. *Palaeogeography, Palaeoclimatology, Palaeoecology*, 168(1–2), 171–186. [https://doi.org/10.1016/s0031-0182\(00\)00254-6](https://doi.org/10.1016/s0031-0182(00)00254-6)
- Wilson, & Wong. (1964). The geology and mineral resources of the Labuan and Padas Valley areas, Sabah, Malaysia. In *Geological Survey Malaysia Memoir 17*.
- Young, S. S., Chul, W. R., Pom-Yong, C., Weon-Seo, K., Jin, Y. S., & Eun-Ju, L. (2013). Distal turbidite fan/lobe succession of the Late Paleozoic Taeon Formation, western Korea. *Geosciences Journal*, 7(1), 9–25. <https://doi.org/10.1007/s12303-013-0016-0>
- Zakaria, A. A., Johnson, H. D., Jackson, C. a. L., & Tongkul, F. (2013a). Sedimentary facies analysis and depositional model of the Palaeogene West Crocker submarine fan system, NW Borneo. *Journal of Asian Earth Sciences*, 76, 283–300. <https://doi.org/10.1016/j.jseaes.2013.05.002>
- Zakaria, A. A., Johnson, H. D., Jackson, C. a. L., & Tongkul, F. (2013b). Sedimentary facies analysis and depositional model of the Palaeogene West Crocker submarine fan system, NW Borneo. *Journal of Asian Earth Sciences*, 76, 283–300. <https://doi.org/10.1016/j.jseaes.2013.05.002>
- Zhang, C., Li, X., Mattern, F., Mao, G., Zeng, Q., & Xu, W. (2015). Deposystem architectures and lithofacies of a submarine fan-dominated deep sea succession in an orogen: A case study from the Upper Triassic Langjiexue Group of southern Tibet. *Journal of Asian Earth Sciences*, 111, 222–243. <https://doi.org/10.1016/j.jseaes.2015.07.013>
- Zhu, M., Graham, S., & McHargue, T. (2011). Characterization of Mass-Transport Deposits on a Pliocene Siliciclastic Continental Slope, Northwestern South China

Sea. *Mass-Transport Deposits in Deepwater Settings*, 111–125.
<https://doi.org/10.2110/sepm.096.111>

Universiti Malaya